6-1-2009

Characterization of the underwater light environment and its relevance to seagrass recovery and sustainability in Tampa Bay, Florida

Christopher J. Anastasiou
University of South Florida

Follow this and additional works at: http://scholarcommons.usf.edu/etd

Part of the American Studies Commons

Characterization of the Underwater Light Environment and Its Relevance to Seagrass

Recovery and Sustainability in Tampa Bay, Florida

by

Christopher J. Anastasiou

A dissertation submitted in partial fulfillment
of the requirements for the degree of
Doctor of Philosophy
College of Marine Science
University of South Florida

Major Professor: Kendall Carder, Ph.D.
Paula Coble, Ph.D.
Penny Hall, Ph.D.
Mark Luther, Ph.D.
John Walsh, Ph.D.

Date of Approval:
November 10, 2009

Keywords: light attenuation, seagrass, spectral, flow-through, fluorescence, absorption, optical model, water clarity, water quality

Dedication

To my parents, who always encouraged my intense curiosity and wonder about the sea, and instilled in me the determination to pursue my dreams, and to never let anything keep me from them.

...that which we are, we are;
One equal temper of heroic hearts,
Made weak by time and fate, but strong in will,
To strive, to seek, to find, and not to yield.

Alfred, Lord Tennyson

Acknowledgements

I thank my major professor, Dr. Ken Carder, for his academic, professional, and moral support over these many years. I am truly honored to be counted as one of Dr. Carder's former students. I also thank my committee for all of their support and dedication, specifically, Dr. Paula Coble for her insight and expertise in colored dissolved organic matter, Dr. John Walsh for his "big picture" perspective and for keeping me on task, Dr. Mark Luther for his insight on residence times and hydrodynamic circulation in Tampa Bay, and Dr. Penny Hall for her expertise in seagrass ecology.

I thank Holly Greening and the Tampa Bay Estuary Program for their financial support, the Florida Department of Environmental Protection for in-kind services and for providing me the opportunity to complete this research, the Florida Fish and Wildlife Research Institute for in-kind services, and the University of South Florida Ocean Optics Laboratory for the use of their optical sensors.

I am grateful to the following individuals for their technical support: Jennifer Kunzelman for the many hours spent in the field, Dave English for his support with the flow-through system, Jennifer Cannizzaro for her laboratory support, Walt Avery and Roger Johansson for their institutional knowledge of Tampa Bay, Jim Ivey for his technical expertise and support, Keith Reynolds for his GIS support, and many others.

I also wish to thank all my friends and family for their encouragement and support over the past 5 years. Finally, I am deeply indebted to my beautiful wife Wendy for her unconditional support, encouragement, and unwavering confidence in my ability to finish this project.

Note to Reader

The original of this document contains color that is necessary for understanding the data. The original dissertation is on file with the USF library in Tampa, Florida.

Table of Contents

List of Tables

List of Figures

List of Definitions and Acronyms

Symbol	Definition	Units
$A_L(\lambda)$	Specific leaf absorptance	nm^{-1}
$a_\phi(\lambda)$	Spectral absorption coefficient of phytoplankton	m^{-1}
$a_d(\lambda)$	Spectral absorption coefficient of detritus	m^{-1}
$a_g(\lambda)$	Spectral absorption of CDOM	m^{-1}
$a_p(\lambda)$	Spectral absorption coefficient of particulate matter	m^{-1}
$a_t(\lambda)$	Total spectral absorption coefficient	m^{-1}
$b(\lambda)$	Total scattering coefficient	m^{-1}
$c(\lambda)$	Beam attenuation coefficient	m^{-1}
CDOM	Colored Dissolved Organic Matter	
Chl a	Chlorophyll a concentration	$\mu g\ L^{-1}$
$E_d(\lambda)$	Spectral downwelling irradiance	$W\ m^{-1}$
$K_d(\lambda)$	Spectral downwelling attenuation coefficient	m^{-1}
LIDAR	Light Detection and Ranging	
PAR(λ)	Wavelength-specific Photosynthetically Active Radiation	$\mu mol\ m^{-2}\ s^{-1}$
PUR(λ)	Wavelength-specific Photosynthetically Useable Radiation	$\mu mol\ m^{-2}\ s^{-1}$
SMA	Seagrass Management Area	
FL_{CDOM}	CDOM fluorescence	V
FL_{Chl}	Chlorophyll fluorescence	V
$Tr(\lambda)$	Wavelength-specific transmittance	$V\ nm^{-1}$
VDC	Voltage Direct Current	V

Characterization of the Underwater Light Environment and Its Relevance to Seagrass
Recovery and Sustainability in Tampa Bay, Florida

Christopher J. Anastasiou

Abstract

The availability of light is a primary limiting factor for seagrass recovery and
sustainability. Understanding not only the quantity but the quality of light reaching the
bottom is an important component to successful seagrass management and the key focus
of this study. This study explores the spectral properties of the sub-surface light field in
four shallow Seagrass Management Areas (SMA) in Tampa Bay. Wavelength-specific
photosynthetically active radiation (PAR(λ)) and the spectral light attenuation coefficient
($K_d(\lambda)$) are used to estimate the percent blue, green, and red light remaining at the
bottom relative to the surface. LIDAR Bathymetry is combined with $K_d(\lambda)$ to produce
high-resolution maps of percent subsurface light along the seagrass deep edge. The
absorptance spectra from two seagrass species together with PAR(λ) is used to calculate
the photosynthetically useable radiation (PUR(λ)), a term describing the actual
wavelengths of light being used by the seagrass. Based on the average annual $K_d(\lambda)$,
32% - 39% percent of PAR reached the bottom at the seagrass deep edge, while only
14% - 18% of blue light reached bottom, suggesting that seagrass may be blue-light
limited. Analysis of PUR(λ) data further confirmed that seagrass are blue-light limited.

Each SMA was characterized in terms of the inherent optical properties (IOP) of
absorption and scatter. Tampa Bay is considered a chlorophyll-dominated estuary.
However, in this study, colored dissolved organic matter (CDOM) was the major

x

absorber of blue light, accounting for 60% of the total absorption. To infer past light conditions, the IOPs were related to parameters more commonly used in routine monitoring programs. To estimate $K_d(\lambda)$ an empirically-derived model using only the total absorption and scatter coefficients was used and resulted in a good fit between measured $K_d(480)$ and modeled $K_d(480)$.

A deck-mounted flow-through system was used to survey each SMA for CDOM and chlorophyll *a* fluorescence, among other properties. A series of SMA-specific predictor equations were empirically derived to relate raw fluorescence to the IOPs. The Kitchen SMA was used as a case study. Survey results show a strong connection between CDOM-rich waters and the mangrove-dominated shoreline.

Introduction

Seagrass are extremely productive estuarine and coastal resources, and are critical habitat for a number of fish, shrimp, and crab species (Zieman and Zieman 1989). These systems are experiencing world-wide decline, due in large part, to coastal eutrophication (Duarte et al. 2007). A major priority of the resource management community in Tampa Bay is to protect and restore seagrass habitat to the greatest extent possible (TBNEP 1996). Seagrass have among the highest light requirements of any organism in the plant kingdom (Gallegos 1994). Light is the primary limiting factor for most seagrass, and its availability is determined by physical, chemical, and biological conditions (Duarte 2002; Duarte et al. 2007; Kirk 1994; Miller 1995). In Tampa Bay, resource management agencies tasked with protecting and restoring these resources have established a minimum light target of 20.5% of total light reaching the bottom as the primary metric to achieve this objective (Dixon and Leverone 1995; TBNEP 1996; Tomasko and Lapointe 1991). Other proposed minimum light requirements for Tampa Bay and other systems throughout Florida are between 20% - 40% depending on species, location, and method used (Dennison et al. 1993; Dixon and Leverone 1995; Fourqurean et al. 2003; Gallegos 1994; Kenworthy and Fonseca 1996; Steward et al. 2005).

Typically light is measured in terms of the photosynthetically active radiation (PAR). By definition, PAR is a broadband quantity, in units of μmol photons m^{-2} s^{-1}, integrated across the visible spectrum (400nm - 700nm) (Mobley 1994). While it is true that a photon induces the same chemical change within a molecule of chlorophyll irrespective of the photon energy state, photons of different wavelengths are not equally likely to be absorbed by chlorophyll (Mobley 1994). While PAR is a relatively good indicator of light quantity, it does not take into account the spectral properties of the light field nor does it provide any indication that the photons available for photosynthesis are actually being used by the seagrass. Since seagrass are considered the "end users" of the incoming light field, it is important to express light quality in terms of the specific absorption characteristics of the light harvesting pigments found in seagrass. Like all higher plants, seagrass are reliant mostly on light within the blue and red color bands,

1

though the presence of accessory pigments can increase the operational window beyond the blue and red wavelengths. The term photosynthetically useable radiation ($PUR(\lambda)$) has been used to quantify the fraction of radiant energy that can be absorbed by a given plant for a given wavelength (Carder 1995; Morel 1978; Morel 1991). Operationally $PUR(\lambda)$ is the product of the $PAR(\lambda)$ and the seagrass leaf-absorptance. As a result of absorption and scatter of the incoming solar flux, $PAR(\lambda)$ diminishes with depth in an approximately exponential manner (Kirk 1994). The downwelling light attenuation coefficient ($K_d(\lambda)$) describes the loss of light with depth and can be calculated as the slope of the natural logarithm of $PAR(\lambda)$. With $K_d(\lambda)$, the percent subsurface $PAR(\lambda)$ can be estimated along the seagrass deep edge. $PUR(\lambda)$ can then be used to compare what is available for photosynthesis with what is actually being used by the seagrass at the deep edge.

Blue light is a common limiting factor in marine waters and results from absorption by phytoplankton and CDOM (Hoge et al. 1993; Menon et al. 2006) and is likely the case in Tampa Bay, especially along the seagrass deep edge. Estimating the $PUR(\lambda)$ at the seagrass deep edge can provide valuable insight into seagrass light utilization in areas that may be blue-light limited. Accessory light harvesting pigments, including chlorophylls *b* and *c*, and photosynthetic carotenoids, expand the light harvesting capabilities across the visible spectrum (Kirk 1994; Malick 2004) and may be a primary mechanism for surviving blue-light limited environments. If blue light is severely depleted along the deep edge, light-harvesting by the accessory pigments in the red and even green wavelengths may be only means of survival in these environments.

Technology in recent years has advanced to where it is now feasible to incorporate spectral light readings as part of routine monitoring programs. Using a geographic information system (GIS) approach, the percent subsurface $PAR(\lambda)$ can be calculated and mapped for a given seagrass area by specifying the $K_d(\lambda)$ and bathymetry. Values of the percent subsurface $PAR(\lambda)$ reaching the bottom along the deep edge can be extracted from the map product.

Defining the contributions of water, CDOM, phytoplankton, and detritus to the optical properties of the water column is a fundamental objective of bio-optical

oceanography (Kiefer and Soohoo 1982; Nelson and Robertson 1993; Prieur and Sathyendranath 1981; Smith and Baker 1978). Such information is also essential for estimating the concentration and composition of particulate and dissolved materials using remote sensing and *in situ* optical techniques (Nelson and Robertson 1993). Blue light in coastal and estuarine waters can be limited through absorption by phytoplankton, CDOM and detritus (Hoge et al. 1993; Nelson and Robertson 1993). Understanding the relative contribution and magnitude of these inherent optical properties (IOP) is critical to understanding the root causes of seagrass light limitation. Absorption by phytoplankton is typically expressed in terms of the phytoplankton absorption coefficient $(a_\phi(\lambda))$ in units of m^{-1}(Kirk 1994; Mobley 1994). Similarly, CDOM and detritus absorption can be described in terms of their absorption coefficients $(a_g(\lambda)$ and $a_d(\lambda)$, respectively).

In Tampa Bay, seagrass management has been predicated on the assumption that light attenuation is controlled largely by increased chlorophyll caused by excessive nitrogen loading (Cannizzaro 2004; Janicki Environmental 2001). This paradigm was developed during a time when wastewater effluent and untreated stormwater were directly discharging into the bay (TBNEP 1996). Today, advances in wastewater treatment and stormwater management have resulted in significant decreases in both nitrogen loads and chlorophyll concentrations. This decrease in the relative contribution of chlorophyll in the bay may have caused an increase in the relative importance of CDOM and detritus to blue light absorption. If CDOM is the dominant light attenuator, there may be little resource management agencies can do to improve light quality at the seagrass deep edge. However, it is likely that phytoplankton absorption is still contributing a significant amount to the total absorption of blue light, and evidence from recent work suggests that the relationship between nitrogen and phytoplankton productivity, though complex, does hold true in Tampa Bay and other CDOM-rich estuaries along the west coast of Florida (Janicki et al. 2003; Janicki and Wade 1996; Pribble et al. 2001; Tomasko and Ott 2001).

Most resource management agencies do not measure the inherent optical properties (IOP), such as $a_\phi(\lambda)$, $a_g(\lambda)$, and $a_d(\lambda)$, but collect quasi-inherent optical properties such as chlorophyll *a* concentration, color, and turbidity. Chlorophyll *a*

concentration is a relatively good proxy for phytoplankton absorption (Bricaud et al. 1995), though differences in photosynthetic efficiencies among phytoplankton and pigment packaging effects, can cause significant errors in this relationship (Bissett 1997; Kirk 1994). Color is reported in platinum cobalt units (PCU) and is visually determined according to the EPA approved method (EPA-140-A). Despite this crude method, the relationship between PCU color and $a_g(440\lambda)$ can be relatively strong (Gallegos 2005). Turbidity is reported in Nephelometric turbidity units (NTU) and, using the EPA approved Method l80.1, is based upon a comparison of the intensity of light, scattered at an angle of 90° by a sample, with the intensity of light scattered by a standard reference suspension, at the same scattering angle (USEPA 1999). Turbidity can be expressed as a function of the total scattering coefficient $b(\lambda)$ and the backscattering coefficient $b_b(\lambda)$ among other variables (Gallegos and Kenworthy 1996). Because chlorophyll a concentration, PCU color, and turbidity have been collected on a monthly basis for as long as 35 years in Tampa Bay (E.P.C.H.C. 2007) and are still widely collected by regulatory and resource management agencies throughout the state of Florida, it is important to couple these parameters with the IOPs (Gallegos and Kenworthy 1996; Gallegos 2001; Gallegos 2005; Lee 1998).

For resource managers, $K_d(\lambda)$ is one of the most relevant metrics for assessing seagrass habitat suitability largely because together with depth, $K_d(\lambda)$ can be used to calculate the percent subsurface PAR(λ). However, PAR is an apparent optical property (AOP) and contains error due to variations in the ambient conditions at the time of sampling. For example, variable cloud cover, sea state, time of day, and time of year all contribute to unaccounted variability in $K_d(\lambda)$. Because of the multiple scattering that takes place in natural systems, and the inherent variability in the angular distribution of the light field, there is no analytical expression to directly calculate $K_d(\lambda)$ from the IOPs (Kirk 1981). An alternative approach has been to develop an empirical relationship between $K_d(\lambda)$ and the IOPs using Monte Carlo procedures (Gallegos 2001; Kirk 1981; Kirk 1984). This method has proven to be very accurate and holds for most turbid estuaries with an scattering to absorption ratio less than 30 (Kirk 1994).

Obtaining adequate spatial and temporal data about the underwater light field, though critical to successful seagrass management, can be costly and time consuming to collect and analyze. A useful approach to supplement discrete water samples and provide calibration of satellite and airborne remote sensing is the use of a continuous flow-through system. Many of these systems have been constructed, but most have been deployed on larger research vessels in blue-water or coastal ocean environments (Madden and Day 1992; Twardowski et al. 2005). One such system has been modified to operate aboard a small open-hull boat in shallow seagrass areas. This deck-mounted flow-through system has all of the necessary sensors to fully characterize the optical light environment. The absorption coefficients $a_\phi(\lambda)$ and $a_g(\lambda)$ are not directly measured, but modeled using chlorophyll and CDOM fluorescence (Belzile et al. 2006; Ferrari and Dowell 1998; Ferrari 1996). The relationships between fluorescence and absorption are site-specific and therefore must be calibrated to the specific survey area. A contouring program can be used to map $a_\phi(\lambda)$, $a_g(\lambda)$, or any other flow-through parameter producing a synoptic snapshot of a given survey area. A deck-mounted flow-through system is not only useful for seagrass management but for any shallow water operation where optical information is desired.

This dissertation is divided into three main parts. Chapter 1: Estimating the photosynthetically available and useable radiation at the seagrass deep edge, focuses on the quantity and quality of light penetrating the bottom of selected Seagrass Management Areas in Tampa Bay to (1) evaluate the appropriateness of the current minimum light targets, (2) examine the relationship between bottom PAR(λ) and PUR(λ) along the seagrass deep edge, (3) use a GIS-based modeling approach to estimated percent subsurface PAR(λ) along the seagrass deep edge and test the hypothesis that the seagrass deep edge is blue-light limited, and (4) propose spectrally relevant minimum light targets for PAR(λ).

Chapter 2: Relative contribution and magnitude of phytoplankton, CDOM, and detritus absorption to the total absorption coefficients in shallow seagrass areas, (1) tests the hypothesis that CDOM is the major absorption component to the total absorption of blue light, (2) challenges the current seagrass management paradigm by comparing the

SMA-specific IOPs with specific environmental variables, (3) establishes SMA-specific predictor equations to model the IOPs based on the quasi-IOPs, and (4) utilizes an empirically-derived spectral attenuation model to relate the IOPs to $K_d(\lambda)$.

Finally, Chapter 3: Synoptic surveillance of the underwater light field using a continuous deck-mounted flow-through system (1) designs a framework for surveying the optical properties of the light field in very shallow seagrass areas, (2) develops SMA-specific correlations between the IOPs and raw flow-through data, and (3) applies this framework to survey the spatial and temporal distribution of CDOM and chlorophyll using the Kitchen SMA as a case study.

Chapter 1. Estimating Photosynthetically Available and Useable Radiation at the Seagrass Deep Edge in Tampa Bay, Florida

1.1. Abstract

Seagrass are among the most productive habitats in the world and are a vital component to maintaining a healthy estuary. To properly manage this resource requires both a solid understanding of light-seagrass relationships and a framework by which to monitor these complex relationships. A major challenge in managing seagrass is setting appropriate minimum light targets, and in Tampa Bay, resource management agencies have adopted a bay-wide minimum light target of 20.5% of photosynthetically available radiation (PAR). This target was based on a single species growing under optimal conditions and may not be appropriate as a bay-wide estimate. PAR is a broadband quantity and does not take into consideration the spectral properties of the light field, nor does it consider the specific absorption characteristics of the seagrass themselves. By multiplying $PAR(\lambda)$ with leaf absorptance ($A_L(\lambda)$), a measure of the photosynthetically useable radiation ($PUR(\lambda)$) can be easily obtained. To address the need for better monitoring tools, a GIS-based modeling approach was used to couple high resolution bathymetry with the light attenuation coefficient to map the percent subsurface $PAR(\lambda)$ reaching the bottom along the seagrass deep edge. Percent subsurface $PAR(\lambda)$ was also calculated using direct measurements at the seagrass deep edge. $PAR(\lambda)$ was grouped into blue, green, and red color bands whose wavelengths were based on the specific absorption characteristics of the seagrass species *Thalassia testudinum* (Banks ex. König) and *Halodule wrightii* (Asch.), both major species found in Tampa Bay. In all cases, the light field was depleted of blue light accounting for as little as 5.3 percent of the total PAR at the bottom. Green light accounted for approximately half the total PAR at bottom while red light accounted for about one third. Based on annual average light attenuation coefficients, seagrass received 31.7 – 38.9 percent of surface PAR and 13.6 – 18.1 percent of surface blue light along the deep edge. In August, during the rainy season, seagrass at the deep edge received as little as 2.51 percent of surface blue light while still receiving 17.5 percent of surface PAR, 19.1 percent of surface green light, and 26.8

percent of surface red light. Under the lowest light conditions measured in this study, seagrass were primarily dependent on red light and, to a lesser extent, on blue-green and yellow light. Bottom PUR(λ) at the deep edge was 13.0 μmol m^{-2} s^{-1} for blue light and 66.0 μmol m^{-2} s^{-1} and 56.3 μmol m^{-2} s^{-1} for red and green light, respectively. The relatively high PUR(λ) for the green wavelengths suggests that when blue light is limited, the accessory pigments chlorophylls *b*, *c*, and the carotenoids, may be most important to maintaining photosynthesis and ultimately plant survival.

1.2. Introduction

Seagrass are important primary producers in estuarine systems around the world and provide critical habitat and food for many commercially and recreationally important fish. Seagrass also play a key role in biogeochemical processes, sediment stability, as well as many other functions (Bortone 2000; Hemminga and Duarte 2000; Thayer et al. 1984). Because of the perceived importance of seagrass to maintaining a healthy estuary, resource management agencies have focused on restoring and protecting seagrass to the greatest extent possible. Light is the primary limiting factor for most seagrass ecosystems. For this reason, most management plans attempt to set minimum light targets along the deep edge typically in terms of the photosynthetically available radiation (PAR).

1.2.1. Minimum light targets in Tampa Bay

While seagrass meadows are highly productive systems, they are vulnerable to light limitation due in part to their high light requirements (Abal et al. 1994; Major and Dunton 2002; Zimmerman 2003). Seagrass depth limits are strongly related not only to the percent of incoming solar radiation reaching the bottom and the rate at which it is attenuated but the light field's spectral quality (Figure 1-1) (Dennison 1987; Duarte 1991; Durako 2007; Nielsen et al. 2002).

In most systems, including Tampa Bay, seagrass are light limited (Janicki Environmental 2001; Kenworthy and Fonseca 1996). For this reason, most management plans attempt to set minimum light targets to maximize seagrass coverage along the deep edge.
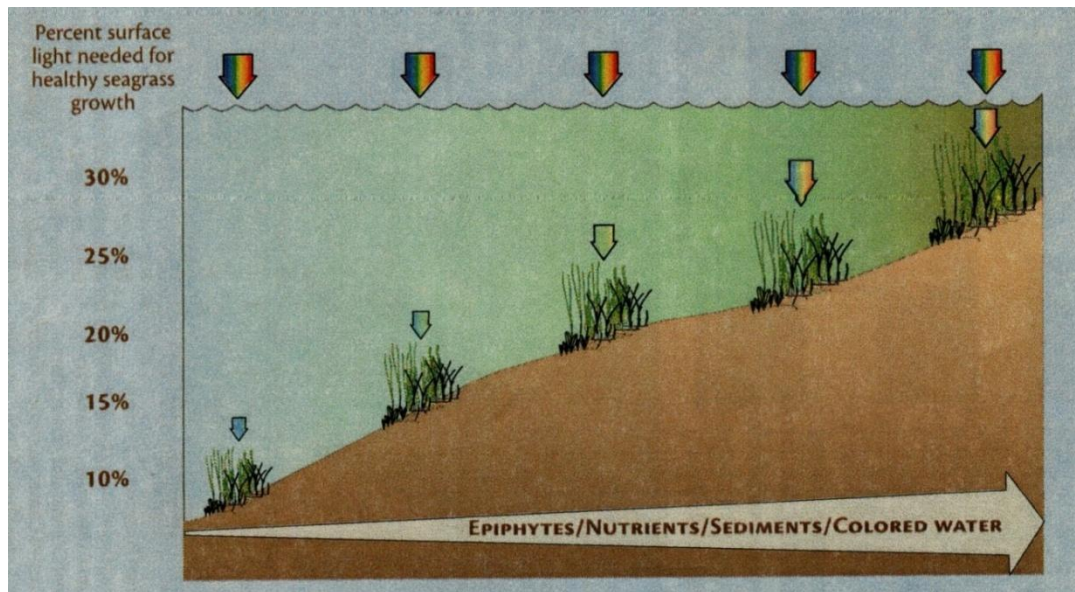
Figure 1-1. Conceptual diagram of light loss with depth. The percent subsurface irradiance is defined as the percent of PAR(λ) or PUR(λ) reaching the bottom relative to just below the water surface. Source: Center for Environmental Science, University of Maryland

Over-development and pollution in Tampa Bay has resulted in a decrease in seagrass coverage by 75% between the years of 1950 and 1985. Since 1985, improvements in wastewater treatment and stormwater management have seen large improvements in water quality resulting in increased light penetration with a corresponding increase in seagrass coverage. Despite these large increases, total seagrass coverage is still below that of the 1950s. The development of a minimum light target for seagrass is a major part of the restoration and management plan for seagrass in Tampa Bay. Though imperfect, it has provided a context by which site suitability can be easily measured.

The Tampa Bay Estuary Program and its partners established a minimum light target for Tampa Bay of 20.5% of the total incoming PAR in units of μmol photons m^{-2} s^{-1} (TBNEP 1996). This target was largely based on work that focused on a single species growing in lower Tampa Bay under optimal conditions

(Dixon and Leverone 1995). The goal of this early work was to determine the annual light regime along the deep edge of a stable *Thalassia testudinum* (Banks ex. König) bed where light limitation was believed to be the limiting factor (Hall et al. 1991). Based on annual water column PAR at the maximum seagrass depth limits for this species, the average percent subsurface light reaching the bottom was determined to be 22.5% (Dixon and Leverone 1995). As Dixon and Leverone (1995) clearly indicate, this value must be used with caution as it is only representative of the light attenuation for the given conditions at those sample locations. The decision to extrapolate the findings of Dixon and Leverone (1995) to include the entire bay and to reduce the established target from 22.5% to its current value of 20.5% was largely a policy decision (H. Greening, personal communication). Other researchers have proposed minimum light targets for other seagrass species including *Halodule wrightii* (Asch.) and *Syringodium filiforme* (Kutz). For example, estimates of between 24% - 37% of subsurface PAR have been proposed for the Indian River Lagoon along the east coast of Florida (Kenworthy and Fonseca 1996). In 2007, the Tampa Bay Estuary Program began an extensive re-evaluation of this light target. This dissertation is a large part of that evaluation.

To apply this minimum light target to the entire bay requires accurate delineation of the seagrass deep edge. Since 1988, the Southwest Florida Water Management District (SWFWMD) has been mapping the spatial extent of seagrass along the west coast of Florida, including Tampa Bay, using aerial photography collected roughly every two years. After the images are georectified and orthorectified, they are analyzed by certified photointerpreters who delineate seagrass polygons and classify them as either patchy (>25% of a polygon is unvegetated) or continuous (<25% is unvegetated) (Kurz 2002). Stringent quality control measures are used to establish the accuracy of identifying each polygon with the correct seagrass classification. A 90% accuracy rate is required for polygons greater than 0.4 hectares in size (Kurz 2002). These maps are the basis for tracking long-term seagrass coverage in Tampa Bay. The 2006 maps are used here to estimate the extent of the mapped seagrass deep edge within the study areas. For the purposes of this study, no distinction is made between the patchy and continuous coverage classifications. It is recognized that seagrass can grow beyond this mapped edge

11

but at densities that are too small to be detected. It is estimated that these grasses represent a very small percentage of the total seagrass area. Therefore, the mapped edge is considered to be the seagrass deep edge for management purposes and is defined as such here.

1.2.2. Wavelength-specific light utilization for photosynthesis

It is important to think of PAR in terms of its flux of quanta as opposed to its energy state because once a quantum has been absorbed by a plant cell, its contribution to photosynthesis is the same regardless of its wavelength-specific energy (Kirk 1994; Mobley 1994). Of course, a given photon must first be absorbed by one of the wavelength-specific photosynthetic pigments. The usefulness of a given light field for photosynthesis is not simply a function of the total intensity of PAR, but how well the spectral distribution of PAR matches the absorption spectrum of a given aquatic macrophyte or phytoplankton (Kirk 1994).

Because PAR, by definition, is a broadband quantity, it does not take into account the spectral variability of light reaching the bottom. Spectral PAR (PAR(λ)) provides much more information on the shape of the incoming light field than simply measuring PAR. However, neither PAR nor PAR(λ) provide any indication that the photons available are actually being absorbed. Since seagrass are considered the "end users" of the incoming light field, it is important to express light quality in terms of the specific absorption characteristics of the light harvesting pigments found in seagrass. Like all higher plants, seagrass are reliant mostly on light within the blue and red color bands, though the presence of accessory pigments can increase the operational window beyond the blue and red wavelengths (Figure 1-2).
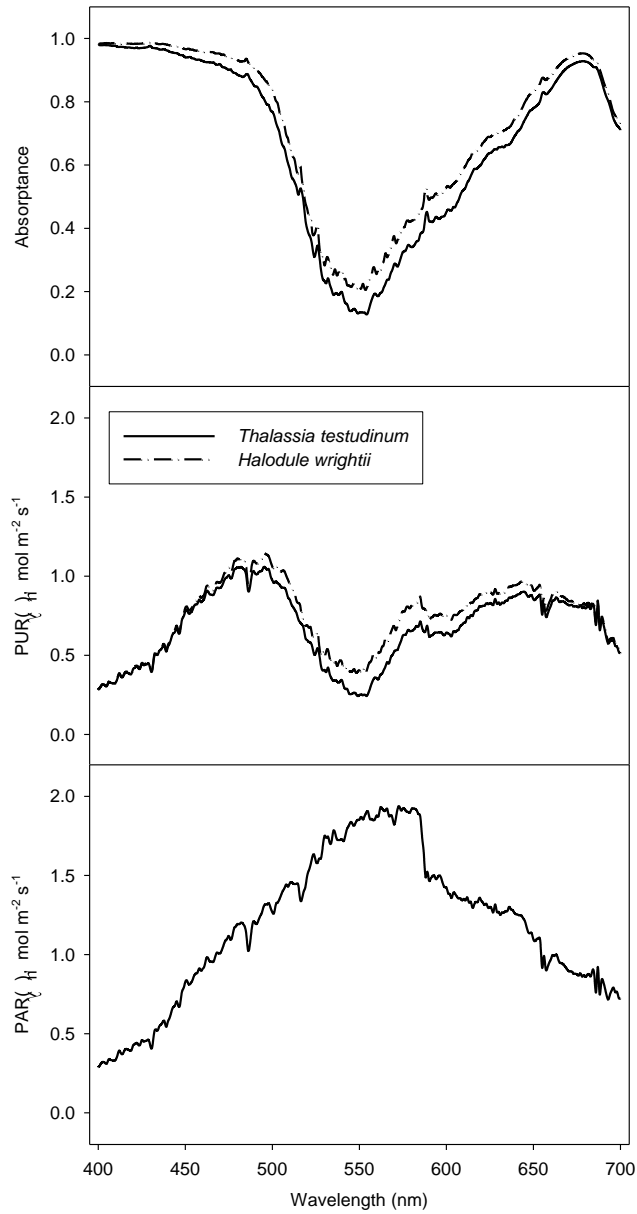
Figure 1-2. Absorptance spectra and PUR(λ) for two species of seagrass *Thalassia testudinum* (Banks ex. König) and *Halodule wrightii* (Asch.), and bottom PAR(λ) measured in Tampa Bay. PUR(λ) is the product of the leaf absorptance and PAR(λ).

Light-harvesting pigments associated with photosynthesis include the chlorophylls *a*, *b*, and *c*, and the carotenoids (Kirk 1994). The chlorophylls are the primary pigments for light harvesting but the presence of carotenoids expands the absorbing capabilities into the near-UV and blue-green wavelengths (Kirk 1994). Of the chlorophylls, chlorophyll *a* is the primary light absorbing pigment, with a primary absorption peak centered near 440nm and a secondary peak near 660nm (Figure 1-2). Seagrass do not posses antennae pigments capable of efficient harvesting of green light (Cummings and Zimmerman 2003) unlike some species of red and blue-green algae that contain green-light harvesting billiproteins (Kirk 1994). Green light should not be thought of as being useless to seagrass, however some of the carotenoids can extend the absorption range of seagrass well into the blue-green region up to about 560nm (Kirk 1994).

Photosynthetically useable radiation (PUR) is a spectrally integrated quantity, defined as the fraction of the radiant energy that can be absorbed by a given plant, in this case seagrass (Morel 1978; Morel 1991). Both PAR and PUR can be expressed in terms of their spectral quantities and are given the symbols PAR(λ) and PUR(λ), respectively. PUR(λ) is calculated by multiplying PAR(λ) by some dimensionless quantity that is proportional to the leaf absorption per wavelength (Kirk 1994). This dimensionless quantity is commonly defined by phytoplankton researchers as the ratio of the phytoplankton absorption coefficient to the maximum absorption coefficient, typically at 440nm (Morel 1978; Morel 1991). Typically, seagrass researchers express this dimensionless quantity in terms of the leaf absorptance (A_L).

While pigment concentrations can vary significantly both within and among various seagrass species, leaf optical characteristics are quite similar because of the strong package effect, partially due to the chloroplasts being limited to the leaf epidermis (Cummings and Zimmerman 2003; Durako 2007; Enriquez 2005). A comparison of the relative absorption curves of *Thalassia testudinum* (Banks ex. König) and *Halodoule writtii* (Asch.) reveals very little difference in the peak absorption wavelengths (Figure 1-2). This does not mean that the absorption efficiencies are the same. Seagrass photoacclimate to changing irradiance levels by varying leaf pigment concentrations

14

(Abal et al. 1994; Cummings and Zimmerman 2003; Dennison and Alberte 1982; Zimmerman 2003). As a result, chlorophyll content can vary significantly among different species and habitats in response to low-light conditions (Cummings and Zimmerman 2003; Dennison and Alberte 1982; Herzka and Dunton 1997). This acclimation strategy has been found to be largely inefficient due in part to the strong package effect caused by the structural configuration of the leaf tissue restricting the chloroplasts to the epidermal layer (Cummings and Zimmerman 2003).

For resource managers, it is far too complicated to address light quality on a per nanometer basis. It is more practical both operationally and conceptually to combine wavelengths into broad color bands based on the absorption characteristics of the seagrass (Figure 1-2). In this study, three color regions or bands are defined (Table 1-1).

Table 1-1. Selected wavelength ranges of the color bands blue, green, and red and the pigments that are represented by each. Only the red algae, blue-green algae, and the cryptophytes contain billiproteins that allow them to harvest green light.

	Blue	Green	Red
Wavelength Range	400nm-490nm	490nm-600nm	640nm-690nm
Pigments	Chlorophyll/Carotenoid Protein Complex	Billiproteins	Chlorophylls
Found in Seagrass	Yes	No	Yes

These regions correspond to the absorption peaks associated with the chlorophylls and the carotenoids. There is an inherent danger of over simplifying what is a very complex process by simply binning wavelengths and this issue is examined in some detail by comparing these bulk color bands with measurements of PUR(λ).

1.2.3. Measuring transparency in shallow waters

Historically, light measurements have been rather crude. One of the oldest techniques and still a very common method is to use a Secchi disk. This approach has

several limitations when applied to seagrass management, the most common of which is that often in very shallow waters, Secchi depth is greater than bottom depth. In other words, if one sees the bottom, Secchi disk cannot be used and in most cases, when dealing with seagrass, the bottom is visible. A more quantitative approach commonly employed is to use an irradiance or quanta meter that measures the quantity of light as PAR. Because PAR is a single number, it gives no indication of the spectral quality of the light field. Further, it gives no indication of the amount of light that is useable by seagrass.

Limitations in the current methods for measuring water clarity and estimating the attenuation coefficient have necessitated the development of an alternative approach to measuring light. Of primary significance is this lack of spectral information. While PAR is a good bulk estimator of the subsurface light field, isolating specific PUR wavelengths allows a much more surgical approach to establishing relevant seagrass targets. Advances in technology have made it relatively easy to acquire spectral data in very shallow waters. Presented here is a framework for determining not only the quantity of light reaching the bottom but also the spectral shape of the underwater light field. With this information a light attenuation coefficient is calculated and the percent subsurface light reaching the bottom is determined.

A potential source of error in setting light and depth targets is that most light data have been and continue to be collected in deeper waters well beyond seagrass depth limits. The current method widely used for measuring PAR requires a minimum depth of 1.5m. The use of a Secchi disk is an alternative method commonly used in Tampa Bay for estimating water clarity but it is of no use in seagrass beds where Secchi depths are typically greater than the bottom. The method presented here allows for detailed measurements of spectral downwelling irradiance in water depths of less than 0.5m. This method also employs a simple tool to determining percent subsurface irradiance at depth at any wavelength or range of wavelengths of interest.

1.3. Materials and Methods

1.3.1. The Seagrass Management Area concept

As part of the Tampa Bay Estuary Program's seagrass management plan re-evaluation, Tampa Bay was subdivided into 30 individual Seagrass Management Areas (SMA) (Figure 1-3) (EPCHC 2007). For this study, four SMAs were selected based on *a priori* knowledge of the optical properties and historical seagrass coverage. Within each SMA two fixed stations were established from which all *in-water* irradiance measurements were collected. For each SMA, except for Egmont Key, a nearshore and an offshore station were established (Table 1-2).

Table 1-2. Fixed stations for each SMA where in-water irradiance measurements were collected. Meter marks correspond to the approximate distance from the shoreline. The seagrass *Halodule wrightii* disappeared from the offshore Wolf Branch and Kitchen sites mid-way through the study. Depth is relative to MSL.

SMA	Strata	Meter Mark	Depth (m)	Seagrass Species
Coffeepot Bayou	near shore	100	0.92	*Thalassia testudinum, Halodule wrightii*
	offshore	900	1.18	*Thalassia testudinum*
Wolf Branch	near shore	300	0.85	*Thalassia testudinum, Halodule wrightii*
	offshore	1100	1.50	*Halodule wrightii* (disappeared)
Kitchen	near shore	600	0.88	*Halodule wrightii*
	offshore	1300	1.16	*Halodule wrightii* (disappeared)
Egmont Key	near shore	100	1.59	*Thalassia testudinum*

The nearshore sites were located within relatively healthy seagrass beds where light limitation was assumed not to be a factor. Originally the offshore sites were to be located at the deepest extent of seagrass growth, where light limitation was likely to be the primary limiting factor. In the Kitchen and Wolf Branch offshore areas, seagrass coverage was extremely sparse during the beginning of the study and had disappeared completely by the end of the study period. Because these SMAs were so shallow, the nearshore sites were actually located along the deep edge of the persistent seagrass bed.
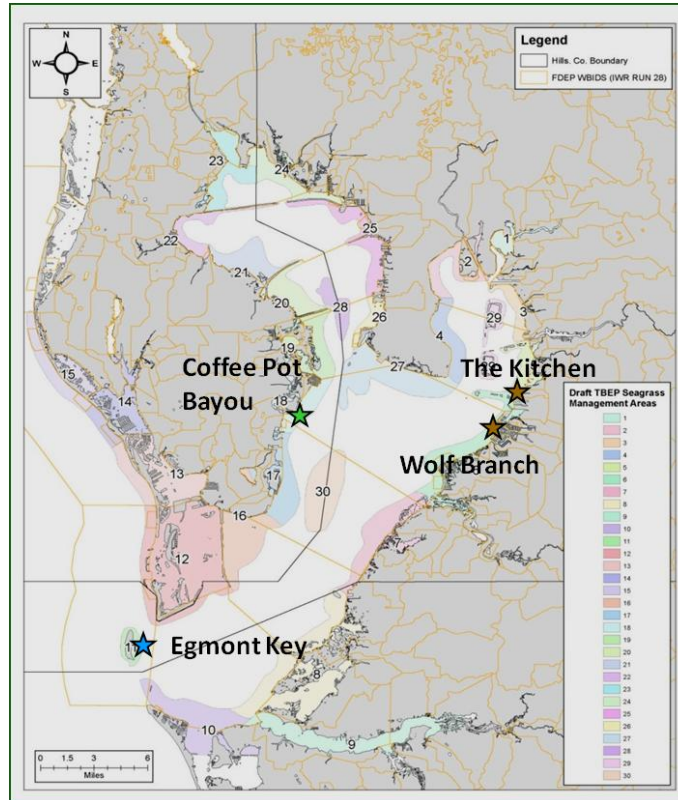
Figure 1-3. Seagrass Management Areas of Tampa Bay.

The Kitchen (SMA 5) is located in eastern Tampa Bay (Figure 1-3) and has an area of approximately 776ha. There have been significant increases in seagrass coverage over the past two decades from approximately 40ha in 1996 to over 142ha in 2007 (HCEPC 2007). The area can be thought of as being hydraulically isolated with the Alafia Banks to the north, spoil islands 2D and 2E to the west, Port Sutton berths to the south, and the shoreline to the east boxing in the area (Figure 1-4). The shoreline is mostly mangrove with some salt marsh. The only direct freshwater inflow is from Bullfrog Creek, a 3km long tidal creek that drains mostly agriculture and some urban development. Additonal freshwater inflow can come from the Alafia River just to the north. The nearshore and an offshore site were located approximately 600m and 1300m from the shoreline (Figure 1-4). The offshore site had very sparse *Halodule wrightii* (Asch.) at the beginning of the study, but by October, what little grass there was had completely disappeared. Given the extremely shallow nature of this SMA, the nearshore

site actually represents the deep edge of the persistent seagrass bed. Presumably, light conditions at this nearshore site are representative of the minimum light conditions necessary for seagrass persistence.
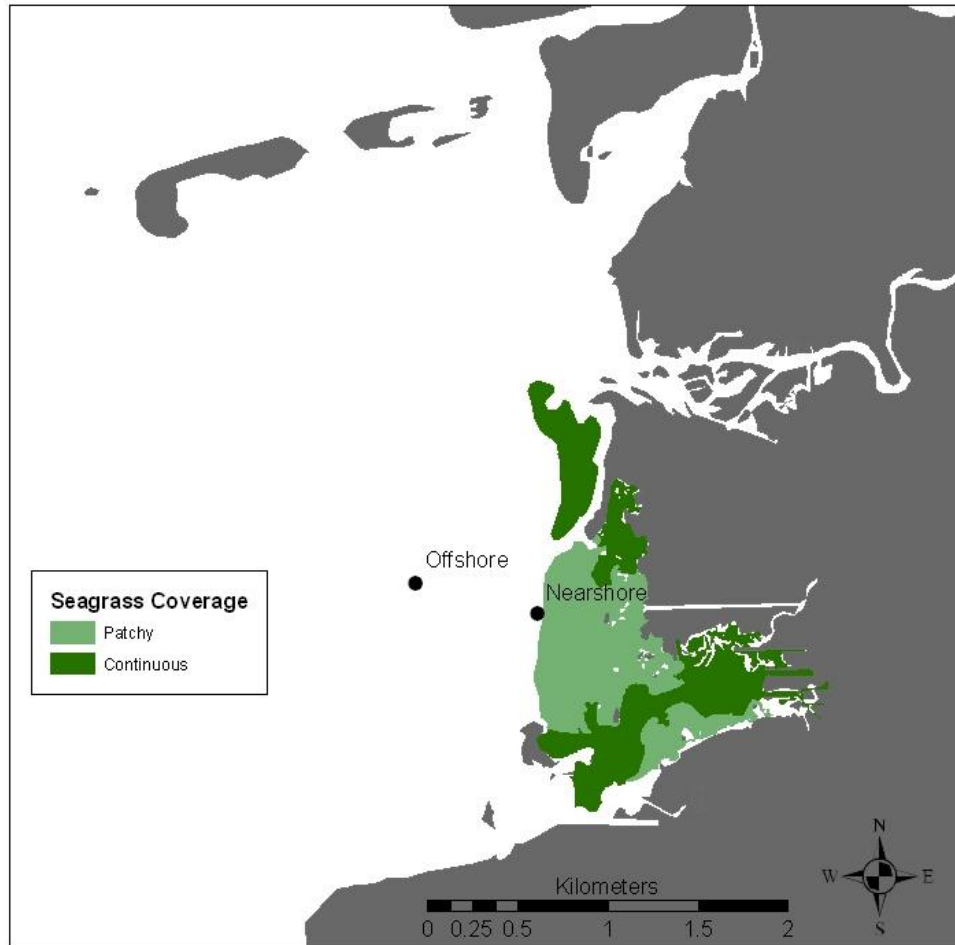
Figure 1-4. Map showing the spatial extent of seagrass coverage in the Kitchen SMA. Coverage is based on 2006 aerial photography.

      Wolf Branch (SMA 6) is located along the eastern shore of Middle Tampa Bay and is immediately to the south of the Kitchen (Figure 1-3). Wolf Branch is approximately 1554ha, roughly double the size of the Kitchen (Figure 1-3). Unlike the Kitchen, seagrass in Wolf Branch have been on a continual decline over the past twenty years, from 283ha in 1996 to 162ha in 2006 (HCEPC 2007). Both Wolf Branch and Kitchen are very rich in colored dissolved organic matter (CDOM) and routinely have

among the highest chlorophyll concentrations of any SMA. The shoreline is dominated by mangroves and some salt marsh communities but no major creeks or rivers, though several small tidal tributaries are located along the complex mangrove shoreline. Within this expanse of mangroves are numerous mosquito ditches dug in the 1960s for mosquito and flood control. These ditches provide a direct conduit for surface runoff and may also be a significant conveyance for CDOM-rich water. A nearshore and an offshore site were established approximately 300m and 1100m from the shoreline (Figure 1-5). Like the Kitchen, the offshore location at Wolf Branch contained very sparse *Halodule wrightii* (Asch.). at the beginning of the study and disappeared by mid-study. Also like the Kitchen, the nearshore site is located near the deep edge of the persistent seagrass bed at 0.85m MSL.

Figure 1-5. Map showing the spatial extent of seagrass coverage in the Wolf Branch SMA. Coverage is based on 2006 aerial photography.

Coffeepot Bayou (SMA 18) is located along the western shore of Middle Tampa Bay and is approximately the same size as Wolf Branch. Seagrass beds within the Coffeepot Bayou SMA have declined over the twenty years going from 243ha in 1997 to 162a in 2007 (HCEPC 2007). Coffeepot Bayou receives large amounts of storm-water from the adjacent urban watershed often resulting in high chlorophyll concentrations greater than 30μg L^{-1} during the rainy season, from July through September. Because the bayou drains an urban watershed with little to no vegetation and because the seawall shoreline has no salt marsh or mangrove vegetation, Coffeepot Bayou is not thought to be a CDOM-rich environment but rather more chlorophyll dominated. A nearshore and an offshore site were located with the nearshore site located approximately 100m from the shoreline and the offshore site 900m from the shoreline (Figure 1-6). The nearshore site at Coffeepot Bayou was well inshore of the seagrass deep edge and it was assumed that seagrass growing here were not light limited. The offshore site was located near the deep edge of the persistent seagrass bed at a depth of 0.90m MSL.
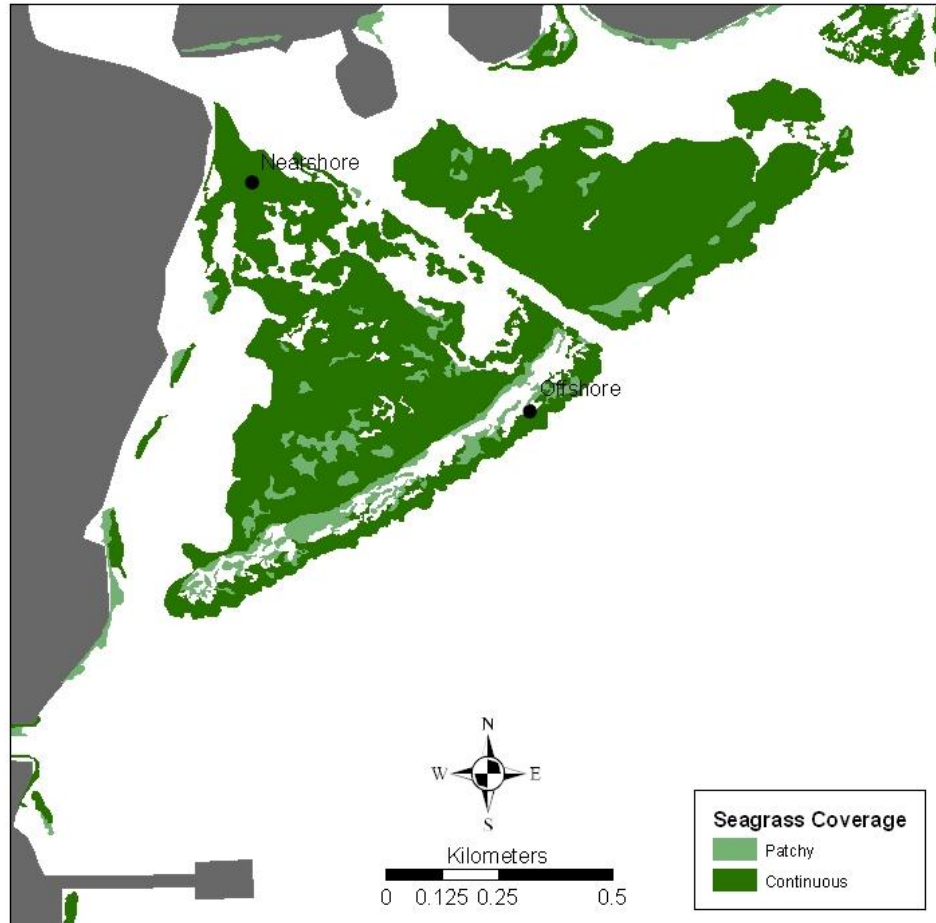
Figure 1-6. Map showing the spatial extent of seagrass coverage in the Coffeepot Bayou SMA. Coverage is based on 2006 aerial photography.

Egmont Key (SMA 11) is nearest to the Gulf of Mexico and is adjacent to a small 162ha island that is both a State Park and a National Wildlife Refuge. Given the unique conditions that exist here, it was assumed that the light conditions would be markedly different from the other three SMAs. This is the smallest of the four SMAs included in this study and covers an area of approximately 518ha. Though small in area, seagrass here are quite healthy growing deeper than in most other areas in Tampa Bay. Over the past twenty years, seagrass coverage has increased from 24ha in 1996 to 40ha in 2006 (HCEPC 1997). Seagrass here only extend to about 200m offshore, beyond which depths

become too great to support seagrass. Given the small aerial extent of the seagrass beds here, only one station was established approximately 100m offshore at a depth of 1.6m MSL (Figure 1-7).
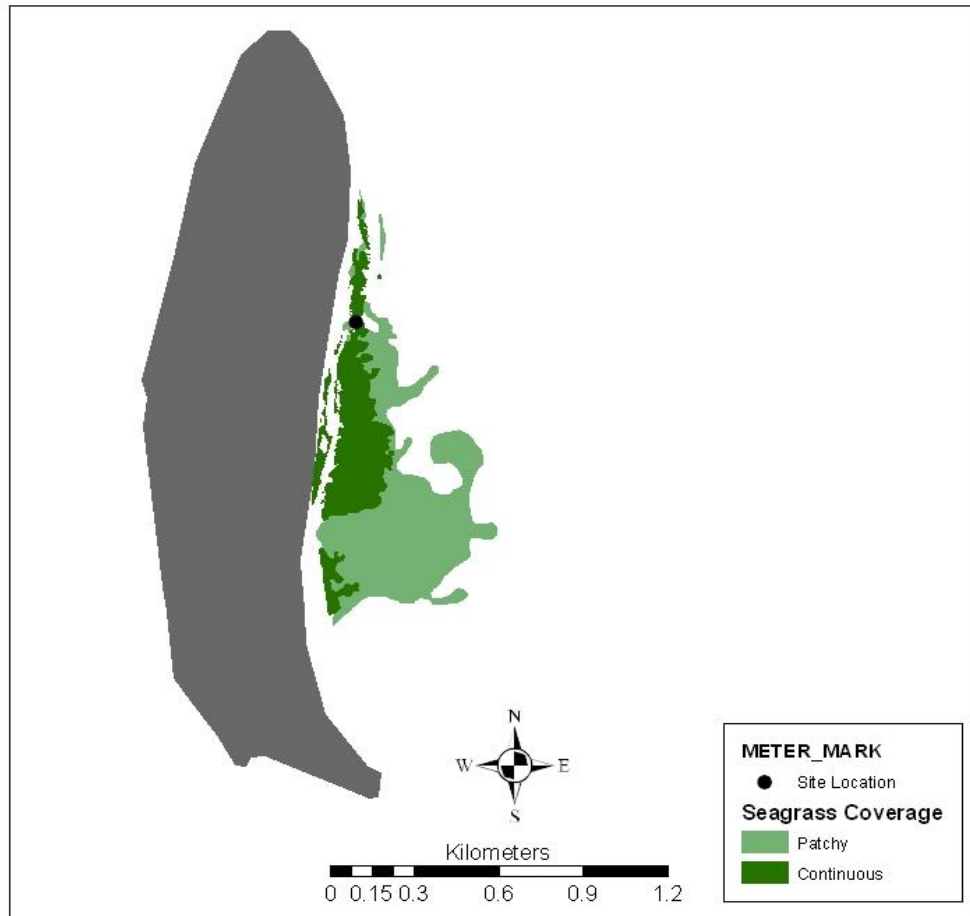
Figure 1-7. Map showing the spatial extent of seagrass coverage in the Coffeepot Bayou SMA. Coverage is based on 2006 aerial photography.

1.3.2. Measuring $E_d(\lambda)$, PAR(λ), and PAR

A planar irradiance cosine collector (Hobi Labs, Inc., Bellevue, WA) was mounted onto a PVC measuring rod. The cosine collector was then connected via a fiber optic cable to a portable spectrometer (HR2000, Ocean Optics, Dunedin, FL). A field laptop PC (Panasonic Toughbook, Panasonic Corporation, New York, NY), running the Ocean Optics program OOI Base32, provided the spectrometer's command and control.

All data were stored on the PC. A planar irradiance cosine collector was chosen over a spherical sensor to remove any inherent bias caused by bottom reflectance. This makes it easier to compare different sites and provides a conservative estimate of $E_d(\lambda)$.

Once onsite, the boat was anchored using a hydraulic anchor pole instead of a traditional anchor to minimize sediment disturbance. Every effort was made to measure $E_d(\lambda)$ under uniform sky conditions, always on the sunny side of the boat, and as far away as possible from the boat's reflection. The measuring rod was kept perpendicular to the water surface to within $\pm 5^o$ of nadir. For each discrete depth, three consecutive scans were taken one second apart and averaged to create a composite scan. Multiple scans were taken to account for any variation caused by waves and movement of the sensor off nadir. Initial measurements were taken in the air just above the water surface followed by a surface reading approximately 0.01m below the water surface. Following the surface reading, scans were taken at 0.25m intervals. The maximum scan depth was 1.75m because of limitations in the fiber optic cable length. In reality, depths were never more than 1.50m so this limitation was not an issue. Because $E_d(\lambda)$ is an apparent optical property, it is dependent on time of day, sun angle, sky conditions, and sea state. These factors are often overlooked in most monitoring programs and over long time periods become less significant. In order to mimic the type of data that would be collected during routine monitoring runs, only time of day was considered and an operational window between 1000 and 1400 standard time was set. Some bias toward an incoming or slack high tide was unavoidable given the extremely shallow depths in certain areas.

At each discrete depth, the three scans were averaged and then converted, first, from raw digital counts to $E_d(\lambda)$ in units of W m^{-2} nm^{-1}, and then, from $E_d(\lambda)$ to PAR(λ) in units of photon flux (μmol m^{-2} s^{-1}). A typical depth profile of PAR(λ) is shown in Figure 1-8.
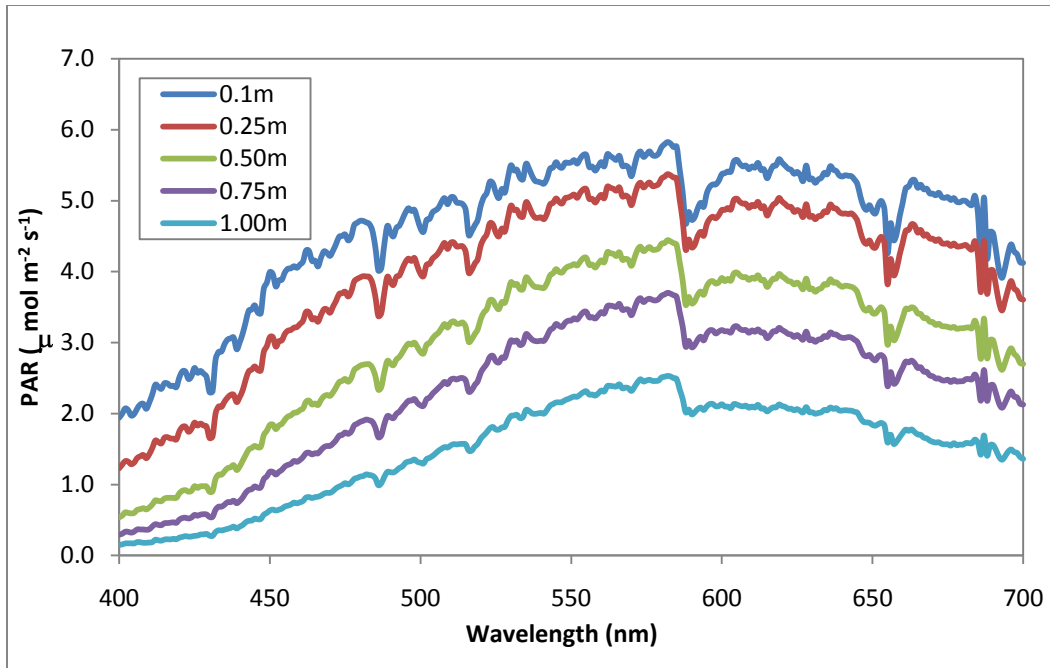
Figure 1-8. Spectral scans of PAR(λ) with depth collected in August 2008 at Wolf Branch in eastern Tampa Bay.

The depressions located throughout the curve are called Fraunhofer lines and are caused by the absorption of light by the cooler gases in the sun's outer atmosphere at frequencies corresponding to the atomic transition frequencies of these gases.

To obtain PAR, PAR(λ) was grouped to the nearest nanometer using a linear interpolation procedure in MATLAB (The MathWorks, Inc., Natick, MA). PAR was then calculated by integrating across the visible spectrum (400nm-700nm) using a trapezoidal integration routine in MATLAB (Kirk 1994; Mobley 1994):

$$PAR(z) = \int_{400nm}^{700nm} \frac{\lambda}{hc} \text{PAR}(z, \lambda) \, d\lambda \qquad \text{Eq. 1.1}$$

where λ is the wavelength (nm), h is Planck's constant and c is the speed of light.

The loss of PAR(λ) with depth for a given wavelength can be described by the diffuse light attenuation coefficient ($K_d(\lambda)$):

$$K_d(\lambda) = \frac{d\ln PAR(\lambda)}{dz} = -\frac{1}{PAR(\lambda)}\frac{dPAR(\lambda)}{dz}$$
<div align="right">Eq. 1.2</div>

Because $K_d(\lambda)$ is not constant with depth, it is more accurate to use the average $K_d(\lambda)$ over a depth interval from 0 to z (Kirk 2003):

$$\overline{K}_d(z;\lambda) \equiv \frac{1}{z}\int_0^z K_d(z';\lambda)dz'$$
<div align="right">Eq. 1.3</div>

The symbology, $K_d(\lambda)$, is used here to indicate the average attenuation coefficient across the depth interval 0 to z. A more accurate measure of $K_d(\lambda)$ is to take the slope of a linear regression line fitted to a plot of the natural logarithm of $PAR(\lambda)$ with respect to depth (Kirk 1994). $K_d(PAR)$ is simply the slope of the natural log of PAR with respect to depth. The same procedure can be used to determine the $K_d(\lambda)$ for $PUR(\lambda)$ instead of $PAR(\lambda)$.

The light attenuation coefficient varies with wavelength (Figure 1-9) and therefore must only be compared to attenuation coefficients of the same wavelengths. The wavelength specific nature of $K_d(\lambda)$ can be attributed to the concentration and composition of the constituent absorption and scatter.
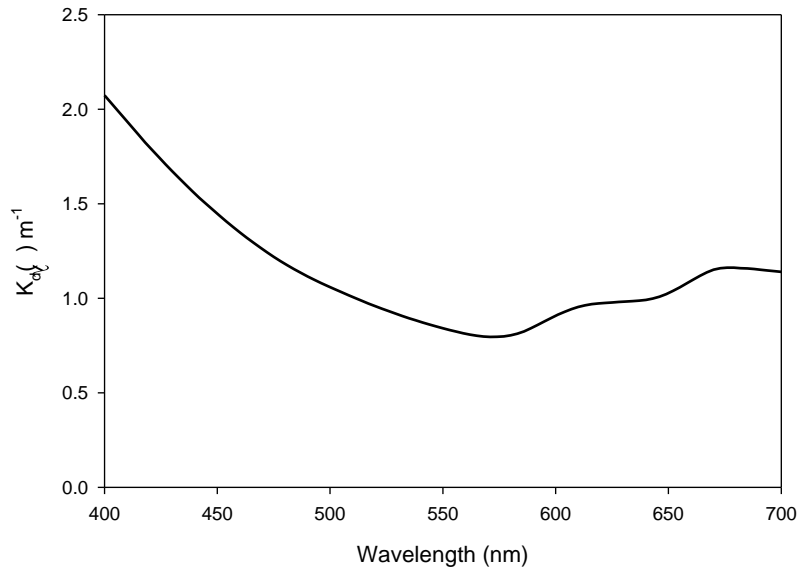
Figure 1-9. The light attenuation coefficient as a function of wavelength. Data from the Wolf Branch Seagrass Management Area collected in October 2008.

1.3.3. Estimating the percent subsurface PAR(λ) and PUR(λ)

        Using $K_d(\lambda)$ calculated from measured PAR(λ) and PUR(λ) at selected locations, the percent subsurface irradiance, expressed in terms of either PAR(λ) or PUR(λ), can be determined at any depth (*d*) for any given $K_d(\lambda)$. For seagrass management purposes, determining the percent subsurface irradiance at the bottom, along the seagrass deep edge, will ultimately determine minimum light targets. Total depth is defined as the total depth of the water column at mean sea level (MSL). This was chosen because it represents the average condition at a given location. The fraction of surface irradiance is calculated as:

$$PAR(\lambda) = \left[\frac{\left(e^{-(K_d(\lambda)z)}\right)}{e}\right] \qquad \text{Eq. 1.4}$$

where z is the total depth in meters at MSL. Multiplying Eq. 1.4 by 100 gives the percent subsurface PAR(λ). The percent PAR(λ) for the blue, green, and red color bands is determined by using the $K_d(\lambda)$ integrated across the wavelength range for each color band. For calculating percent subsurface PAR, the $K_d(\lambda)$ integrated across the visible spectrum (400nm-700nm) is used.

        PUR(λ) is calculated by multiplying the PAR(λ) by the single leaf specific absorptance ($A_L(\lambda)$). Single leaf absorptance for a given species is expressed as $1 - Tr(\lambda)$, where $Tr(\lambda)$ is the transmittance across a single seagrass leaf and represents the ratio of the amount of light that passes through the seagrass leaf to the amount of light incident on the leaf surface. A PUR(λ) is calculated for each wavelength and binned to the nearest nanometer using the same MATLAB linear interpolation procedure as was used for calculating PAR(λ). To calculate the PUR(λ) for each of the three color regions, PUR(λ) was summed across the wavelengths corresponding to the blue, green, and red color bands (Table 1-1). PUR was calculated by summation across the visible spectrum.

        To determine $A_L(\lambda)$, healthy *Thalassia testudinum* (Banks ex. König) and *Halodule wrightii* (Asch.) leaves were harvested from Coffeepot Bayou and scanned onsite using an Ocean Optics DR2000 field spectrometer (Ocean Optics, Inc., Dunedin,

FL) and a fiber optic cable connected to a black mounting bracket. All scans were taken near solar noon. Before leaves were scanned, they were carefully wiped clean of any epiphytes or other particulate matter. Leaves were then placed across the mounting bracket and the bitter end of the fiber optic cable was adjusted until making contact with the leaf surface. The apparatus was positioned to face the sun and the spectrometer integration time was adjusted to avoid saturation of the signal. Scans were collected using the same methodology for measuring $E_d(\lambda)$. Immediately after scanning the leaf, a scan of the incoming solar radiation was collected. This procedure was repeated four times for each species using different leaves each time. Results were compared to literature values to ensure consistency with other researchers (Cummings and Zimmerman 2003; Durako 2007; Zimmerman 2003).

1.3.4. Mapping percent subsurface irradiance

A major limitation in understanding the seagrass light-depth relationship is accurate bathymetric data. Airborne laser bathymetry, also known as Light Detection and Ranging (LIDAR), can help overcome this limitation. LIDAR is a technique for measuring shallow waters using a pulsed laser beam from an airborne platform. This technology has been in use since the mid-1960s (Hickman and Hogg 1969). At that time, laser technology was brand new and used primarily for anti-submarine warfare by the U.S. Navy. Today airborne LIDAR is routinely used for hydrographic surveys and has evolved into an accurate operational technique.

In 2007, selected areas of Tampa Bay were mapped using NASA's Experimental Advanced Airborne Research LIDAR (EAARL) (Figure 1-10).
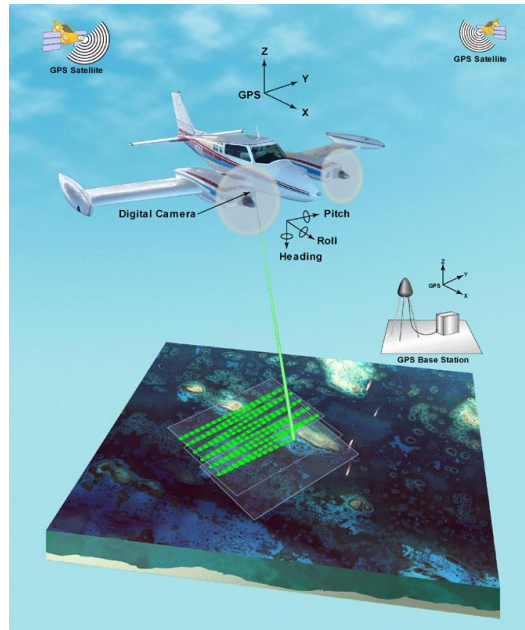
Figure 1-10. Concept of operations of the NASA Experimental Advanced Airborne Research LIDAR (EAARL) (Image source http://ngom.usgs.gov).

The EAARL system has a maximum measureable water depth of 26m and is determined by the strength of the bottom return signal and water clarity (Brock et al. 2002; Guenther et al. 2000). The minimum operating depth is 30cm and has a nominal depth accuracy of 4.0cm ± 1.0 (Brock et al. 2002). In Tampa Bay, the average maximum measureable water depth was approximately 2.6m MSL (Tyler et al. 2007). In depths greater than 0.5m, LIDAR data were cross checked with depth data collected using a ship-borne acoustic system called the System for Accurate Nearshore Depth Surveys (SANDS) (Hansen et al. 2005). The Kitchen, Wolf Branch, and Coffeepot Bayou SMAs were mapped using this technique.

Bathymetry for the Kitchen SMA is very shallow with most of the area less than 0.5m MSL (Figure 1-11). Depth penetration is a function of the optical properties of the water column and the bottom sediment composition (Brock et al. 2002; Guenther et al. 2000). The deep area toward the center of the image is the original Alafia River channel while the deep shaded areas toward the bottom of the SMA are old dredge holes.
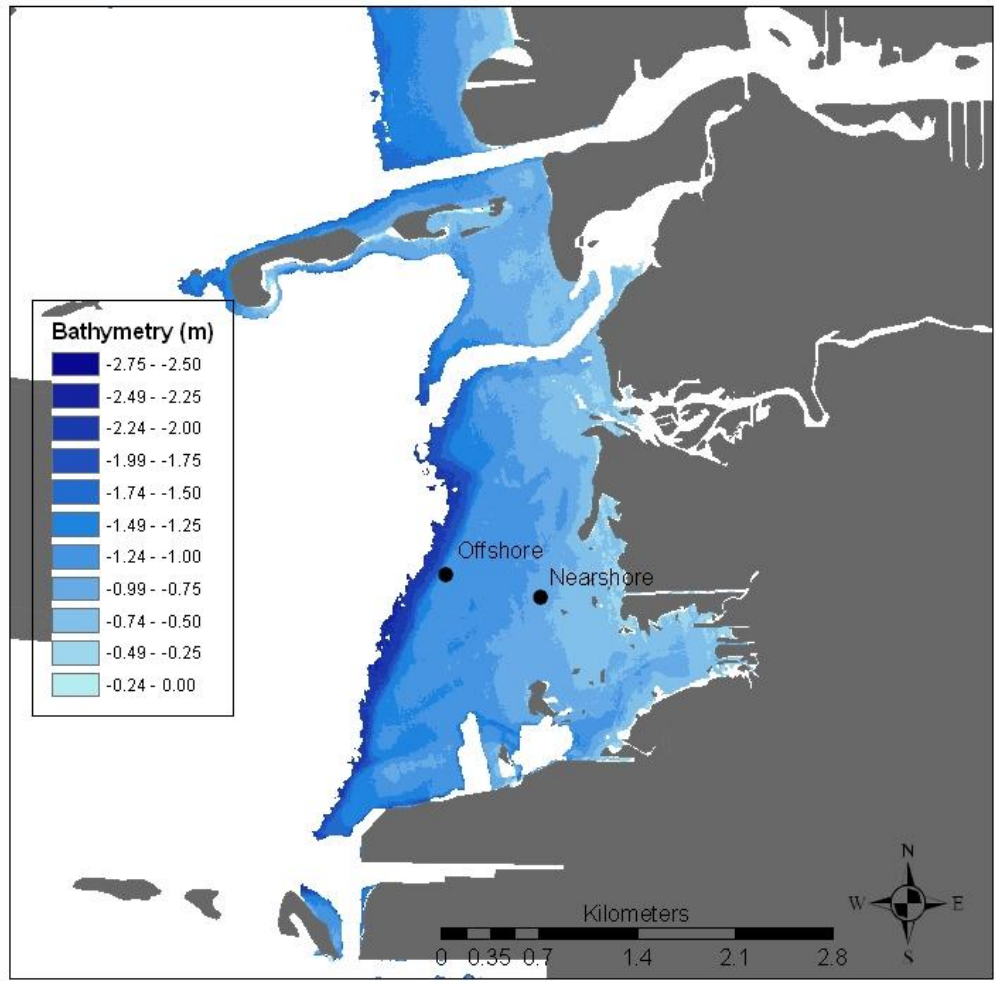
Figure 1-11. Bathymetry of the Kitchen Seagrass Management Area.
Bathymetry was collected in 2007 using NASA's Experimental Advanced Airborne
LIDAR system. Unshaded areas exceed the maximum measureable depth of 2.75m.

The Wolf Branch SMA sits on a relatively flat shelf with a gradual slope terminating approximately 1500m from the shoreline (Figure 1-12).
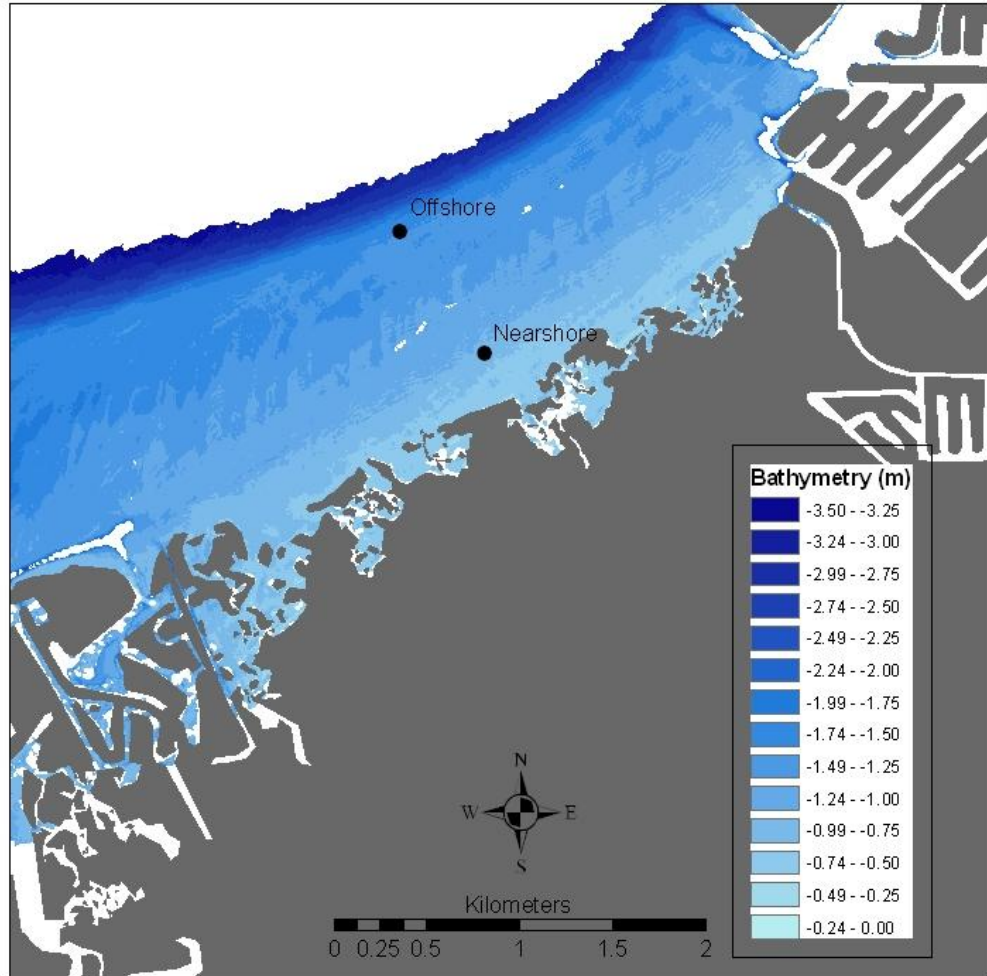
Figure 1-12. Bathymetry of the Wolf Branch Seagrass Management Area. Bathymetry was collected in 2007 using NASA's Experimental Advanced Airborne LIDAR system. Unshaded areas exceed the maximum measureable depth of 3.50m.

The Coffeepot Bayou SMA is characterized by a large shelf with a relatively sharp break approximately 1000m offshore (Figure 1-13). The large unshaded areas to the southwest and northeast are dredged areas greater than 4.00m. All of the areas that exceed the maximum measurable depth also exceed the maximum seagrass depth limit.

31
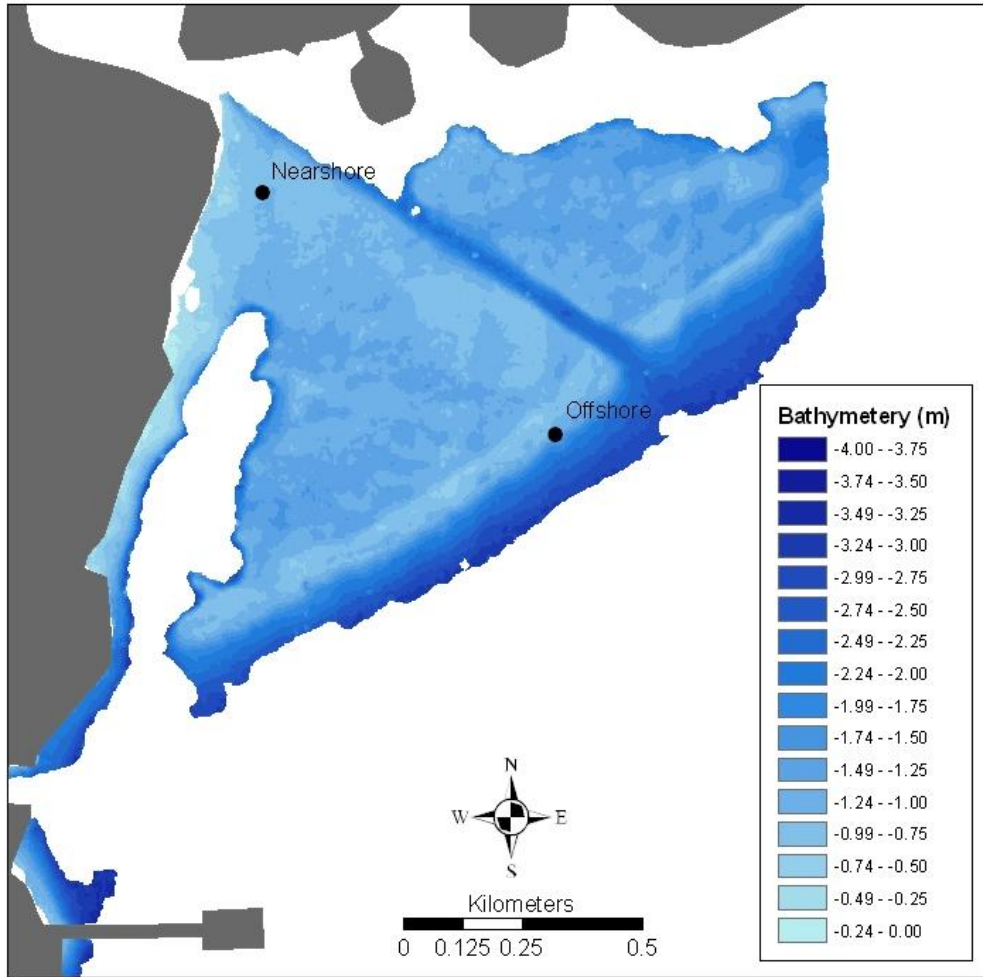
Figure 1-13. Bathymetry of the Coffeepot Bayou Seagrass Management Area. Bathymetry was collected in 2007 using NASA's Experimental Advanced Airborne LIDAR system. Unshaded areas exceed the maximum measureable depth of 4.00.

To calculate the percent PAR(λ) for any location, only the total depth and $K_d(\lambda)$ are necessary. For the Kitchen, Wolf Branch, and Coffeepot Bayou SMAs, a GIS-based modeling approach was employed to merge the LIDAR bathymetry with site-specific $K_d(\lambda)$ and using Eq. 1.4 to calculate the percent PAR(λ) for each cell in the bathymetric grid. It was assumed that the $K_d(\lambda)$ was the same throughout a given Seagrass Management Area. This simplification was necessary to run the GIS model with the caveat that spatial differences in $K_d(\lambda)$ do exist but that this method is a good first cut in

the absence of high resolution attenuation information. In all cases the $K_d(\lambda)$ used for a given Seagrass Management Area was the average annual $K_d(\lambda)$ for both the nearshore and offshore sites.

1.4. Results and Discussion

1.4.1. $K_d(\lambda)$ and PAR(λ) relationships across SMAs

For Coffeepot Bayou, the annual average $K_d(\lambda)$ for blue light (K_d(blue)) was greater at the seagrass deep edge, than at the nearshore site, though not statistically significant (ANOVA; $p > 0.10$) (Table 1-3). This may be a function of differences in residence time and flushing rates in this SMA. The proximity of the nearshore station to relatively deep channels may increase the amount of water flow past this station. While the offshore site sits on the end of a large bar covered with seagrass which may act to impede water flow and increase residence times.

Table 1-3. Annual average light attenuation coefficient for nearshore and offshore stations for the blue color band (400nm-490nm). Stations depths are in parentheses and are relative to MSL.

	K_d(blue) μmol m^{-2} s^{-1}	Standard Deviation	Maximum	Minimum
Coffeepot Bayou				
Nearshore (0.924m)	1.37	0.477	2.13 (Jun)	0.959 (Apr)
Offshore (1.18m)	1.65	0.526	2.34 (Aug)	0.814 (Apr)
Kitchen				
Nearshore (0.880m)	2.42	0.833	3.47 (Dec)	1.53 (Jun)
Offshore (1.16m)	1.63	0.322	2.15 (Aug)	1.34 (Apr)
Wolf Branch				
Nearshore (0.852m)	2.07	1.16	4.33 (Aug)	1.19 (Jun)
Offshore (1.50m)	1.40	0.404	2.04 (Apr)	0.846 (Jun)
Egmont Key				
Nearshore (1.60m)	0.917	0.200	1.28 (Aug)	0.708 (Dec)

The reverse pattern was observed in the Kitchen and Wolf Branch SMAs where K_d(blue) was significantly higher (ANOVA; $p > 0.05$) at the nearshore sites relative to the offshore sites (Table 1-3), and was most likely a function of shoreline morphology. The relatively natural shorelines of both Kitchen and Wolf Branch are heavily vegetated with mostly mangroves and some salt marsh. The increased attenuation at the nearshore sites is likely a result of increased loads of dissolved and particulate organic material from shore. For the Kitchen, there is also direct discharge of organic-rich waters from Bullfrog Creek and indirect discharge from the Alafia River just to the north. K_d(blue) was lowest at Egmont Key where direct mixing with Gulf of Mexico waters helps to buffer water originating from the upper parts of Tampa Bay.

Graphically, it is easy to see that light loss with depth occurs at different rates for the different color bands and for PAR (Figure 1-14). Blue light attenuated much more rapidly than either green or red light in all cases.
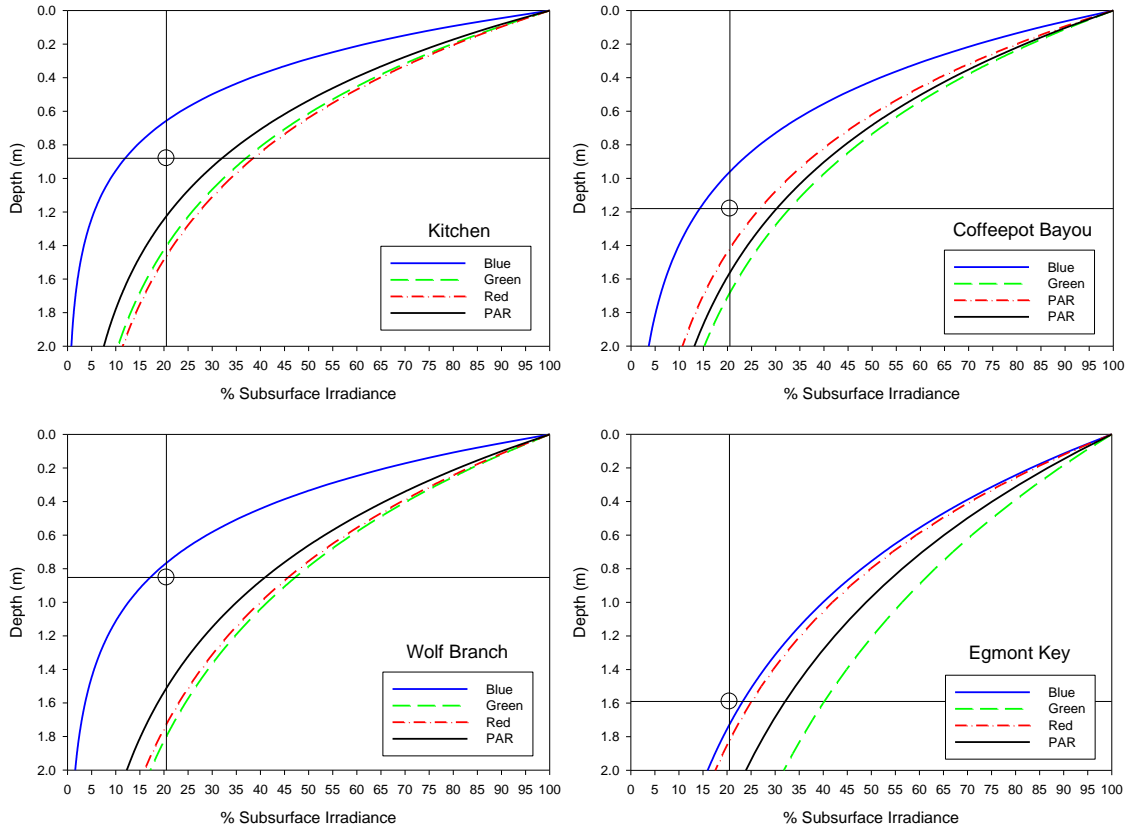
Figure 1-14. Annual average light loss with depth by color band for each Seagrass Management Area. The intersection of the vertical and horizontal lines represents the current minimum light target of 20.5% at the deep seagrass edge. Depths are in meters relative to MSL.

On an annual average basis, the percent subsurface PAR for all four SMAs well exceeded the minimum light target of 20.5% (Figure 1-14). Over the course of this study, the minimum light target was met or exceeded for all but three sampling events (Table 1-4).

Table 1-4. Monthly percent subsurface irradiance at bottom relative to just below the water surface for each representative color band. Data were collected at the deep edge of the persistent seagrass bed. Total depth at each deep edge is in parentheses and is relative to MSL. No data were collected for the Kitchen in December due to technical difficulties.

PAR	April	June	August	October	December	Annual Average
Wolf Branch (0.85m)	40.8	62.0	17.5	53.0	49.7	40.9
Kitchen (0.88m)	46.8	52.0	26.5	34.1	-	39.8
Coffeepot Bayou (1.18m)	57.1	36.1	15.5	28.8	32.5	30.1
Egmont Key (1.60)	33.5	40.5	18.3	34.4	39.8	32.1

BLUE	April	June	August	October	December	Annual Average
Wolf Branch	19.5	36.4	2.51	27.7	30.6	17.1
Kitchen	23.4	26.0	5.25	16.1	-	17.7
Coffeepot Bayou	38.2	8.93	6.30	14.9	23.1	14.2
Egmont Key	24.1	29.7	13.1	22.4	32.4	23.3

GREEN	April	June	August	October	December	Annual Average
Wolf Branch	48.0	71.9	19.1	61.7	57.9	47.2
Kitchen	54.4	60.6	30.7	39.8	-	46.4
Coffeepot Bayou	67.2	26.9	18.6	34.7	38.8	32.8
Egmont Key	42.1	50.6	22.7	43.7	50.3	40.2

RED	April	June	August	October	December	Annual Average
Wolf Branch	43.7	63.3	26.8	54.8	50.0	45.8
Kitchen	49.1	56.2	35.6	39.3	-	45.0
Coffeepot Bayou	51.9	23.0	16.9	28.3	29.3	26.6
Egmont Key	26.9	31.6	14.3	27.6	30.1	25.1

August percent subsurface PAR for Wolf Branch, Coffeepot Bayou, and Egmont Key were 17.5, 15.5, and 18.3, respectively while Kitchen was 26.5. This could lead to the incorrect conclusion that seagrass along the deep edge at the Kitchen site were the least light-limited. However, the percent subsurface blue light for August tells a different story. In August, the Kitchen had the second lowest value at 5.25. Wolf Branch had the lowest value at 2.51 and Egmont Key had the greatest value at 13.3, followed by Coffeepot Bayou at 6.30. August percent subsurface irradiance for green and red light while lower than any other month, were greater than percent subsurface blue light. This suggests that blue light was the limiting factor for seagrass during the month of August. The minimum light target for Tampa Bay was based on annual average PAR (Dixon and

Leverone 1995). Annual average percent subsurface PAR at the deep edge, during this study, ranged from 30.1 – 40.9. This range is 10% – 20% higher than other estimates (Bortone 2000; Dennison and Alberte 1982; Duarte 1991; Kenworthy et al. 1993; Steward et al. 2005) though Kenworthy, et al. (1993) reported light requirements as high as 37% in seagrass beds of Northeastern Saudi Arabia. Most estimates do not take into consideration epiphyte load. Dixon (2000) reported that average annual epiphyte attenuation in Tampa Bay accounted for 32.0% – 36.5% and while the minimum light target of 20.5% subsurface PAR may be appropriate for healthy seagrass with light epiphytic loads but where loads are moderate to heavy, the amount of light needed may be greater (Dixon 2000). While no attempts to quantify the epiphyte loads on the seagrass in this study were made, qualitative observations were taken and suggest that epiphyte loads were heavier in the Kitchen and Wolf Branch SMAs along eastern Tampa Bay and less so in Coffeepot Bayou and Egmont Key.

Minimum light target estimates also do not take into account pulsed events such as turbidity plumes like those documented in the Gulf of Carpentaria in northern Australia (Longstaff and Dennison 1999). In Tampa Bay, especially in eastern Tampa Bay, pulsed events may be more likely to cause high colored dissolved organic matter (CDOM) conditions. Heavy rain events during summer months may also bring pulsed nutrient loads that can lead to increases in phytoplankton biomass. Most likely, the drastic decrease in both percent subsurface PAR and blue light in August was the result of a pulsed rain event. The relatively moderate values in percent subsurface red light indicate that CDOM and/or detritus may have been the dominant light attenuators during this dark water event. Whatever the cause, the sharp decrease in percent subsurface PAR and blue light indicates that this was not a localized event.

Rainfall plays a major role in regulating the light field in Tampa Bay, either in terms of direct runoff or increases in river discharge. Heavy rainfall during the 30 days preceding the August sampling was likely responsible for the anomalous low-light conditions. For Kitchen and Wolf Branch, the rainfall amount recorded at Tampa International Airport during the 30 days prior to sampling was 29.5cm. For Coffeepot Bayou and Egmont Key, rainfall amounts recorded at the St. Petersburg Airport were

24.3cm and 16.4cm, respectively. More rain fell prior to the August sampling than for any other sampling. When the 30 day average rainfall is plotted against the monthly light attenuation coefficients for blue light, there is a correlation and this correlation appears to be stronger for the Kitchen and Wolf Branch than for Coffeepot Bayou or Egmont Key (Figure 1-15).
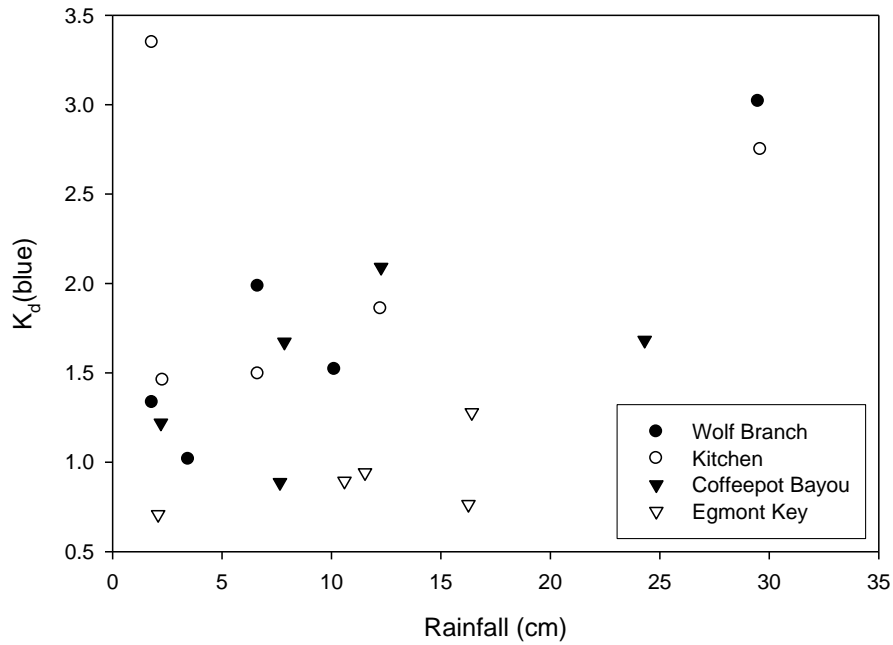
Figure 1-15.   Relationship between $K_d(blue)$ and the 30-day running average for rainfall for each Seagrass Management Area. Rainfall data were taken from the nearest ASOS weather station. Rainfall data source: National Weather Service, NOAA.

One anomalously high $K_d(blue)$ reading occurred in December for the Kitchen and was most likely a function of wind driven sediment re-suspension coupled with a very shallow measured depth (0.25m). A strong north wind following the passage of a cold front exacerbated the already shallow conditions by pushing water offshore, further adding to the likelihood of wind driven re-suspension and shallow depth as the likely cause of this anomaly.

Blue light made up only 5.3% of total PAR reaching the bottom at the seagrass deep edge for Wolf Branch during the relatively wet month of August, whereas during a June dry period, blue light made up 13% of the total PAR (Table 1-5). Both green and red light were similar irrespective of wet or dry weather conditions. Green light made up about half of the total PAR at the bottom for all SMAs irrespective of rainfall. The percent of red light that made up PAR was less in wet periods relative to dry periods but only slightly (Table 1-5).

Table 1-5. Proportion of the blue, green, and red color bands relative to total bottom PAR at the seagrass deep edge during wet and dry periods for each SMA. Rainfall is the total amount for the 30 days prior to sampling.

	Rainfall (cm)	Blue (400nm - 490nm)	Green (490nm- 600nm)	Red (640nm- 690nm)
Coffeepot Bayou				
Wet	24.3	11	51	20
Dry	7.65	18	48	16
Kitchen				
Wet	29.6	6.7	50	26
Dry	2.28	13	48	20
Wolf Branch				
Wet	29.5	5.3	48	29
Dry	3.45	15	48	19
Egmont Key				
Wet	16.4	18	51	14
Dry	2.08	22	47	15

Despite the fact that there appears to be plenty of light based on the percent subsurface PAR at bottom, it is probable that these grasses are blue-light limited. For resource managers, relying only on PAR measurements without having any information about the spectral properties of the light field could lead to the wrong conclusions.

1.4.2. PUR(λ) relationships

While a photon may be available for photosynthesis, there is no guarantee that it will be used. The usefulness of a given photon is dictated by the plant of interest. In this case, seagrass are the "end-users" and monitoring the light field for seagrass management

should focus on those usable wavelengths. In this study, the spectral regions for the usable color ranges of blue and red were estimated using spectral absorption ranges for seagrass light-harvesting pigments found in the literature (Cummings and Zimmerman 2003; Durako 2007; Zimmerman 2003). While this is a good first approximation, a more sophisticated way to determine spectral significance is through the use of PUR(λ).

The poorest light conditions occurred during the month of August across all SMAs and corresponded to a relatively rainy period. Under these worst case conditions, PUR(λ) approached zero at 440nm increasing to near 1.0 μmol m^{-2} s^{-1} at 490nm (Figure 1-16).
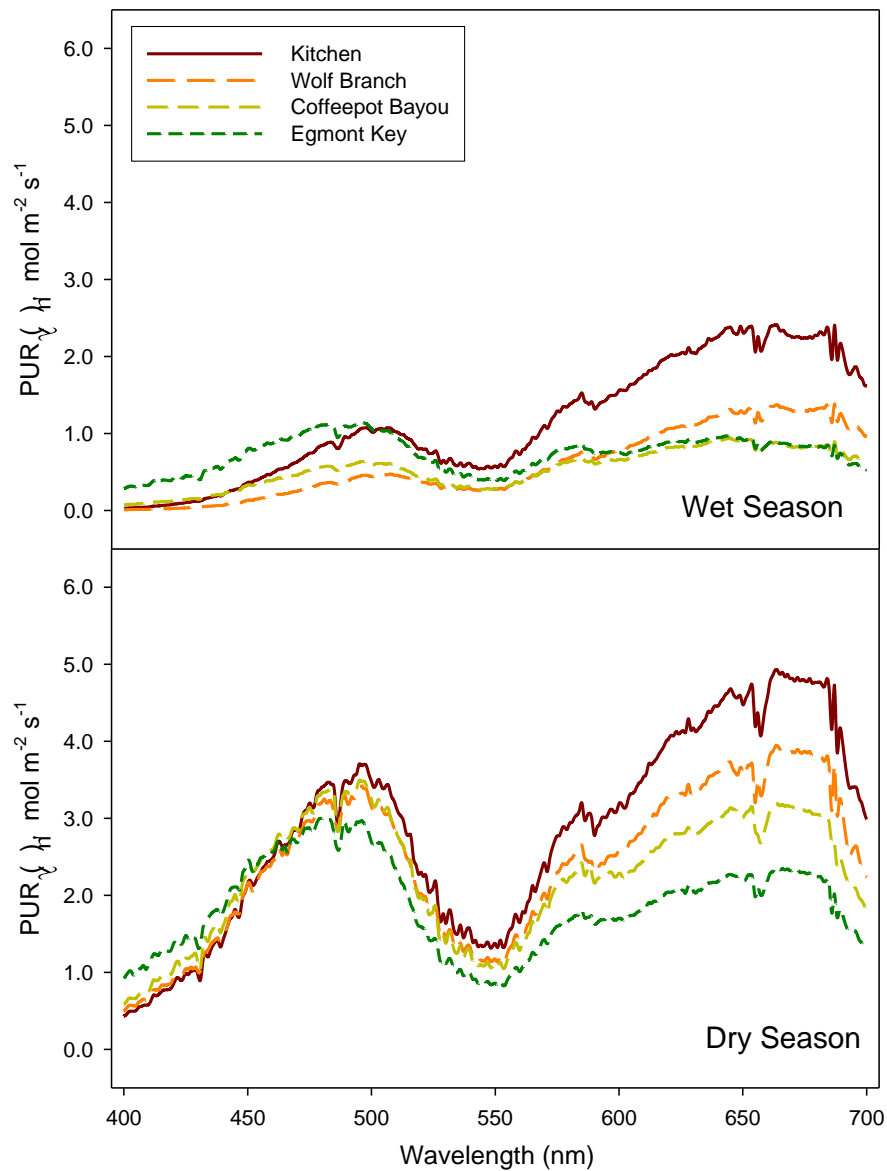
Figure 1-16. PUR(λ) curves for each of the four Seagrass Management Areas sampled in this study under wet conditions and dry conditions.

The small rise in PUR(λ) centered between 490nm and 500nm is likely absorption by the accessory chlorophyll *b* and *c* as well as the carotenoids. A second, more gradual rise, in PUR(λ) between 550nm and 700nm is likely a function of chlorophyll *c* and perhaps to a lesser extent chlorophylls *a* and *b*. There was a more pronounced rise in the

yellow to red region for the Kitchen (Figure 1-16). This same pattern was seen under the best light conditions though the magnitudes of PUR(λ) was much greater (Table 1-6).

Table 1-6. PAR and PUR for each SMA under wet and dry conditions for each representative color band. All values are in units of μmol m^{-2} s^{-1}.

	Coffeepot Bayou		Kitchen		Wolf Branch		Egmont Key	
	Wet	Dry	Wet	Dry	Wet	Dry	Wet	Dry
PAR (400nm – 700nm)	250	1060	513	1320	255	1130	354	859
Blue (400nm – 490nm)	28.1	187	34.5	177	13.4	174	65.3	193
Green (490nm – 600nm)	127	513	258	629	123	540	181	403
Red (640nm – 690nm)	49.4	173	131	266	74.4	212	49.9	127
PUR (400nm – 700nm)	161	680	348	858	179	734	223	566
Blue (400nm – 490nm)	27.2	181	33.4	171	13.0	168	63.1	186
Green (490nm – 600nm)	58.3	236	118	289	56.3	248	83.2	185
Red (640nm – 690nm)	43.9	154	117	236	66.0	188	44.3	113

The seagrass growing along the deep edge in Tampa Bay are blue-light limited as evidenced by the sharp decrease in PUR(λ) from 490nm to 400nm (Figure 1-16). Peak PUR(λ) for the Kitchen and Wolf Branch SMAs was located in the red color region and not the blue region, suggesting that these grasses are acclimated to absorbing red light. CDOM-rich water removes most of the blue light while much of the red light remains intact, although absorption due to water becomes significant at longer wavelengths.

Average annual percent subsurface red light ranged from a maximum of 45.8 at Wolf Branch to a minimum of 25.1 at Egmont Key (Table 1-4) suggesting an ample supply of red light even when light conditions are minimal.

While leaf absorptance is minimal at 550nm, it is not zero. In fact, there is a significant amount of absorptance occurring in the green region (Figure 1-2). PUR(λ) for the green region under the best light conditions during this study was as high as 289 μmol m-^{2} s^{-1} measured in the Kitchen during a June dry spell (Table 1-6). Even under low light conditions, a PUR(λ) for the green region was 118 μmol m-^{2} s^{-1} measured in Wolf Branch. It is evident that there is absorption taking place in the green color region and

further study is needed to isolate the pigments responsible and to understand the physiological mechanisms behind this apparent acclimation. The light harvesting pigments largely responsible for absorption in the blue-green region are the carotenoids but it is not clear what percentage are acting as photo-protective pigments. Along the deep-edge it is doubtful that leaves have much in the way of photo-protective pigments. One supposes that most production will be in the form of light-harvesting pigments for photosynthesis.

1.4.3. Mapping spectral light and depth targets

Seagrass in Coffeepot Bayou are depth limited as evidenced by the relatively sharp shelf break at the offshore terminus (Figure 1-13). Most of the seagrass beds along the flat shelf behind this slope are classified on the 2006 seagrass map as continuous (Figure 1-6). Visually, these grasses appear to be in good health and are persistent. Depths along the shelf break are between 1.25m – 1.50m MSL. The annual average K_d(PAR) of 1.51 m^{-1} was used to map the percent subsurface PAR for the Coffeepot Bayou SMA (Figure 1-17).
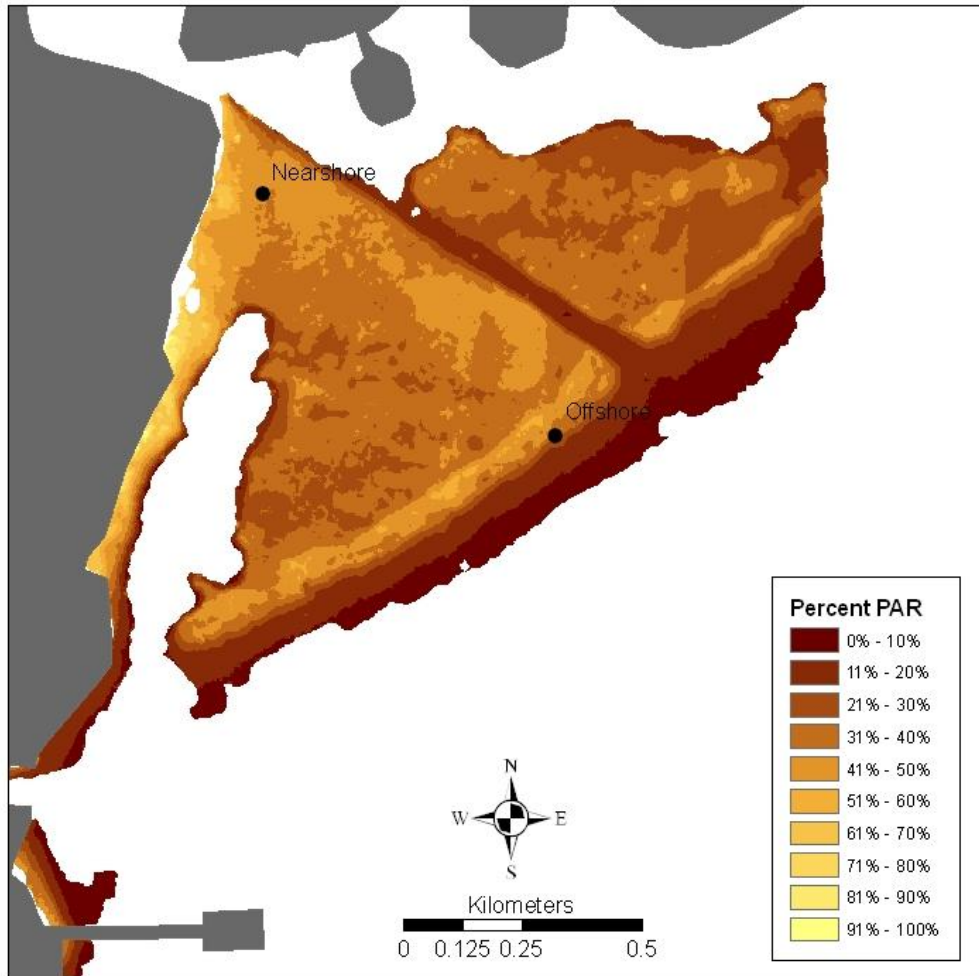
Figure 1-17. Percent subsurface PAR reaching the bottom for Coffeepot Bayou calculated using the annual average $K_d(PAR)$ and LIDAR bathymetry.

Extracting the percent subsurface PAR reaching the bottom along the mapped seagrasss

deep edge yielded an average of 31.7 ± 6.7 (Table 1-7).

Table 1-7. Total measured depth, percent subsurface blue light, and percent subsurface PAR relative to surface conditions along the mapped seagrass deep edge. These data were extracted using a sub-routine in GIS in which percent subsurface irradiance was collected for each pixel that fell along the seagrass deep edge.

	% Blue Light	% Green Light	% Red Light	%PAR	MSL Depth (m)
Coffeepot Bayou					
Mean ± standard deviation	13.6 ± 3.5	48.5 ± 5.1	30.7 ± 7.3	31.7 ± 6.7	1.21 ± 0.30
Median	13.8	48.9	31.5	32.7	1.14
Max	24.1	87.15	43.6	43.6	2.05
Min	4.5	26.26	13.6	15.5	0.82
Kitchen					
Mean ± standard deviation	17.3 ± 2.7	44.5 ± 3.2	40.7 ± 2.72	38.7 ± 3.25	0.87 ± 0.08
Median	17.4	44.8	40.3	38.9	0.86
Max	29.6	57.15	51.8	51.8	1.09
Min	11.0	36.26	35.0	30.3	0.60
Wolf Branch					
Mean ± standard deviation	18.1 ± 4.9	45.1 ± 5.6	40.7 ± 5.7	38.9 ± 5.8	0.97 ± 0.15
Median	18.0	45.4	40.9	39.1	0.95
Max	27.8	55.0	50.9	49.2	1.29
Min	18.0	34.4	29.8	28.1	0.72

By contrast, the percent of blue light reaching the bottom was only 13.6% (Figure 1-18).

The percent of green and red light reaching the bottom was 48.5% and 30.7%,

respectively (Table 1-7).
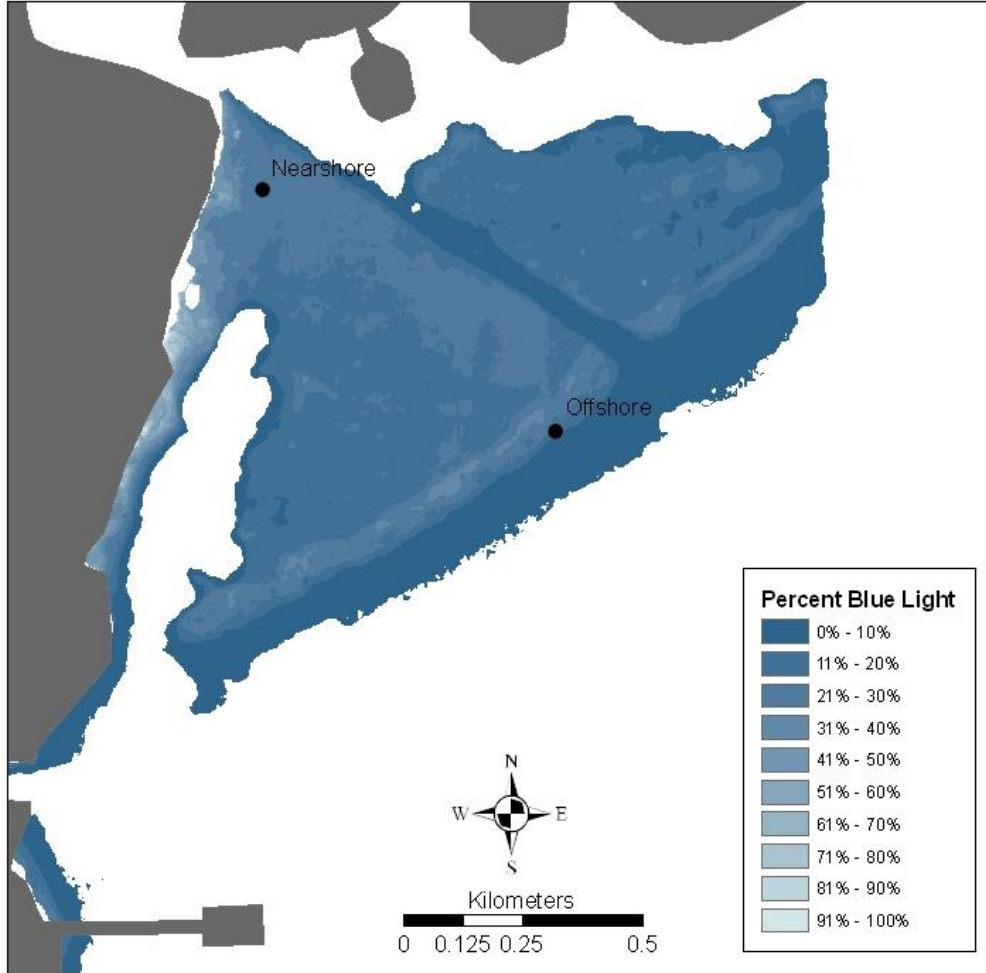
Figure 1-18. Percent subsurface blue light reaching the bottom for Coffeepot Bayou calculated using the annual average K_d(blue) and LIDAR bathymetry.

Using the annual average K_d(PAR) of 0.985 m^{-1} for Wolf Branch yielded a percent subsurface PAR along the mapped seagrass deep edge of approximately 39% (Table 1-7). For Wolf Branch, the 30% - 40% range for subsurface PAR was located approximately 250m offshore (Figure 1-19) and corresponded to the mapped seagrass deep edge (Figure 1-5).
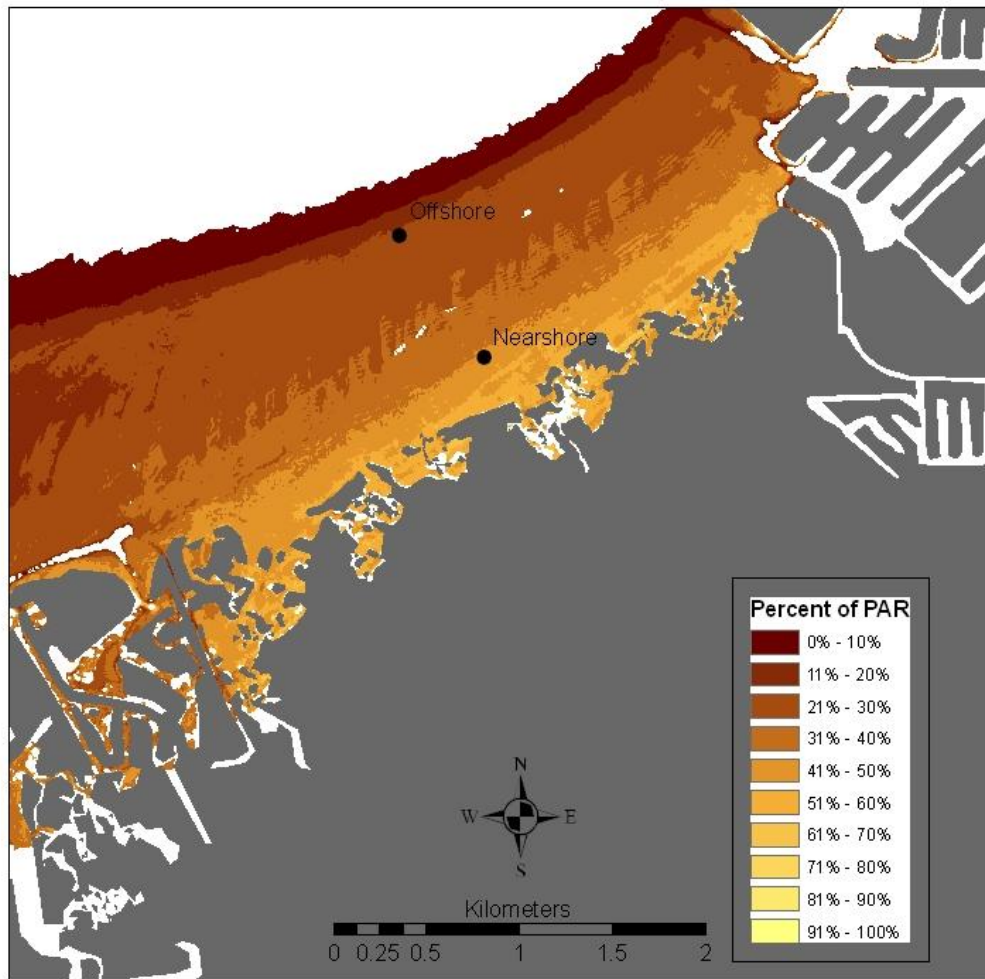
Figure 1-19. Percent subsurface PAR reaching the bottom for Wolf Branch calculated using the annual average K_d(PAR) and LIDAR bathymetry.

The modeled percent subsurface blue light at bottom was 17% along the mapped seagrass deep edge using a K_d(blue) of $1.78 m^{-1}$ (Figure 1-20). Near the offshore sample station, 1300m from the bank, is the approximate location of the minimum light target of 20.5% (Figure 1-20). Based on this target, there should be seagrass at this offshore station. While there were very sparse seagrass at the beginning of this study, after six months, the few shoots that were there had disappeared. The percent subsurface blue light along this same 20.5% PAR line was between 0% - 10%, further supporting the

hypothesis that this is a blue-light limited environment. Using only percent subsurface PAR without any information of the amount of blue light reaching the bottom, would lead to the conclusion that this area is meeting its minimum light requirement.
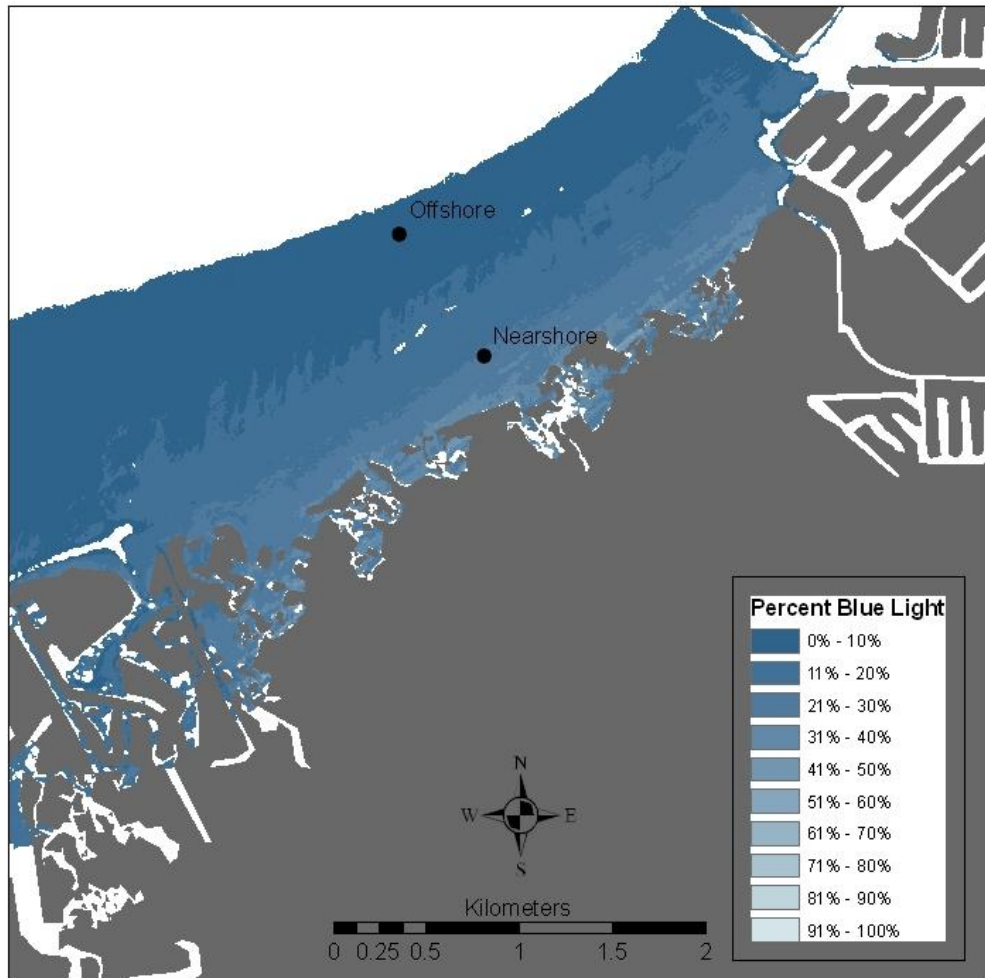
Figure 1-20. Percent subsurface blue light reaching the bottom for Wolf Branch calculated using the annual average K_d(blue) and LIDAR bathymetry.

Spatial patterns in the Kitchen SMA were similar to those found at Wolf Branch (Figure 1-21). Percent subsurface PAR at the deep edge was 38.9% using an average $K_d(PAR)$ of $2.07m^{-1}$.
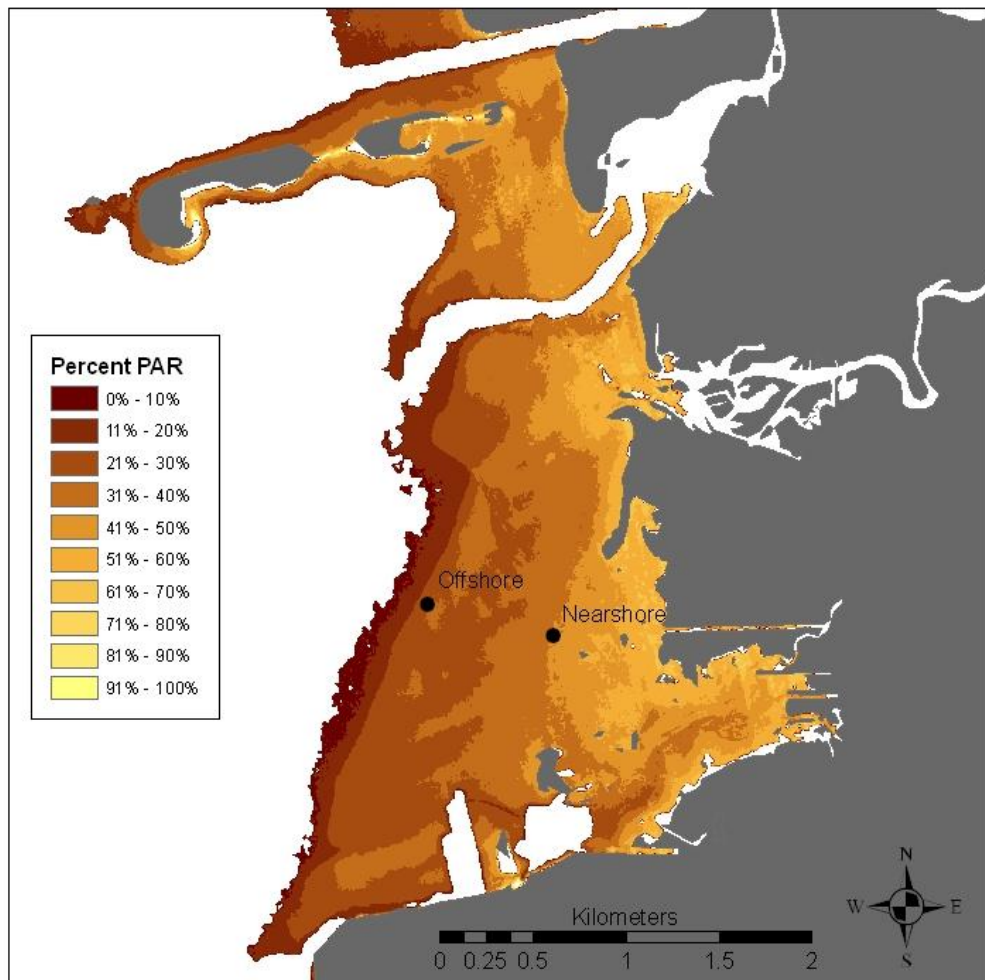
Figure 1-21. Percent subsurface PAR reaching the bottom for the Kitchen calculated using the annual average $K_d(PAR)$ and LIDAR bathymetry.

For the Kitchen, where there were persistent seagrass (Figure 1-4), the percent subsurface blue light had a range of 20% - 40% (Figure 1-22). Like Wolf Branch, at the beginning of the study, the offshore station had very sparse seagrass that disappeared during the rainy season. At this location, the percent subsurface blue light was approximately 10% (Figure 1-22) while the percent subsurface PAR was near 25%. Again, this further suggests that these areas are blue-light limited and that site suitability based solely on the minimum subsurface PAR could be misleading.
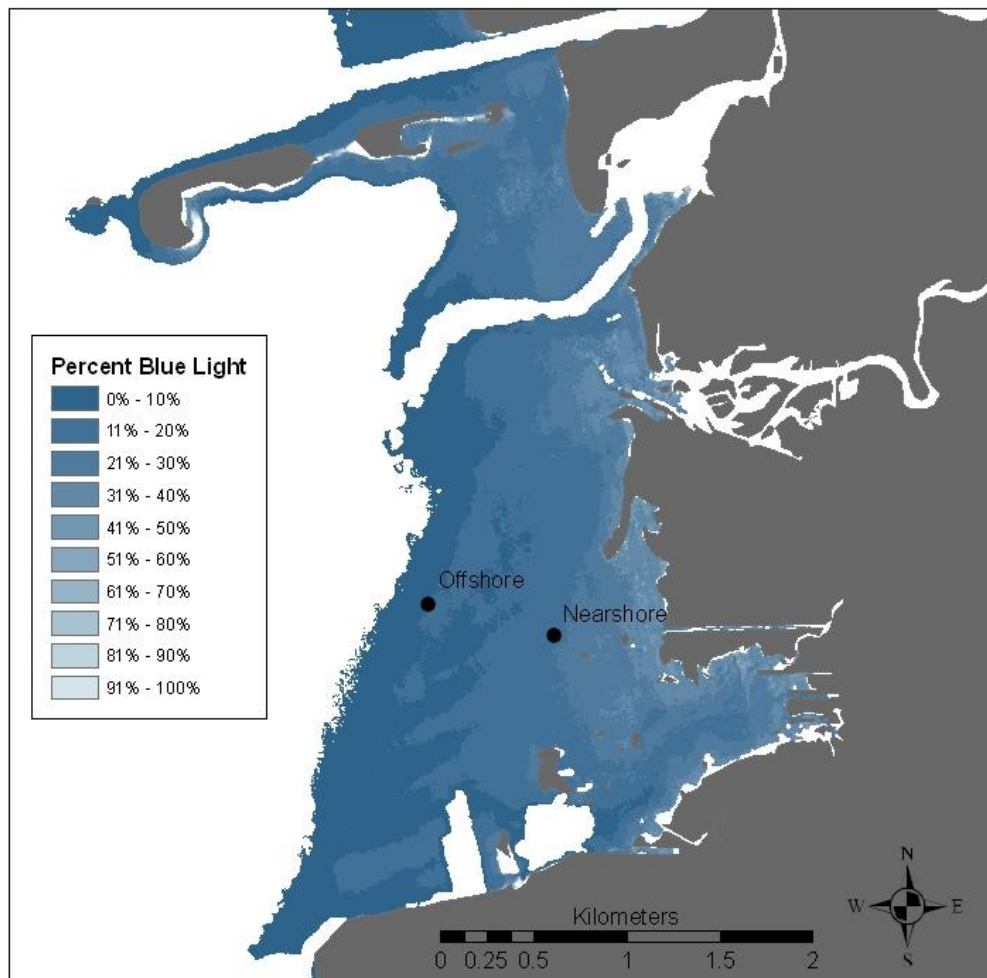
Figure 1-22. Percent subsurface blue light reaching the bottom for the Kitchen calculated using the annual average K_d(blue) and LIDAR bathymetry.

1.5. Conclusions

In the context of the existing minimum light target of 20.5% PAR, the seagrass deep edge should not be light-limited. Based on the results presented here, this target may be too low and should be increased to 30% or higher. While this may seem like more than enough light, it is important to remember that much of the photosynthetically useable blue light has been attenuated by the time the light reaches the bottom. Results presented here suggest that a target of 20% may actually be an appropriate blue light target. Because there were no significant differences in either K_d(blue) or K_d(PAR) for Coffeepot Bayou, Kitchen, and Wolf Branch, applying a bay-wide target may be appropriate and the need to develop Seagrass Management Area-specific targets unnecessary.

Having access to high resolution bathymetry like that collected by NASA's EAARL system, greatly enhances the ability to model the spatial distribution of light. Unfortunately, such data are few and far between but none the less imperative to accurate model development. The GIS-based model presented here is an effective tool to quickly assess the status of the subsurface light field on an area-wide basis and does not necessarily need such high resolution bathymetry. What is necessary is an accurate understanding of the spatial and temporal variability in PAR(λ) and $K_d(\lambda)$. The framework presented here is relatively straightforward and can quantify the spectral properties of the subsurface light field in a way that is cost effective and can be readily integrated into existing water quality monitoring programs. Because this system is designed to work in very shallow waters, makes it an ideal tool for seagrass applications. While understanding the spectral characteristics of the light field is a critical first step, it is not enough simply to know how much light is there at the bottom. It is equally important to understand the underlying causes of light attenuation and if these causes can be managed to facilitate improvements in water clarity, and ultimately to provide an environment suitable for seagrass recovery and growth.

Chapter 2. Relative Contribution and Magnitude of Phytoplankton, CDOM, and Detritus Absorption to the Total Absorption Coefficient in Shallow Seagrass Areas

2.1. Abstract

The quality of light plays a major role in limiting the distribution of seagrass. In sub-tropical estuaries like Tampa Bay, seagrass are blue light limited along the deep edge. But it is not enough simply to know this. To effectively manage seagrass, the causes of blue light attenuation must also be understood. The total absorption of light is a function of phytoplankton, colored dissolved organic matter (CDOM), and detrital material. Historically, Tampa Bay has been considered a chlorophyll dominated estuary and seagrass management efforts have focused on chlorophyll as the primary target for increasing light along the seagrass deep edge by reducing the total nitrogen load into the bay. However, while bay-wide chlorophyll concentrations have decreased over the past decade, there has been no major expansion of seagrass into deeper areas. Mounting evidence suggests that the major light attenuator in these shallow seagrass areas is not chlorophyll but CDOM. This hypothesis was tested in selected Seagrass Management Areas (SMA) by comparing the relative contribution and magnitude of the various components of the total absorption. Results confirmed that CDOM is the major absorption component, and at 440nm, accounted for an average of 60% of the total absorption. Detrital absorption, at 440nm, accounted for an additional 20%, leaving only 20% of the total absorption attributable to phytoplankton absorption. The magnitude of the absorption coefficients varied as a function of the 30-day running average for total rainfall. The correlation between rainfall and $a_g(440)$ was directly related to distance up the bay from the mouth. Rainfall and $a_\phi(440)$ correlated with rainfall for all SMAs, though the magnitude of $a_\phi(440)$ increased with increasing distance up the bay from the mouth. It is important to infer past light conditions in terms of the inherent optical properties (IOP). Predictor equations were developed relating chlorophyll a to $a_\phi(440)$, turbidity to the scatter coefficients $b(480)$ and $b(660)$, and PCU color to $a_g(440)$. The correlation coefficients were relatively strong ranging from 0.68 to 0.89. An empirically-derived spectral attenuation model was used to relate the IOPs with the light attenuation

coefficient ($K_d(\lambda)$) using the equation $K_d = 1/\mu_0 \left[a^2 + G(\mu_o)ab\right]^{1/2}$, where μ_o is the cosine of the solar zenith angle, and $G(\mu_o)$ is a coefficient that determines the relative effect of scattering on the total attenuation of irradiance. SMA-specific $a_t(480)$ and $b(480)$ were used to generate modeled $K_d(480)$ which agreed well with measured $K_d(480)$ ($p < 0.01$; $r^2 = 0.78$). While this model was originally calibrated for the turbid waters of San Diego Harbor, it worked fairly well in Tampa Bay.

2.2. Introduction

Chapter 1 explored the spectral attenuation of light in four Seagrass Management Areas (SMA) in Tampa Bay and found that seagrass along the deep edge are blue light limited. This chapter explores the root causes of blue light loss in shallow SMAs of Tampa Bay by comparing the relative contribution and magnitude of the inherent optical properties for each area. Because the inherent optical properties are independent of the ambient conditions at the time of sampling, they are considered the "gold standard" for understanding the radiance distribution of the underwater light field. An empirical optical model is employed to couple these inherent optical properties with the light attenuation coefficient ($Kd(\lambda)$), a term derived from the apparent optical properties. Light limitation is the factor determining seagrass depth distribution in many subtropical estuaries like Tampa Bay. Seagrass provide critical habitat for many commercially, recreationally, and ecologically important species of fish (Bortone 2000; Hemminga and Duarte 2000; Hill 2002; Kenworthy et al. 1993; Zieman and Zieman 1989). Seagrasses in Florida provide juvenile nursery and adult feeding areas for red drum, spotted seatrout, spot, silver perch, sheepshead, snook, shrimp, and the bay scallop (Zieman and Zieman 1989).

Light quantity reaching the bottom is often expressed in terms of the photosynthetically available radiation (PAR) (Morel 1978; Smith and Baker 1978). Photosynthetically useable radiation (PUR) is a spectrally integrated quantity, defined as the fraction of the radiant energy that can be absorbed by the light-harvesting pigments (Morel 1978; Morel 1991). Both PAR and PUR can be expressed in terms of their spectral quantities and are given the symbols PAR(λ) and PUR(λ), respectively. PUR(λ) can be thought of as a measure of the quality of light relative to a given target species. Plant pigments typically absorb at blue-green wavelengths whereas the maximum transparency of most Tampa Bay waters occurs at the greenish-yellow wavelengths, consistent with the color of CDOM-rich waters. Models based upon white-light concepts such as PAR do not allow calculation of the photosynthetically useable radiation (PUR) (Carder 1995; Morel 1978; Smith and Baker 1978) that seagrass require to thrive or even survive (Zimmerman 2003).

To effectively manage these seagrass systems, it is not enough simply to know the amount of PAR or even the quality of light (PUR) reaching the bottom, but also the causes of light loss. As light propagates down through the water column, its attenuation is governed by a combination of absorption and scatter (Kirk 1994). The primary causes of water column absorption are phytoplankton, colored dissolved organic matter (CDOM), and detrital material (Kirk 1994; Mobley 1994).

2.2.1. The inherent optical properties

The term inherent optical property (IOP) is rooted in radiative transfer theory with equations providing the theoretical framework for predicting and interpreting underwater light fields in terms of the physical, chemical, and biological constituents of natural water bodies (Mobley 1994). These properties refer to those intrinsic properties of the aquatic medium which are dependent solely on the radiance distribution and independent of the ambient conditions at the time of measurement (Kirk 1984; Mobley 1994; Preisendorfer 1961). The IOPs include the absorption coefficients, the scattering coefficients, and the beam attenuation coefficients (Table 2-1). By contrast, the apparent optical properties (AOP) depend both on the radiance distribution of the aquatic medium and the ambient light conditions at the time of sampling (Kirk 1984; Mobley 1994). Typical AOPs include downwelling irradiance, the diffuse attenuation coefficient, and photosynthetically active radiation (PAR) (Table 2-1).

Table 0-1. Common parameters associated with the inherent and apparent optical properties of water.

Parameter	Symbol	Unit
Inherent Optical Properties		
Absorption coefficient	$a(\lambda)$	m^{-1}
Scattering coefficient	$b(\lambda)$	m^{-1}
Beam attenuation coefficient	$c(\lambda)$	m^{-1}
Apparent Optical Properties		
Diffuse attenuation coefficient	$K_d(\lambda)$	m^{-1}
Downwelling irradiance	$E_d(\lambda)$	$W\ m^{-2}$
Photosynthetically active radiation	PAR	$\mu mol\ m^{-2}\ s^{-1}$

Absorption of light by constituents in the water column is the most common cause of light loss with depth. In hydrologic optics, the parameter most commonly used to describe absorption is the spectral absorption coefficient (Mobley 1994). The total spectral absorption coefficient for a given wavelength λ can be expressed as a function of its component parts

$$a_t(\lambda) = a_w(\lambda) + a_\phi(\lambda) + a_g(\lambda) + a_d(\lambda) \qquad \text{Eq. 2.1}$$

Where $a_t(\lambda)$ is the total absorption coefficient, $a_w(\lambda)$ is the absorption by water, $a_\phi(\lambda)$ is the absorption by phytoplankton chlorophyll, $a_g(\lambda)$ is the absorption by CDOM, and $a_d(\lambda)$ is the absorption by detrital material. Of these components, $a_w(\lambda)$ can be treated as a constant because it is dependent on the molecular properties of pure water. The contribution of $a_w(\lambda)$ to $a_t(\lambda)$ is small in the blue and the green regions of the visible spectrum but increases exponentially above 550nm (Kirk 1994) (Figure 2-1). For photosynthetically useable blue light, $a_w(\lambda)$ is insignificant relative to $a_\phi(\lambda)$, $a_g(\lambda)$, and $a_d(\lambda)$. For example, $a_w(440)<0.01\ m^{-1}$ (Morel and Prieur 1977; Pope and Fry 1997; Smith 1981) while typical absorption coefficients for phytoplankton, CDOM, and detritus in Tampa Bay range anywhere from $0.10\ m^{-1}$ to greater than $1.0\ m^{-1}$.
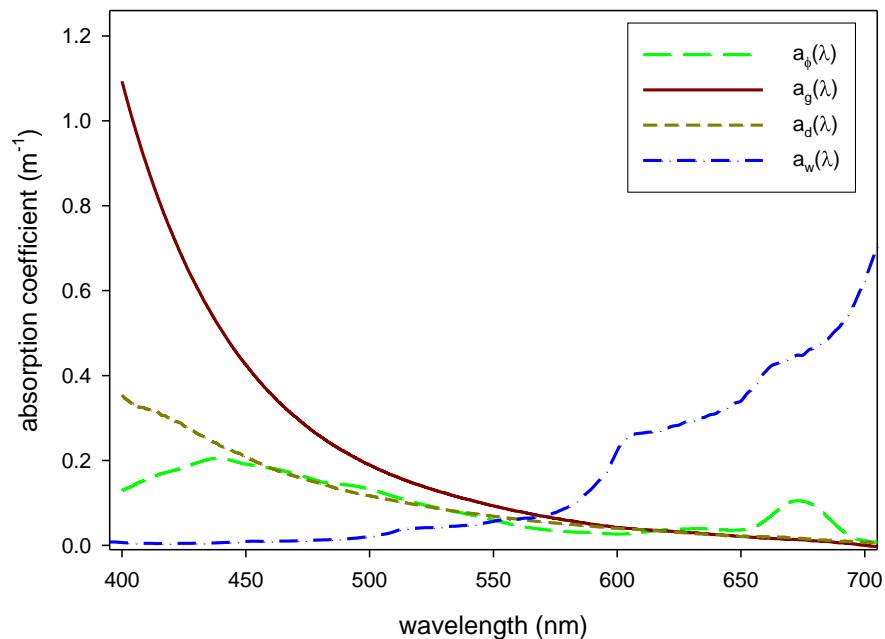
Figure 2-1. Typical phytoplankton, CDOM, and detrital absorption spectra measured in Tampa Bay, FL. Pure water absorption spectrum is taken from Pope and Fry (1997).

Absorption by phytoplankton is accomplished primarily by photosynthetic and photoprotective pigments (Bricaud et al. 1995; Bricaud and Stramski 1990; Gordon 1983; Kirk 1994). While there are many varieties of light-harvesting pigments found in phytoplankton, each with unique absorption spectra, all phytoplankton contain chlorophyll *a* (Kirk 1994). In living phytoplankton cells, almost all of the chlorophyll and most of the carotenoids in the chloroplasts are complexed to proteins (Kirk 1994). There are two broad absorption peaks for $a_\phi(\lambda)$. The primary peak is in the blue region centered near 440nm with the secondary peak located in the red region near 660nm (Figure 2-1).

The spectral shape of phytoplankton absorption is a function of the absorption characteristics of chlorophyll *a* and the accessory pigments chlorophyll *b* and *c*, the carotenoids, and the billiproteins. Billiproteins are chloroplast pigments found in certain types of red and blue-green algae (Kirk 1994; Rowan 1989). These pigments extend the absorption window into the yellow and green wavelengths. For example, the absorption maxima for phycoerythrin, a billiprotein, lies between 490nm and 600nm, and between

490nm and 640nm for the billiprotein phycocyanin (Kirk 1994). As higher plants, seagrass species do not have billiproteins and thus are not capable of harvesting much light in the green region.

In many subtropical estuaries like Tampa Bay, $a_g(\lambda)$ can be a significant contributor to $a_t(\lambda)$. CDOM is operationally defined as that component of the total dissolved organic matter pool that absorbs light over the visible and ultraviolet spectrum (Coble 2007; Conmy 2008). There are many different names for CDOM in the literature including gelbstoff, gilvin, yellow matter, and chromophoric dissolved organic matter. The definition of CDOM can be further broken down into its component parts. Organic matter is any material that contains carbon and hydrogen and is of biological origin. An operational definition for "dissolved" is the mechanical separation of water samples using filtration, centrifugation, or other techniques to remove particles larger than some minimum diameter (Coble 2007). Often 0.2μm is used as the operational cutoff between dissolved and particulate constituents (Hansell and Carlson 2002; Twardowski et al. 2004). The term "colored" refers to the optical properties giving CDOM its characteristic yellow, or iced-tea, color. CDOM absorbs and fluoresces in the ultraviolet to blue wavelengths. CDOM has been shown to play a major role in light attenuation, even in clear, open ocean waters like the Sargasso Sea (Siegel and Michaels 1996a). CDOM is the principal light-absorbing constituent of the DOM pool in seawater (Blough and Vecchio 2002). Due to its complex nature, absorption spectra are broad and unstructured. CDOM absorption spectra decrease exponentially with increasing wavelength in the range 300nm-700nm. Absorption magnitudes vary significantly and increase with increasing proximity to terrestrial sources. Typically CDOM absorption increases along a continuum from open-ocean to river water. The absorption spectrum for $a_g(\lambda)$ can be approximated with the following equation:

$$a_g(\lambda) = a_g(\lambda_o)e^{-S(\lambda-\lambda_o)}$$
Eq. 2.2

where $a_g(\lambda)$ is the CDOM absorption coefficient at wavelength λ, $a_g(\lambda_o)$ is the CDOM absorption coefficient at some reference wavelength λ_o, and S is the spectral slope.

Differences in S can be indicative of CDOM origin such that lower slopes are typical of freshwater and coastal environments while steeper slopes are more indicative of offshore, photobleached marine waters (Coble 2007; Hansell and Carlson 2002). Spectral slope varies depending on the wavelength range used to calculate the slope (Coble 2007; Hansell and Carlson 2002; Stedmon et al. 2000; Stedmon 2003).

Detrital material is essentially the non-living particulate portion of the total organic matter pool that is left behind after a water sample has been passed through a 0.2μm filter. Because the chemical compounds that make up the detrital fraction are similar to those found in CDOM, the spectral shape of $a_d(\lambda)$ is very similar to that of $a_g(\lambda)$ though typically at much lower concentrations (Figure2-1). In shallow coastal lagoons, wind-driven suspension of particulate matter can be a significant control on light attenuation (Lawson et al. 2007).

Understanding the behavior of light requires knowledge of the scattering properties of the water (Kirk 1981). At the most fundamental level, scattering of light arises from interactions between photons and molecules (Mobley 1994). In natural waters, scatter is dependent on particle size, phytoplankton species, particle mineralogy, detritus composition, and particle concentration (Coble 2007; Weidemann and Bannister 1986). The total scattering coefficient ($b(\lambda)$) can be calculated as:

$$b(\lambda) = a(\lambda) - c(\lambda)$$
<div align="right">Eq. 2.3</div>

where $a(\lambda)$ is the total spectral absorption coefficient and is the sum of the component absorption coefficients as stated in Eq (2.1), and $c(\lambda)$ is the total spectral beam attenuation coefficient in units of m^{-1}. The probability of a photon travelling along a specific path length before interacting with some component within the water column, either through absorption or scattering is governed by $c(\lambda)$ (Kirk 1981). The beam attenuation coefficient is calculated by in-water measurement of the beam transmittance of a specific wavelength of light across a fixed pathlength.

2.2.2. Seagrass-light relationships in Tampa Bay

Phytoplankton productivity is directly related to nutrient loads originating from terrestrial runoff, sediment re-suspension, internal cycling, and direct atmospheric deposition. The most cited cause of seagrass decline in coastal systems, including Tampa Bay and Charlotte Harbor, is anthropogenic nutrient enrichment (Janicki Environmental 2001; Tomasko et al. 1996). Pulsed events like hurricanes, regulated discharges from nutrient-rich systems, or accidental nutrient releases can provide the catalyst for high phytoplankton productivity, significantly increasing light limitation for seagrass. Under the current Tampa Bay nitrogen management strategy, seagrass management has been predicated on the assumption that phytoplankton chlorophyll is the major light attenuator limiting seagrass depth distribution (Figure 2-2) (Janicki Environmental 2001).
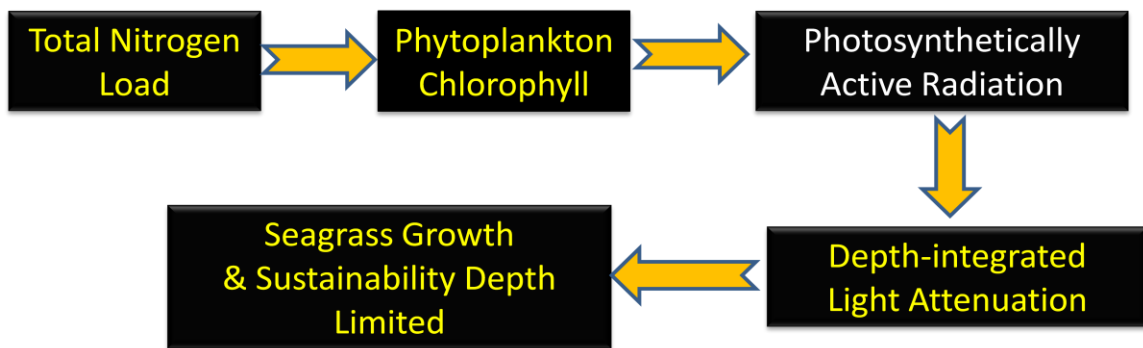
Figure 2-2. Tampa Bay nitrogen management strategy as it relates to light and seagrass sustainability.

This assumption was based on empirical relationships between water quality and light attenuation from an impressive monthly data set collected over several decades by the Hillsborough County Environmental Protection Commission as part of their ambient monitoring program. However, almost all of the stations are located well offshore from existing seagrass beds. Results from a two year study in Old Tampa Bay concluded that light attenuation was greater in shallow seagrass beds immediately along the shoreline than further offshore and that CDOM absorption has more of an impact than previously believed (Griffen and Greening 2004). The City of Tampa's Bay Study Group came to the same basic conclusion in the Kitchen and Wolf Branch areas of the bay (Johansson,

personal communication). In ocean water, CDOM is one of the strongest absorbing constituents often exceeding absorption by phytoplankton in the blue color region (Hoge et al. 1993). Not only can CDOM reduce the PAR and PUR of blue light, it also degrades the accuracy of chlorophyll concentration by satellite color sensors (Carder et al. 1989).

CDOM can come from a variety of sources and sinks in Tampa Bay (Table 2-2). While the primary source of CDOM in the world's oceans is via in-situ biological production, the major source in estuaries like Tampa Bay is from freshwater inflow from rivers and streams such as the Hillsborough River and Alafia River. Along the immediate shoreline, mangrove swamps and salt marshes can also be an important source of CDOM. Groundwater could also be a significant source of CDOM along coastal and estuarine areas where groundwater inputs exist either as discrete springs like Crystal Beach Spring off Pinellas County, or as diffuse groundwater discharge through sediments. CDOM sinks in estuaries like Tampa Bay are mostly through direct export via tidal mixing and flushing. Photobleaching is the dominant process for the degradation of CDOM in shallow oceanic waters (Conmy et al. 2004; Siegel and Michaels 1996b; Warrior and Carder 2005) but in estuarine systems residence times are sufficiently short that CDOM is exported before major degradation can occur.

Table 0-2. CDOM sources and sinks in Tampa Bay summarizing inputs and outputs.

Sources	Sinks
Major Rivers – Hillsborough, Manatee, Alafia	Direct Export – Tidal mixing and Flushing
Minor Rivers and Canals – Bullfrog Creek	Photodegradation
Direct Runoff – Stormwater	Biodegradation
Coastal Vegetation – Mangroves, Salt marsh	
In-situ Biological Production – Water column	
In-situ – Seagrass / Macroalgae	
Direct Groundwater – Sediment flux	

Detrital material can also play a major role in the absorption of light and has been correlated with wind-driven re-suspension of organic particles (Lawson et al. 2007; Steward and Green 2007). If this is the case in the shallow seagrass areas of Tampa Bay, the current seagrass management paradigm should be modified to include the effects of detritus and CDOM absorption on the light field (Figure 2-3).
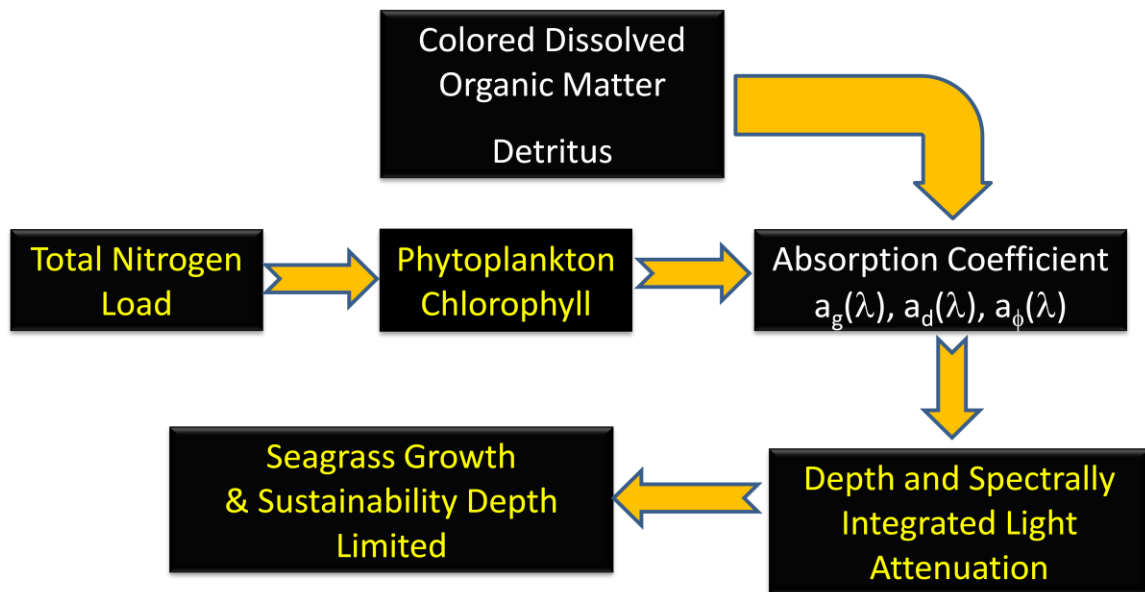
Figure 2-3. Modified Tampa Bay seagrass management strategy that includes spectral absorption by CDOM and detritus.

2.2.3 Coupling the IOPs with the quasi-IOPs and $K_d(\lambda)$

While IOPs are considered to be the "gold standard" for understanding the optical properties of the water, most resource management agencies do not collect these data, and little historical IOP data exist. Today, many agencies are beginning to appreciate the importance of understanding the optical properties of the water as it relates to resource management and have begun to collect IOP data. For example, the City of Tampa's Bay Study Group and the Hillsborough County Environmental Protection Commission now routinely collect CDOM absorption as part of their monitoring programs (R. Johansson, personal communication). Nevertheless, there is wealth of historical data that could be useful to infer historical IOPs. This can be accomplished using empirical relationships between the IOPs and historical quasi-IOPs such as chlorophyll *a* concentration, water color in platinum cobalt units, and turbidity in nephelometric turbidity units. The term quasi-IOP is used to indicate the close relationships between these parameters and the various absorption and scattering coefficients.

The Apparent Optical Properties (AOP) define the light field within the water column and are parameters routinely monitored by limnologists and oceanographers (Kirk 1981). For resource managers, $K_d(\lambda)$ is the most relevant metric that arises from the AOPs and is the fundamental metric for setting seagrass light and depth targets. To relate $K_d(\lambda)$ with the IOPs provides much more insight into the root causes of light loss with depth. Historically there has been a great deal research trying to couple the AOPs with the IOPs (Berwald et al. 1995; Berwald et al. 1998; Kirk 1984; Kirk 1994). Because of the multiple scattering that takes place in natural systems and the variability in the angular distribution of the light field, there is no analytical expression to directly calculate $K_d(\lambda)$ from the IOPs (Kirk 1981). The IOPs however, can be used to specify the probability of absorption and scatter occurring on an individual photon basis.

This study was designed to investigate the relative contribution and magnitude of the IOPs for selected Seagrass Management Areas (SMA) in Tampa Bay. Based on the results presented in Chapter 1, seagrass depth distribution in Tampa Bay is limited by blue light (400nm-490nm). To effectively manage seagrass along the deep edge, the root causes of blue-light loss must be better understood. If CDOM is the dominant attenuator of blue light in these areas, it further challenges the long standing seagrass management paradigm that phytoplankton chlorophyll is the primary light attenuator and that reductions in nitrogen loads will have a significant impact in reducing chlorophyll concentrations significantly enough to increase water clarity (Janicki Environmental 2001). Also, empirical relationships between the IOPs and the quasi-IOPs for these shallow water areas were constructed to couple the IOPs with parameters more commonly measured in resource management and regulatory programs. Finally, the total absorption and scattering coefficients are coupled with the light attenuation coefficient at 480nm using the equation developed by Kirk (1981) and modified by Kirk (1991).

2.3. Methods and Materials

2.3.1. Site Locations

Tampa Bay has been subdivided into 30 individual Seagrass Management Areas (SMA) (Figure 2-4). The SMA concept was proposed by the Tampa Bay Estuary

Program and is based on several factors such as historical seagrass patterns, water quality, sediment type, and watershed land-use (E.P.C.H.C. 2007). A detailed description of each SMA may be found in Chapter 1.
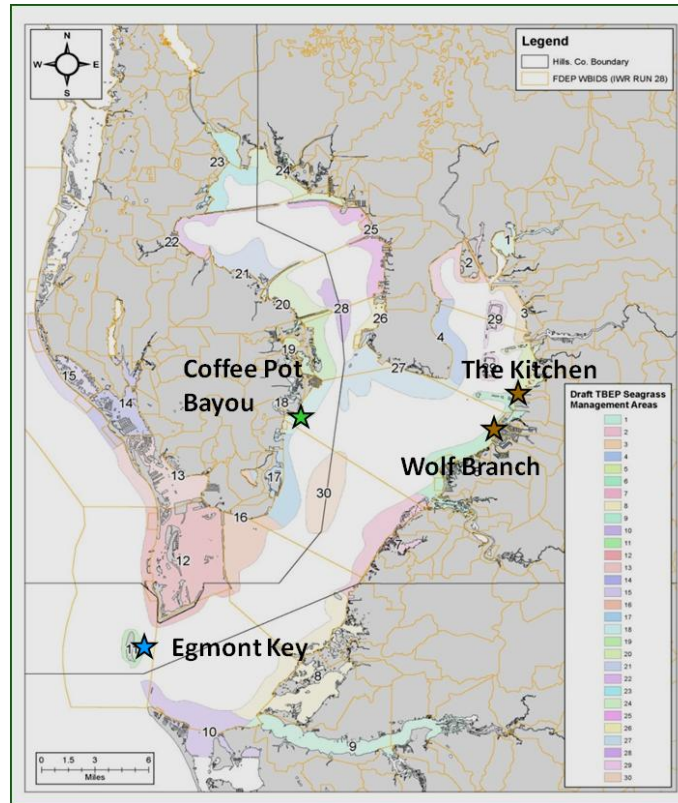
Figure 2-4. Seagrass Management Areas in Tampa Bay and the four areas used in this study.

The Kitchen SMA is located in eastern Tampa Bay and has a well developed mangrove shoreline (Figure 2-5). This is a CDOM and chlorophyll-rich area characterized by average water depths of less than 2.0m mean sea level (MSL). Direct river discharge comes from Bullfrog Creek, a 3km long tidal creek that drains mostly agriculture and some urban developed areas. A second source of river water comes from the Alafia River just to the north of the Kitchen. Discharge from these rivers is typically maximum during the height of the rainy season during the months of August and September.

Figure 2-5. Mangroves dominate the shoreline in (a) the Kitchen and (b) Wolf Branch Seagrass Management Areas. The creek near the center of the Kitchen is Bullfrog Creek. The old mouth of the Alafia River can also be seen just above Bullfrog Creek. No major creeks flow into Wolf Branch. Image scale: 1:32,285.

Wolf Branch is located along the eastern shore of Middle Tampa Bay and is immediately to the south of the Kitchen (Figure 2-4). Like the Kitchen, Wolf Branch also has a well developed mangrove shoreline (Figure 2-5) and is rich in both CDOM and, chlorophyll. Unlike the Kitchen, there are no significant river inputs into Wolf Branch, though several small tidal tributaries are located throughout the area. Additionally, within the mangroves, numerous mosquito ditches were dug in the 1960s for flood control. These ditches provide a direct conduit for surface runoff and may also be a significant conveyance for CDOM-rich water.

65

Coffeepot Bayou is located along western Tampa Bay (Figure 2-4). Shoreline morphology is very different from the Kitchen and Wolf Branch and is mostly seawall with no mangroves. The urban landuse adjacent to Coffeepot Bayou can deliver large amounts of stormwater runoff during wet weather. Because there are no major sources of CDOM, blue-light loss is not thought to be driven by CDOM absorption, but by phytoplankton absorption due to pulsed inputs of nutrient-laden urban runoff during storm events.

The Egmont Key SMA is unique in that it is adjacent to a 162ha island that is both a State Park and a National Wildlife Refuge (Figure 2-4). The largely undeveloped island is located at the mouth of Tampa Bay. Given its proximity to the Gulf of Mexico, CDOM and phytoplankton absorption should be minimal by comparison with the other three SMAs.

2.3.2. IOP field and laboratory methods

For each SMA, a minimum of ten water samples were pseudo-randomly selected every other month during 2008. For each SMA, a 25m by 25m grid was placed on top of the SMA map and each grid cell was assigned a number. Ten randomly generated numbers were selected and placed on the SMA map. Sites locations were adjusted if the randomly generated plot resulted in sites clustered too close together. In some cases, especially in the Kitchen where water depths can be very shallow, station locations were moved to deeper water to allow boat access. The minimum operating depth during this study was 0.20m.

Sampling protocol followed Florida Department of Environmental Protection standard operating procedures (http://www.floridadep.org/labs/qa/sops.htm). Samples were collected approximately 0.10m below the surface using 1L brown plastic bottles and were immediately placed in a cooler of ice. Because some of the shallowest sites were so difficult to reach, attempts were made to sample on an incoming or a slack high tide.

Laboratory analyses were performed following the methods as described in Cannizzaro (2004). The particulate absorption coefficient ($a_p(\lambda)$) is the sum of the phytoplankton absorption coefficient ($a_\phi(\lambda)$) and the detritus absorption coefficient

($a_d(\lambda)$). Absorption spectra for $a_p(\lambda)$ were determined using the quantitative filter technique (Kiefer and Soohoo 1982; Yentsch 1962). Water samples were filtered slowly through 2.5cm GF/F (Whatmans) filters using vacuum pressures less than 15in Hg. The volume of water filtered depended on the concentration of the pigmented particles in the sample. Filters were wrapped in aluminum foil and stored in liquid nitrogen for less than one week prior to being processed. Filters were allowed to thaw slowly at room temperature for 5-10 minutes prior to being placed in a dark petri dish and re-hydrated with a drop of Milli-Q water. The sample filter and a reference filter wetted with Milli Q water were placed on individual 2.4cm diameter glass plates in a custom made light box. Prior to each transmission scan, the filters were slid one at a time over a tungsten-halogen light source that shone through a blue long-pass filter and a quartz glass diffuser. The transmittance of the sample filter ($T_{sample}(\lambda)$) and the reference filter ($T_{reference}(\lambda)$) were each measured in triplicate using a custom-made, 512-channel spectroradiometer with an effective λ range of 350nm-850nm. Particulate absorption was calculated as

$$a_p(\lambda) = \frac{2.3 OD(\lambda)\beta}{1}$$
Eq. 2.4

where $OD(\lambda)$ is the optical density, β is the pathlength amplification factor or beta-factor, and the number one in the denominator is the geometric pathlength equivalent to the volume of water filtered divided by the clearance area of the filter (Butler 1962). $OD(\lambda)$ is the optical density and is calculated as

$$OD(\lambda) = \log_{10}\left[\frac{T_{referance}(\lambda)}{T_{sample}(\lambda)}\right]$$
Eq. 2.5

The beta factor (β) is an empirical formulation defined as the ratio of optical to geometric pathlength that corrects for multiple scattering inside the filter. To correct for pathlength amplification, β was determined from published work (Bricaud and Stramski 1990; Nelson and Robertson 1993) using the equation

Eq. 2.6

67

$$\beta = 1.0 + 0.6\text{OD}(\lambda)^{-0.5}$$

Absorption at 750nm was subtracted from the entire spectra to correct for either residual scattering caused by non-uniformity in wetness between the sample and reference filters or stray light.

Phytoplankton pigments were extracted from the sample filter with ~40-60ml of hot 100% methanol for 10-15 minutes in the dark (Kishino et al. 1985; Roesler et al. 1989). Fluorometric chlorophyll and pheaopigment concentrations were determined on the filtrate using a Turner 10-AU-005 fluorometer (Holm-Hansen and Rieman 1978). Following extraction, the sample filter was rinsed with Milli Q water to remove any excess methanol and to rehydrate the filter. Transmittance spectra were measured on this filter and the reference filter. The absorption spectra for detrital material and non-methanol extractable pigments (e.g. phycobiliproteins) were calculated using Eq. 2-4. Lastly, $a_\phi(\lambda)$ was calculated by subtraction using the following equation:

$$a_\phi(\lambda) = a_p(\lambda) - a_d(\lambda) \qquad\qquad \text{Eq. 2.7}$$

For CDOM absorption, water samples were filtered within four hours of collection, first through a 0.45μm GF/F filter, and then through a 0.2 μm nylon membrane filter. Filtrates were stored in clean 125mL amber bottles at -10°C and processed within one month of sample collection. Prior to measurement, samples were thawed overnight at 6°C and re-filtered through a 0.2 μm syringe filters to remove any particles that may have formed during the freezing and thawing processes. Absorbance measurements were then made using the same spectrophotometer as was used for particulate absorption (Cannizzaro et al. 2009).

The beam attenuation coefficient ($c(\lambda)$) for 480nm and 660nm was calculated using transmittance measurements collected in the field using two C-star beam transmissometers (Wet Labs, Inc., Philomath, OR). Each transmissometer was housed in a flow chamber as part of a larger flow-through system, and sample water was pumped

into the tank via a small pump. Beam attenuation for a given wavelength was calculated from raw transmittance using the following equation:

$$c = -\frac{1}{x}(\ln Tr) \qquad\qquad \text{Eq. 2.8}$$

where x is the pathlength between the light source and the detector, and Tr is transmittance and is calculated as:

$$Tr = \left[\frac{(V_{sig} - V_{dark}}{(V_{ref} - V_{dark})} \right] \qquad\qquad \text{Eq. 2.9}$$

where V_{sig} is the measured output signal, V_{dark} is the unit's dark voltage offset, and V_{ref} is the manufacturer supplied clean water offset.

2.3.3. Coupling the IOPs with the quasi-IOPs

Historically, and still commonly in use by the State of Florida, chlorophyll a concentrations are determined using a spectrophotometer in accordance with Standard Methods 10200H (Eaton et al. 2005; FLDEP 2009). Many environmental laboratories and regulatory agencies have switched to the EPA approved fluorometric method 445.0 which is considered to be a more accurate method (Arar and Collins 1997; Eaton et al. 2005). In the present study, chlorophyll a concentrations were determined based upon this fluorometric method. Samples for chlorophyll a concentration were collected at all water sample locations using one-liter amber plastic bottles. Samples were placed on ice and brought back to the University of South Florida's College of Marine Science Ocean Optics Laboratory for analysis. Using regression techniques, an empirically-derived equation was determined to allow direct conversion of chlorophyll a with a$_\phi$(440).

Additional water samples were collected at selected stations and analyzed for turbidity and color using methods commonly used for regulatory purposes. These samples were collected using 250mL clear plastic bottles, placed on ice, and shipped to

the Florida Department of Environmental Protection Central Laboratory Facility in Tallahassee, FL for analysis.

For regulatory purposes in Florida, water color is reported in units of Platinum Cobalt Units (PCU) and have historically been analyzed using an EPA approved method (EPA-140-A) in which a color wheel is used to visually compare a given sample against a known PCU color scale (Eaton et al. 2005). This method is crude with a resolution of only $\pm$ 5 PCU and a minimum detection limit of 5 PCU. Despite the existence of better methods, it is worthwhile to relate $a_g(\lambda)$ to PCU color given the thirty-year record of color in Tampa Bay (Conmy 2008). In addition, this method is still widely in use by many agencies, including the FDEP Central Laboratory Facility, the laboratory responsible for most of the state's water quality testing. For this reason, and to be consistent with historical determinations of PCU color, water samples collected in this study were analyzed for PCU color using this crude method. To relate PCU color with $a_g(\lambda)$, a linear regression model was fitted to data collected in this study. Local and regional resource management agencies are now switching to the newer EPA method (Method 110.3) that employs the use of a single-wavelength spectrophotometer for determining PCU color at much greater resolution and with lower detection limits compared to the color wheel method (Eaton et al. 2005). Over the past few years, the HCEPC has been collecting side-by-side water samples from various parts of Tampa Bay and analyzing them for spectrophotometrically-determined PCU color and for single-wavelength CDOM absorption. The relationship between PCU color at 345nm and $a_g(440)$ is examined for this larger Tampa Bay data set in the context of the current study.

In turbid coastal waters, turbidity, a quasi-IOP, and the scatter coefficient, an IOP, are directly related and can be used interchangeably (Kirk 1994; Kirk 1991). Most regulatory agencies report turbidity in Nephelometric Turbidity Units (NTU) using an EPA approved method (Method 180.1) (UU 1999). This method is based upon a comparison of the intensity of light scattered at an angle of 90° by a sample with the intensity of light scattered by a standard reference suspension at the same scattering angle. A primary standard suspension is used to calibrate the instrument. A secondary

standard suspension is used as a daily calibration check and is monitored periodically for deterioration using one of the primary standards. To relate this quasi-IOP with the scatter coefficient, a subset of water samples were collected, sent to the FDEP Central Laboratory Facility for turbidity analyses, and compared to b(480) and b(660) as determined by Eq. 2.3. A regression equation was fitted to these data allowing direct conversion of turbidity to the scatter coefficients which then can be used to estimate the light attenuation coefficients.

To model K_d an empirically derived relationship between K_d and the total absorption and scattering coefficients is used. Kirk (1981) established this relationship between K_d and the IOPs by expressing K_d/a as a function of b/a for monochromatic light using Monte Carlo simulation. The values of K_d/a over a range up to $b/a = 30$ fit very closely to the following equation:

$$K_d = [a^2 + gab]^{1/2} \qquad\qquad \text{Eq. 2.10}$$

where g is a constant whose value is dependent on the volume scattering function used (Kirk 1981; Kirk 1984). While this has proven to be a very robust relationship when the solar zenith angle (θ) is zero, K_d increases as the direction of the incident light increases from vertical (Kirk 1984). Using Monte Carlo simulation, Kirk (1984) accounts for differences in (θ) by modifying Eq. 2-6 to the form:

$$K_d = \frac{1}{\mu_o}[a^2 + G(\mu_o)ab]^{1/2} \qquad\qquad \text{Eq. 2.11}$$

where μ_o is the cosine of (θ) and $G(\mu_o)$ is a coefficient that determines the relative effect of scattering on the total attenuation of irradiance (Gallegos 2001; Kirk 1991). $G(\mu_o)$ is a linear function of μ_o and can be expressed as:

$$G(\mu_o) = g_1\mu_o - g_2 \qquad\qquad \text{Eq. 2.12}$$

where g_1 and g_2 are numerical constants. Kirk (1991) determined g_1 and g_2 to be 0.425 and 0.19, respectively using the volume scattering function for San Diego Harbor and found that these values were applicable to most coastal waters where $b{:}a < 30$. Gallegos (2001) reproduced the values for g_1 and g_2 found by Kirk (1984) by conducting 432 model runs allowing a to vary between 0.5 and 4.0 m^{-1} and b to vary between 0.5 and 40 m^{-1}, encompassing a range of $b{:}a$ between 0.5 and 20. Although Eq. 2.11 is entirely empirical, it has proven over the years to be highly accurate and applicable to a wide range of solar angles and $b{:}a$ ratios (Gallegos et al. 1990; Kirk 1981; Kirk 1984; Kirk 1994; Kirk 1991). Values for g_1 and g_2 determined by Kirk (1991) were used in the present study to estimate the $K_d(480)$ using $a_t(480)$ and $b(480)$. To calculate the solar zenith angle, the position and time of day for each sample station was input into the RADTRAN computer program (Sandia National Laboratories) (Weiner et al. 2008).

2.4. Results and Discussion

2.4.1. IOP spatial and temporal patterns

On an average annual basis, absorption coefficients for CDOM, detritus and phytoplankton were higher in the Kitchen than in any other area followed by Wolf Branch, Coffeepot Bayou and Egmont Key. Average annual absorption coefficients for CDOM, detritus, and phytoplankton were greatest in the Kitchen, followed by Wolf Branch, then Coffeepot Bayou, and finally Egmont Key (Figure 2-6).
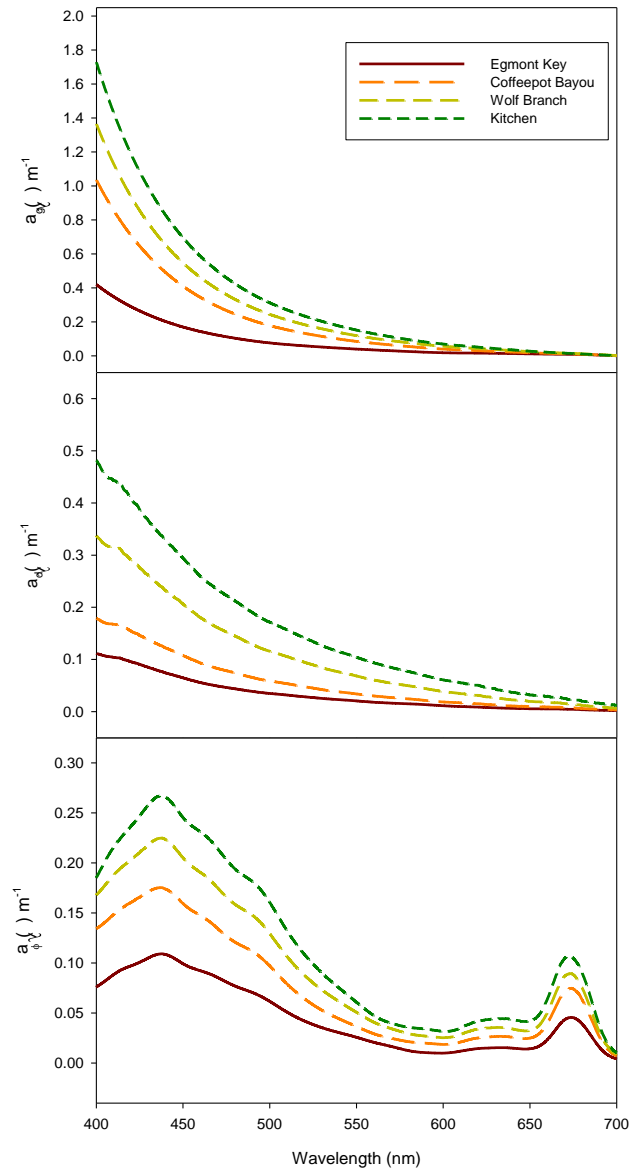
Figure 2-6. Average annual CDOM, detritus, and phytoplankton absorption spectra for each Seagrass Management Area. Note the different scales along the y-axes.

This pattern was inversely proportional to the distance from the mouth of the bay, with the Kitchen being furthest from the mouth and Egmont Key at the mouth. At 440nm in the photosynthetically useable blue region (400nm-490nm), the average annual $a_g(440)$ for the Kitchen was more than four times that of Egmont Key and almost twice that of Coffeepot Bayou (Table 2-3).

Table 0-3. Mean ± standard deviation of the annual chlorophyll concentrations and the annual absorption coefficients at 440nm for chlorophyll, CDOM, detritus, and total absorption.

	Chl a (mg L^{-1})	$a_\phi(440)$ (m^{-1})	$a_g(440)$ (m^{-1})	$a_d(440)$ (m^{-1})	$a_t(440)$ (m^{-1})
Kitchen	9.73 ± 6.62	0.2655 ± 0.129	0.8268 ± 0.459	0.3269 ± 0.131	1.4192 ± 0.568
Wolf Branch	7.40 ± 3.87	0.2233 ± 0.085	0.6509 ± 0.396	0.2315 ± 0.07	1.1057 ± 0.491
Coffeepot Bayou	5.45 ± 3.66	0.1736 ± 0.088	0.4893 ± 0.109	0.1207 ± 0.057	0.7836 ± 0.229
Egmont Key	3.09 ± 1.49	0.1052 ± 0.039	0.2013 ± 0.044	0.0774 ± 0.030	0.3839 ± 0.087

The standard deviation about the mean average annual $a_g(440)$ was greatest in the Kitchen suggesting that this area is subject to CDOM pulses driven largely by rainfall. Most CDOM sources in the Kitchen are locally derived and include a well developed mangrove shoreline, direct inputs from Bullfrog Creek, and secondary inputs from the Alafia River (Figure 2-5a). Similar to Kitchen, Wolf Branch also has a well developed mangrove shoreline, but unlike the Kitchen, has no major creeks (Figure 2-5b).

By contrast, the shoreline along Coffeepot Bayou is contained by a seawall. There are no major freshwater rivers and landuse is urban. Those few wetland systems in Coffeepot Bayou's watershed are impounded as stormwater ponds and have no direct connection to the bay. This results in an overall lower magnitude of CDOM absorption relative to that of Wolf Branch and Kitchen.

An often used and relatively simple method for comparing the characteristics of CDOM from various locations is to compare their $a_g(\lambda)$ spectral slopes (Branco 2005; Coble 2007; Hansell and Carlson 2002; Malick 2004; Minor et al. 2006; Steinberg et al. 2004; Vanderbloemen 2006). Spectral slope did not change much over the course of the study with annual average slopes ranging between -0.0190 to -0.0194. These values are consistent with those found in other parts of Tampa Bay. The spatial and seasonal distributions of CDOM in Tampa Bay indicate that the two largest rivers, the Alafia River near the Kitchen and Hillsborough River further to the north are dominant CDOM sources to most of the bay (Chen et al. 2007).

As with $a_g(440)$ detritus absorption ($a_d(440)$) was greatest at the Kitchen and Wolf Branch relative to Coffeepot Bayou and Egmont Key (Table 2-2). In addition to shoreline morphology and inputs from Bullfrog Creek and the Alafia River, detrital absorption is also a function of re-suspension of organic matter (Lawson et al. 2007). This is especially evident in the Kitchen where extremely shallow water and organic rich sediments are common. As with $a_g(440)$ and $a_d(440)$, average annual $a_\phi(440)$ was also highest in the Kitchen and followed the same pattern of decreasing absorption with proximity to the mouth of the bay. This pattern may be driven by higher nitrogen concentrations in the Kitchen and Wolf Branch resulting in higher phytoplankton productivity. This hypothesis is supported by long-term total nitrogen and chlorophyll data from fixed monitoring stations near the Kitchen and Egmont Key (Figure 2-7).
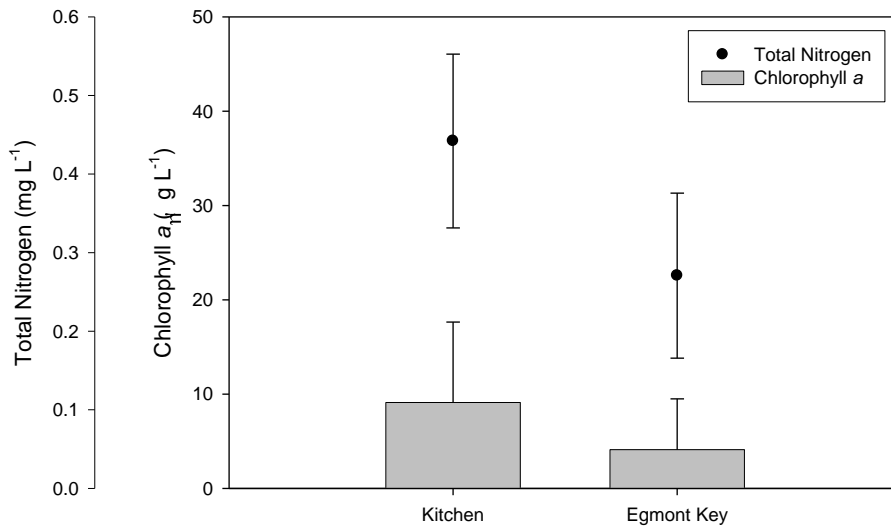
Figure 2-7. Total nitrogen and chlorophyll data from two long-term monitoring stations near the Kitchen and Egmont Key Seagrass Management Areas. Data are reported as averages ± standard deviation for the period 2004 – 2007. The Kitchen and Egmont Key were significantly different for both total nitrogen and chlorophyll a concentration (ANOVA; p<0.01). Source: Hillsborough County Environmental Protection Commission.

Because samples were collected every other month, the temporal resolution was rather coarse. However, seasonality in $a_\phi(440)$ and $a_g(440)$ for both the Kitchen and Wolf Branch is evident with maximum absorption occurring in August and minimum absorption occurring in December (Figure 2-8). Tampa Bay has distinct rainy and dry seasons and maximum absorption coincided with the rainy season, typically between the months of June through September, although the 30-days prior to the June sampling were very dry with rainfall totals of less than 3.0cm.
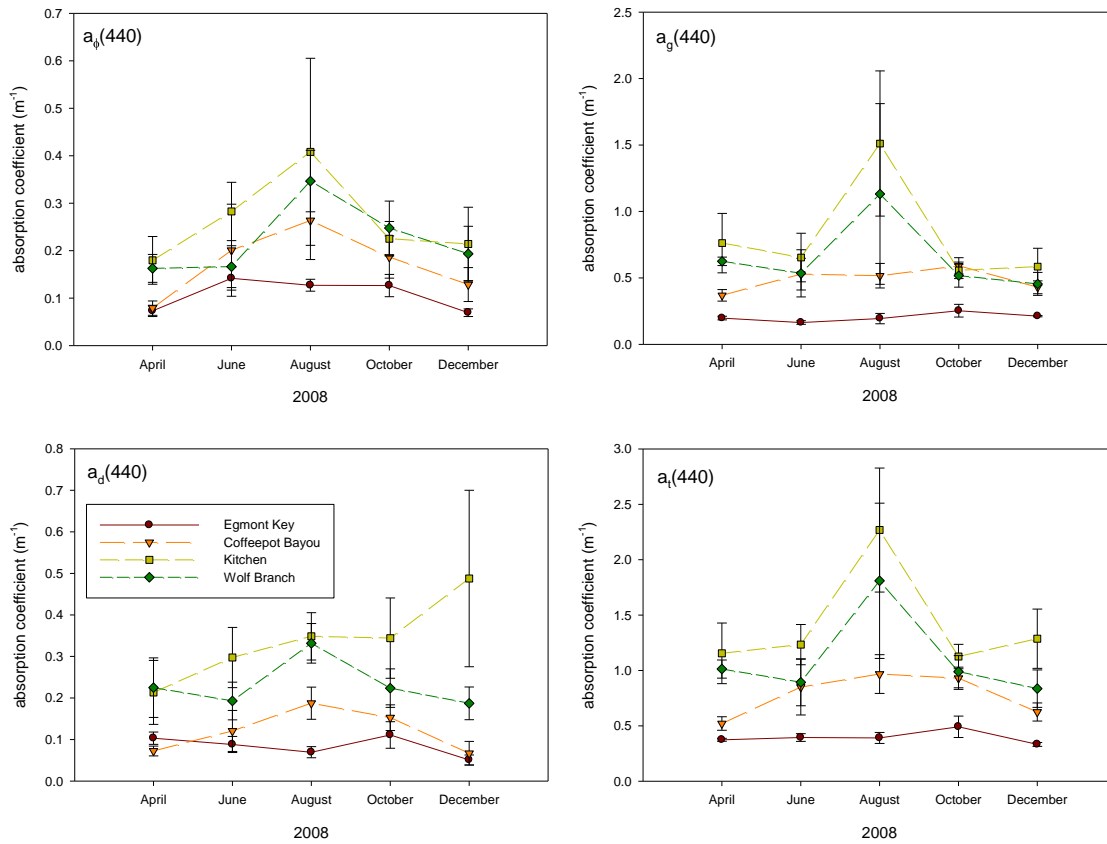
Figure 2-8. Monthly averages ± standard deviation of the mean for the inherent optical properties for the four Seagrass Management Areas.

Rainfall totals at the St. Petersburg station for 2008 was 117cm and was slightly below the average of 126cm. Also, peak rainfall occurred in July rather than the typical peak in August (Figure 2-9).
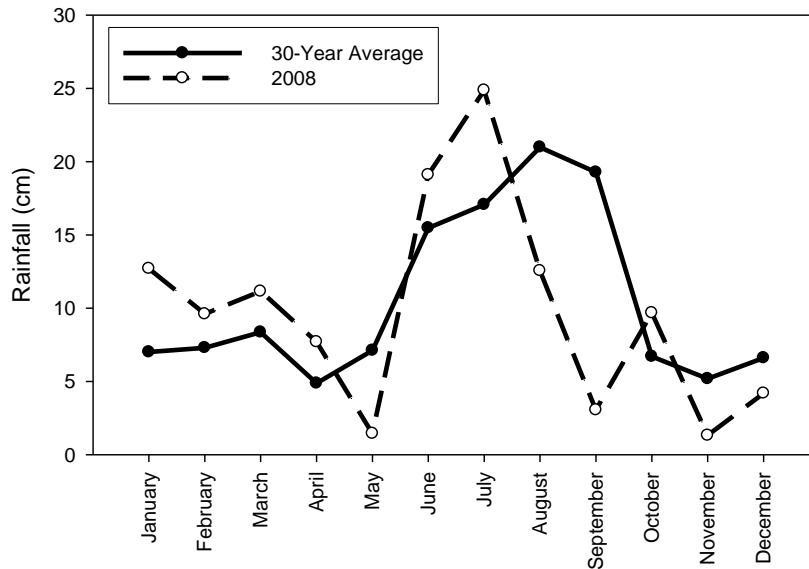
Figure 2-9. Historical monthly average rainfall and average rainfall for 2008 for St. Petersburg, FL. Source: National Weather Service.

Both $a_g(440)$ and $a_\phi(440)$ were compared with average rainfall for the 30-days preceding a given sample event. There was a strong correlation between $a_g(440)$ and rainfall for Kitchen (p<0.01; r^2=0.81) and Wolf Branch (p<0.01; r^2=0.92) but not for Coffeepot Bayou (p>0.05; r^2=0.12) or Egmont Key (p>0.05; r^2=0.16) (Figure 2-10a). The slopes of the best lines ranged from 0.032 in the Kitchen to -2.23 for Egmont Key decreasing with increasing proximity to the mouth of the bay (Figure 2-10a).

The correlation between $a_\phi(440)$ and rainfall was significant (p<0.05) for all four SMAs and exhibited similar patterns (Figure 2-10b). The slopes of the best fit lines from the Kitchen (r^2=0.64), Wolf Branch (r^2=0.88), and Coffeepot Bayou (r^2=0.65) ranged from 6.36 to 6.98 suggesting that while the magnitudes of $a_\phi(440)$ varied among SMAs, the $a_\phi(440)$ response to rainfall was similar. Egmont Key also exhibited a significant correlation between $a_\phi(440)$ and rainfall (p<0.05; r^2=0.67) but at a slightly different slope of 4.79 relative to the other three SMAs, due to the mixing of bay water with the Gulf of Mexico.

78
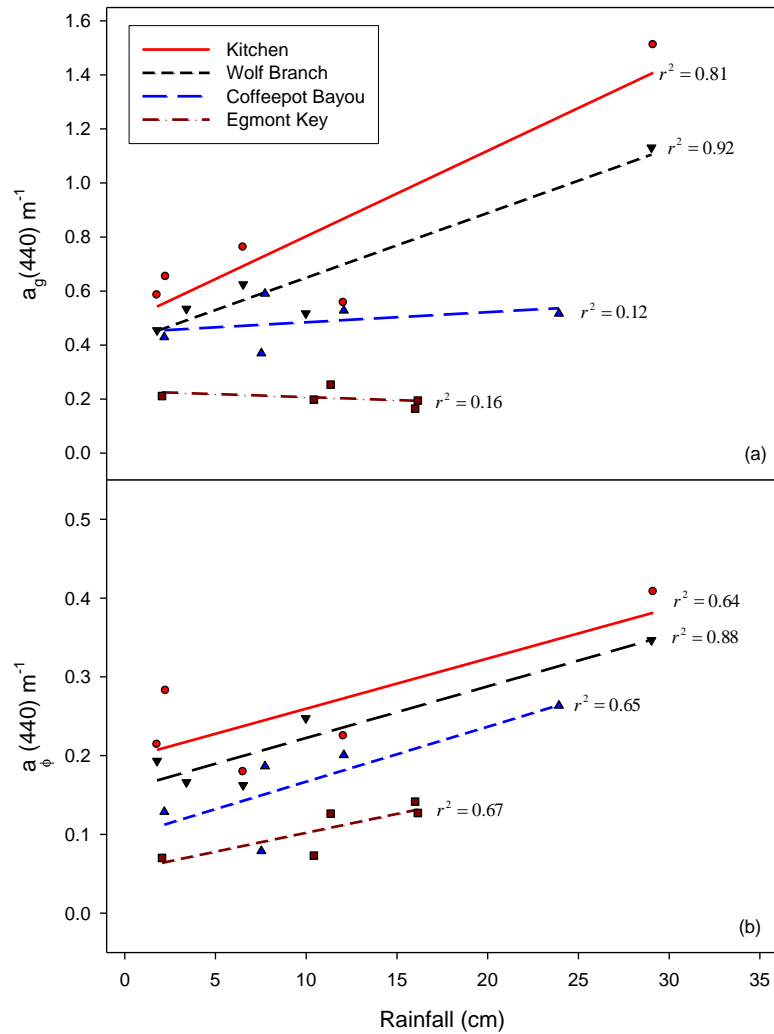
Figure 2-10. Scatter plot and best-fit line of the 30-day running average for rainfall and (a) $a_g(440)$.and (b) $a_\phi(440)$ for each Seagrass Management Area. Simple linear regressions were carried out for each curve with each the resultant r^2 listed to the right of the best-fit line.

Previous research has established a correlation between total nitrogen loads and rainfall in Tampa Bay (Janicki et al. 2003; Pribble et al. 2001). This suggests that the $a_\phi(440)$ response to rainfall may be associated with increases in nitrogen loads during high flow periods. Analysis of monthly HCEPC water quality data from 2004-2007 showed a significant differences between the two fixed stations closest to the Kitchen and

Egmont Key for total nitrogen and chlorophyll *a* concentrations (Figure 2-7) suggesting that the current nitrogen management paradigm may be appropriate for managing chlorophyll concentrations in the bay. However, the effect of reducing chlorophyll concentrations on increasing the amount of blue light at depth in seagrass areas is a function of the relative contribution of $a_\phi(\lambda)$ to $a_t(\lambda)$.

Overall, the relative contributions of $a_g(440)$, $a_\phi(440)$, and $a_d(440)$ to $a_t(440)$ on an annual average basis were very similar for the Kitchen, Wolf Branch, Coffeepot Bayou, and Egmont Key. In all cases, $a_g(440)$ represented approximately 61% of $a_t(440)$, while $a_\phi(440)$ only accounted for 20% of $a_t(440)$, with $a_d(440)$ accounting for the remaining 19% (Table 2-4). Absorption due to water $(a_w(440))$ represented less than 0.1% of the total absorption at 440nm and therefore was considered to be negligible.

Table 0-4. Annual percent contribution to the total absorption coefficient by chlorophyll absorption, CDOM absorption, and detrital absorption.

	$a_\phi(440)$	$a_g(440)$	$a_d(440)$
Wolf Branch	20.2%	58.9%	20.9%
Kitchen	18.7%	58.3%	23.0%
Coffeepot Bayou	22.2%	62.4%	15.4%
Egmont Key	20.8%	63.8%	15.3%

Traditionally the Tampa Bay model assumes that phytoplankton absorption is the primary cause of light attenuation. This assumption is part of a larger model describing an increase in nutrient availability leading to increased phytoplankton productivity and thus reducing the available light for seagrass (Cloern 2001; Janicki Environmental 2001). Most of these conceptual models are based on water quality information collected at stations not representative of the conditions in shallow waters (Lawson et al. 2007). In Tampa Bay, the data most utilized for model development are from fixed stations located throughout the deeper waters. Virtually none of these stations are located anywhere near seagrass areas where the optical properties can differ markedly from offshore areas. The results presented here strongly suggest that the existing model needs to be modified to

account for the dominance of CDOM as the major attenuator of light. At the end of the day, $a_\phi(440)$ may be the only component that can be effectively managed through nitrogen reductions and is much more problematic to manage for CDOM or detritus. Nevertheless, resource managers must take into account reductions in $a_\phi(440)$, although these reductions will affect only 20% of the total absorption.

2.4.2. Relationship between the IOPs and the quasi-IOPs

A multiple regression model was used to determine the contribution of $a_\phi(440)$ and the contribution, if any, of $a_g(440)$ to chlorophyll a concentration. Model results indicated that both $a_g(440)$ and $a_\phi(440)$ were significant at the 95% confidence level with an r^2=0.87.Standard error for $a_g(440)$ and $a_\phi(440)$ was 0.378 and 1.35, respectively. Using only $a_\phi(440)$ as the independent variable yielded similar results with an r^2=0.86 and a standard error of 1.15.

To predict $a_\phi(440)$ from chlorophyll a concentration, a simple linear regression model was applied to the entire data set and to each SMA. In all cases, the predictor equations explained between 68% and 89% of the variation (Table 2-5).

Table 0-5. Predictor equations for $a_\phi(440)$ based on chlorophyll a concentration for each Seagrass Management Area and for all areas combined.

Wolf Branch	$a_\phi(440) = 0.0192 Chl\ a + 0.0814$	$r^2 = 0.75$
Kitchen	$a_\phi(440) = 0.0179 Chl\ a + 0.0913$	$r^2 = 0.84$
Coffeepot Bayou	$a_\phi(440) = 0.0228 Chl\ a + 0.0492$	$r^2 = 0.89$
Egmont Key	$a_\phi(440) = 0.0198 Chl\ a + 0.0497$	$r^2 = 0.68$
All Areas	$a_\phi(440) = 0.0201 Chl\ a + 0.0647$	$r^2 = 0.86$

The weakest correlation was at Egmont Key where lowest chlorophyll a and $a_\phi(440)$ values were reported. Average chlorophyll a concentration for Egmont Key was 3.25 µg L^{-1} ranging from 1.05µg L^{-1} to 6.44µg L^{-1}. Average $a_\phi(440)$ for Egmont Key was

0.1140m[-1] ranging from 0.0571m[-1] to 0.1812m[-1]. These low values may explain why the r^2 for Egmont Key was lower than for the other SMAs.

The chlorophyll a - $a_\phi(440)$ relationship for the areas in this study were consistent with relationships found by other researchers along the West Florida Shelf (Cannizzaro et al. 2008; Cannizzaro et al. 2004) (Figure 2-11). As expected, Tampa Bay data fall on the upper end of the West Florida Shelf curve and are representative of the nearshore end members (Figure 2-11).
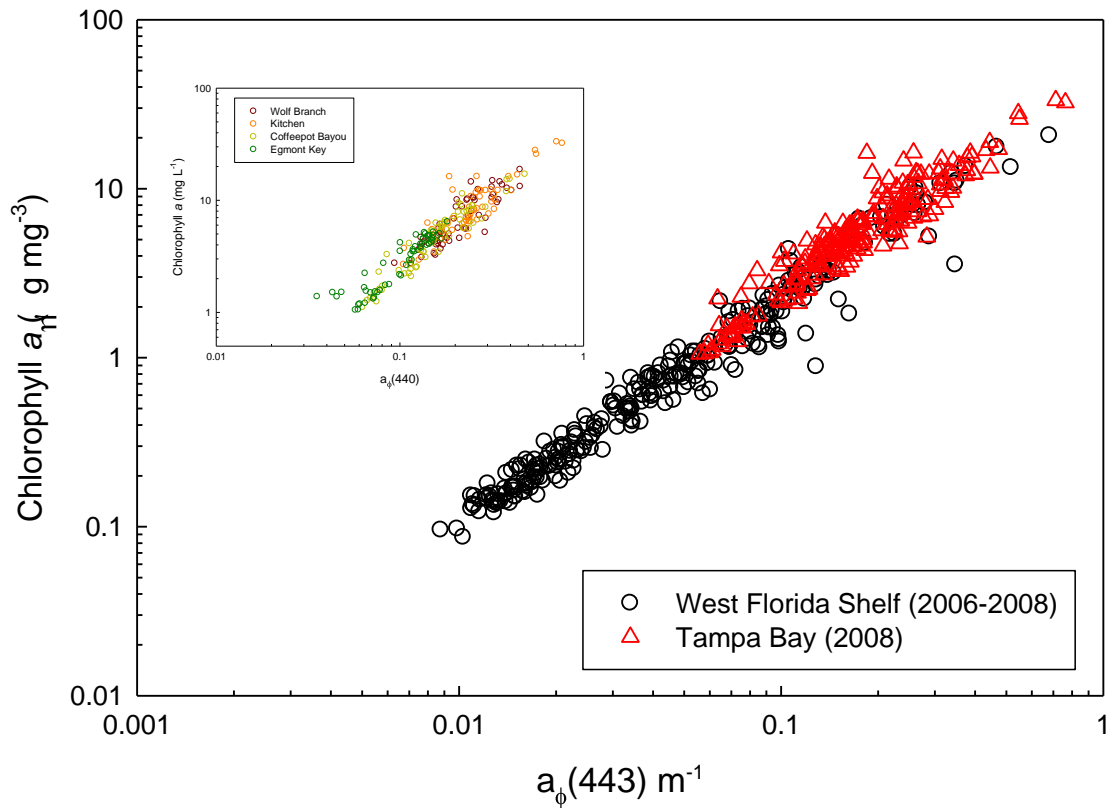
Figure 2-11. Chlorophyll a concentration and $a_\phi(443)$ for Tampa Bay, collected during this study, and data collected for the West Florida Shelf (Cannizzaro et al. 2004). Inset shows chlorophyll a concentration and $a_\phi(440)$ for data collected in this study from each of the four SMAs.

Turbidity is a simple and very common water quality parameter measured using a nephelometric turbidimeter. Essentially, a beam of light is directed along the axis of a cylindrical glass cell containing the sample. Light is scattered from the beam and a photomultiplier is positioned at a scattering angle of 90° (Kirk 1994). The measurement provided is in Nephelometric Turbidity Units (NTU) and is a measure relative to a known standard. Turbidity meters do not provide a direct estimate of any fundamental scattering property of the water, and measurements using these devices can be thought of as quasi-inherent optical properties. Nevertheless, in waters with moderate to high turbidity due to inorganic particles, turbidity should approximate the scattering coefficient such that a linear relationship should bear out. Turbidity data were collected for a subset of sites across each of the four Seagrass Management Areas and when plotted against the total scattering coefficients for 480nm and 660nm yielded a moderately strong relationship (Figure 2-12).
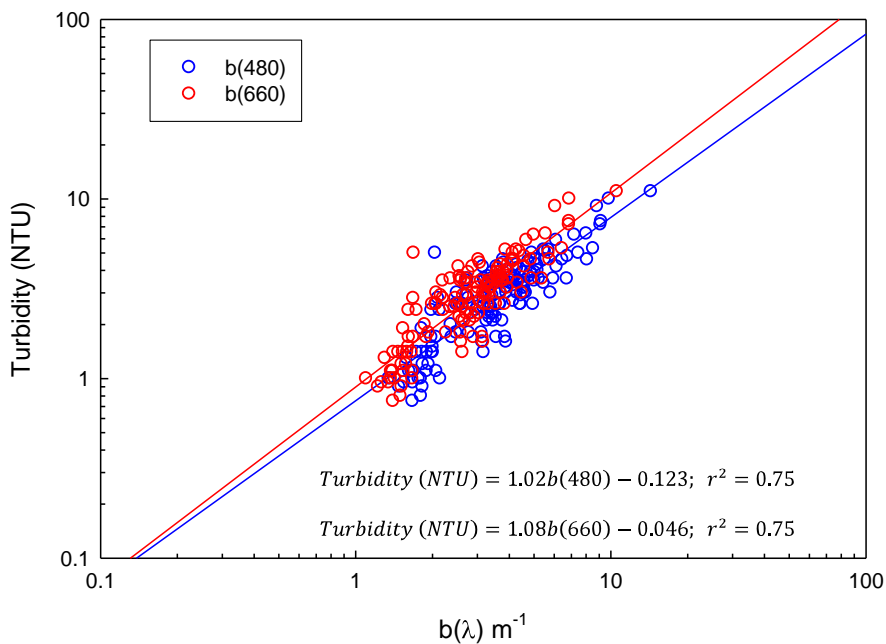
Figure 2-12. Relationship between turbidity and the scattering coefficients for blue light ($b(480)$) and red light ($b(660)$) for selected samples in Tampa Bay.

PCU color and $a_g(440)$ were weakly correlated mostly because of the coarse resolution of color measurements (Figure 2-13). Color was reported in ±5 PCU increments making these data more categorical than continuous. The City of Tampa's Bay Study Group has conducted extensive side-by-side comparisons of PCU color and $a_g(440)$ measurements and has demonstrated an almost one to one relationship between them (Figure 2-14). The City determines color by measuring absorbance at 345nm and then using a platinum cobalt standard, converting absorbance to color in PCU. This provides a much more robust measure of color, and regulatory agency laboratories are slowly making the change to the more quantitative method of measuring color.
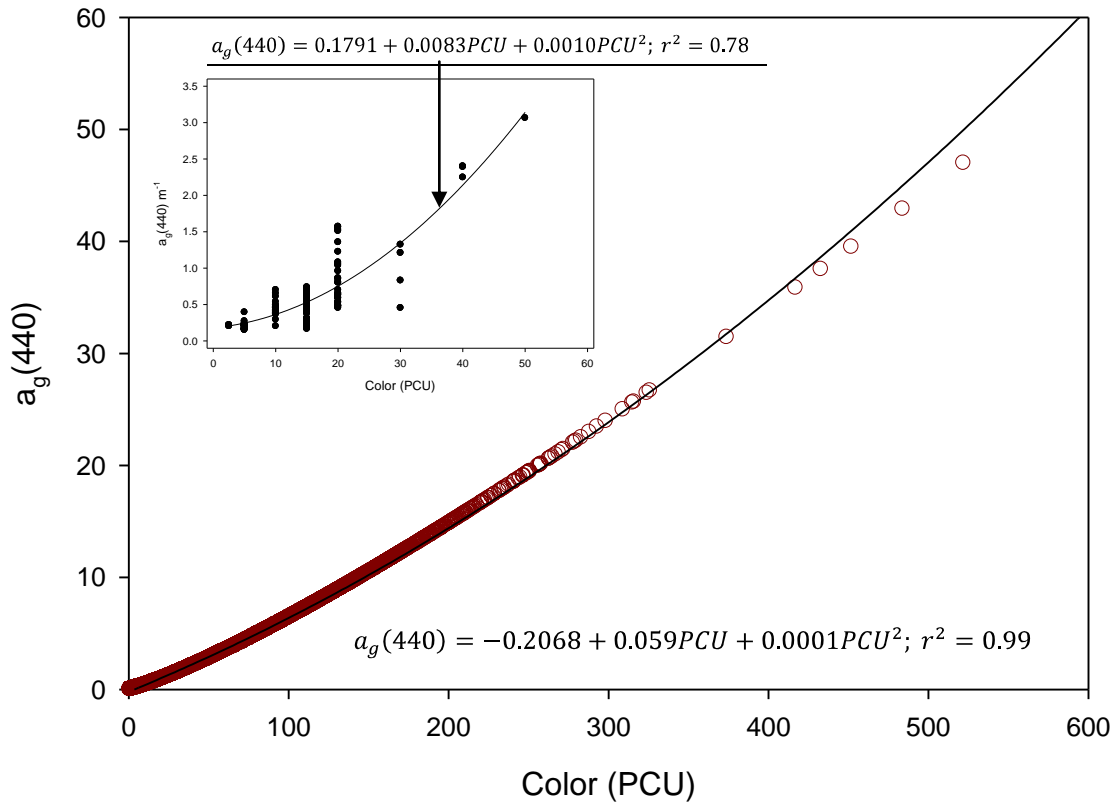
Figure 2-13. PCU color at 345nm plotted against $a_g(440)$ for samples taken throughout Tampa Bay by the City of Tampa's Bay Study Group (unpublished data). Inset shows the relationship between color and $a_g(440)$ for samples collected during this study. The stair step pattern is a result of PCU color being reported in ± 5 PCU increments.

2.4.3. Modeling K$_d$(480) for Tampa Bay

In this study, the attenuation coefficient at 480nm ($K_d(480)$) was calculated using Eq. 2.10 and the values for g_1 and g_2 as determined by Kirk (1991) for selected stations. Measured versus modeled $K_d(480)$ fit well against a 1:1 line with scatter being evenly distributed on either side of the line (Figure 2-14).
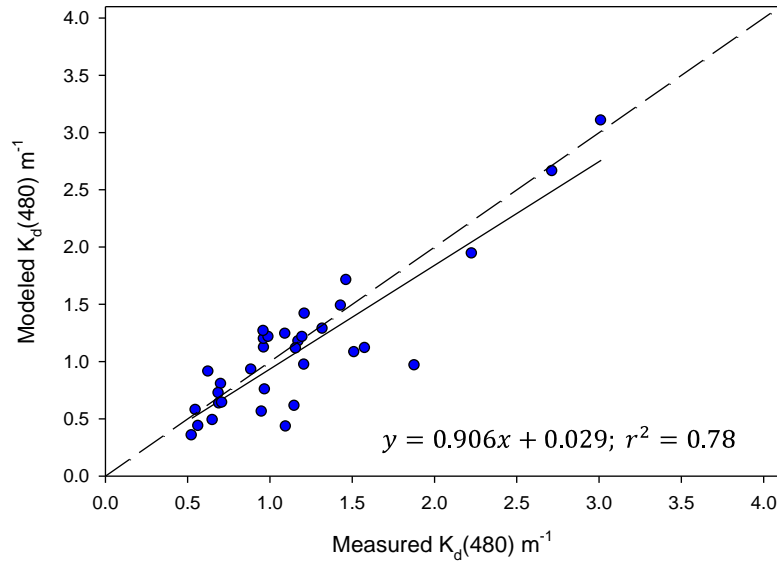
Figure 2-14. Plot of measured $K_d(480)$ against modeled $K_d(480)$.

The ratio of $b(480){:}a(480)$ for this study ranged from 1.74 to 34.4. With the exception of the single 34.4 value, all other values were within the recommended maximum value of 30 (Kirk 1984). Residuals ranged from 0.002 to 0.913 and the sum of the absolute values of the difference between measured and modeled values ($\sum|Err|$) was 7.03. An optimization program adjusted the coefficients g_1 and g_2 but did not yield an improvement in the $\sum|Err|$ term. Using Eq. 2-10, estimates of the $K_d(480)$ for all water samples were calculated and summarized in Table 2-6.

Table 0-6. Average annual summary table for predicted $K_d(480)$, $a_t(480)$, $b(480)$, and $b(480): a(480) \pm$ standard deviation for each Seagrass Management Area.

	$K_d(480)$	$a_t(480)$	$b(480)$	$b(480): a(480)$	N
Wolf Branch	1.16 ± 0.432	0.678 ± 0.357	4.01 ± 1.23	6.64 ± 2.38	60
Kitchen	1.47 ± 0.429	0.830 ± 0.324	5.95 ± 2.16	7.83 ± 2.96	57
Coffeepot Bayou	0.761 ± 0.223	0.439 ± 0.138	2.55 ± 0.962	5.77 ± 1.32	60
Egmont Key	0.459 ± 0.099	0.224 ± 0.051	2.55 ± 1.05	11.928 ± 5.73	56

As expected, the Kitchen had the highest annual average modeled $K_d(480)$ and highest standard deviation, while Egmont Key had the lowest annual average modeled $K_d(480)$ and the lowest standard deviation. Despite the relatively small sample size in this study, the model yielded good results. Nevertheless, further work is needed to refine the coefficients for the various conditions found in Tampa Bay and beyond.

2.5. Conclusions

The results in Chapter 1 of this study indicated that seagrass in Tampa Bay are largely blue-light limited, especially along the deep edges. Management decisions designed to improve the light environment for seagrass growth should focus on the blue wavelengths which are largely dominated by CDOM absorption. The current management paradigm does not address CDOM but focuses exclusively on light attenuation by phytoplankton absorption. Historically, management of nutrient load reductions has been successful in reducing chlorophyll concentrations in the bay, primarily through the increased level of wastewater treatment and improvements in stormwater management. While there is still room for improvement, it is unlikely that the large increases in seagrass coverage, as seen in the 1980s and 1990s, will occur given the already significant reductions in water column chlorophyll and the large fraction of total blue-light absorption due to CDOM.

Based on the results from this study, CDOM was the dominant blue light absorption component accounting for as much as 80% of the total absorption. This supports the conclusions of Chen, et al. (2007) who found on a bay-wide basis, $a_g(443)$ was five times higher than $a_\phi(443)$ in June and ten times higher in August. In the present study, the relative dominance of CDOM to $a_t(440)$ was consistent across all four

86

SMAs, even at Egmont Key which was expected to have a much greater percent contribution from $a_\phi(440)$ given its proximity to the Gulf of Mexico and relative distance from any major CDOM sources.

The contribution of $a_d(440)$ to $a_t(440)$ was not insignificant and in some cases exceeded $a_\phi(440)$. Given the shallow nature of the seagrass beds in Tampa Bay, wind-driven resuspension of organic material may be a primary cause of the relatively high contribution of $a_d(440)$ to $a_t(440)$, especially in areas where major sources of detritus from river inflows are minimal. Lawson, et al. (2007) found bottom stresses from wind-driven waves was the dominant predictor of light attenuation in Hogs Bay, Virginia, a shallow coastal bay off the U. S. mid-Atlantic coast. Lawson, et al. (2007) also points out that these wind-driven forces are episodic and often missed due to fair-weather monitoring or inappropriate sample site locations.

While relative contributions were similar across SMAs, differences in the magnitude of CDOM were largely a function of proximity to the Gulf of Mexico. Temporal variability in CDOM absorption was greatest in the Kitchen and Wolf Branch and was largely a response to pulsed events. There was a strong response to rainfall in both the Kitchen and Wolf Branch. For seagrass, the timing of these pulsed events may be critical to their survival. Typically, the highest rainfall occurs in the summer rainy season with peak rainfall in August and September during the height of the growing season. Anecdotal evidence of increases in seagrass coverage one year following the winter El Niño of 1997/1998 supports the hypothesis that the timing of high CDOM pulses is extremely critical. A better understanding of the impacts of the magnitude and timing of pulsed events is critical to successfully managing seagrass resources, especially in the face of sea-level rise and global climate change.

While there may be little resource management agencies can do to manage CDOM inputs to the bay, it is important to differentiate between anthropogenic and natural sources of light attenuation, especially in the face of growing regulatory pressure to implement numerical criteria for water bodies deemed impaired. One potential management action could be to remove the mosquito ditches adjacent to the Kitchen and Wolf Branch SMAs. These ditches could be increasing the conveyance of CDOM to the

bay by providing a direct conduit. However, more research is necessary to determine if hydrologic restoration of these ditches would in fact significantly change the CDOM load into these areas. There could be unintended consequences of such management actions. For example, reductions in CDOM could potentially result in increased phytoplankton productivity due to less shading, thus offsetting any benefit to removing the ditches.

Typically with high CDOM come high nutrients resulting in higher chlorophyll concentrations and phytoplankton absorption. The pattern of chlorophyll and phytoplankton absorption seen in this study supports this contention. Kitchen and Wolf Branch, the areas with the highest CDOM also had the highest chlorophyll concentrations and phytoplankton absorption coefficients. Comparing nutrient and chlorophyll data from two long-term monitoring stations, one near Egmont Key and the other near the Kitchen, shows a strong correlation between increased total nitrogen and increased chlorophyll concentration. This is good news to resource management agencies spending millions of dollars to reduce nutrient loads into the bay.

By regressing chlorophyll *a*, color, and turbidity with the IOPs, a series of predictor equations were developed and will be very useful in estimating SMA-specific absorption and scatter coefficients. Linking the IOPs with the quasi-IOPs provides a means to infer past optical conditions using historical data. The relationship between $a_\phi(440)$ and chlorophyll concentration yielded similar regression equations across all four areas and is further evidence that while these shallow seagrass areas may be unique relative to the rest of the bay, it is likely that many of the 30 bay-wide SMAs can be merged together to create a simpler framework for management purposes. Of course this will need to be verified for other SMAs and over longer time periods. The relationships determined in this study were based on data collected in 2008, a normal year for rainfall. It is unknown whether these relationships will hold under varying conditions such as during a prolonged La Niña or El Niño or in the aftermath of a major hurricane.

Finally, the utility of using an empirically derived model to estimate the light attenuation coefficient at 480nm was demonstrated by using absorption and scatter coefficients of the same wavelength. This model is very useful in that it links the AOPs with the IOPs and allows much more insight into the underlying causes of attenuation.

For resource management agencies tasked with setting light targets, this model is very powerful in that $K_d(\lambda)$ based targets can be set on the basis of the IOPs that are by definition intrinsic to the optical properties of the water and independent of the ambient light conditions at the time of sampling. This drastically increases the operational tempo of a monitoring program because it relieves the constraints normally associated with measuring AOPs, such as sky cover and sea state. Of course validation of this model must be incorporated into any monitoring program using $K_d(\lambda)$ derived from measured $E_d(\lambda)$ using a spectral light monitoring system like the one described in Chapter 1.

Chapter 2 Synoptic Surveillance of the Underwater Light Field Using a

Continuous Deck-Mounted Flow-Through System

3.1. Abstract

Greater spatial and temporal information about the shallow water light environment is critical to understanding seagrass ecology. The spatial and temporal variability inherent in shallow seagrass areas makes it difficult to accurately assess conditions using discrete measurements. Remote sensing of the water column can also be problematic due to interference from bottom reflectance. The use of a flow-through system designed to operate in water depths of less than 2.5m would provide relevant optical data at spatial resolutions not possible using other techniques. The flow-through system used in this study was modified to operate in a small, open-hulled boat in depths as shallow as 0.25m. The payload included chlorophyll and colored dissolved organic matter (CDOM) fluorometers that were used to estimate the chlorophyll a concentration, as well as the phytoplankton ($a_\phi(\lambda)$) and CDOM ($a_g(\lambda)$) absorption coefficients. To accomplish this, discrete water samples were collected during each survey and analyzed in the laboratory. Empirical equations were derived to calculate $a_\phi(\lambda)$ and $a_g(\lambda)$ from raw chlorophyll (FL_{Chl}) and CDOM (FL_{CDOM}) fluorescence voltage measurements. Relationships between (FL_{Chl}) and $a_\phi(440)$ approximated a linear fit, with correlation coefficients ranging from 0.80 to 0.84. A second-order polynomial equation best fit the relationship between (FL_{CDOM}) and $a_g(440)$ with correlation coefficients ranging between 0.88 and 0.92. This non-linearity was observed across all surveyed areas using two different models of fluorometers, and was a function of the inherent non-linearity within the CDOM absorption spectra. Regressing $a_g(312)$ against FL_{CDOM} approximated a linear fit (p<0.01; r²=0.91). The potential for interferences from $a_\phi(440)$ and the detrital absorption coefficient ($a_d(440)$) on FL_{CDOM} were explored using multiple regression procedures, but resulted in no improvement over the non-linear predictor equations. The Kitchen Seagrass Management Area, a 776 hectare area located along the shoreline of eastern Tampa Bay, is presented as a case study to demonstrate the utility of using a flow-through system approach to detect spatial and temporal differences in

CDOM and chlorophyll *a* concentration. CDOM was concentrated along the immediate shoreline. This CDOM-rich water mass only extended out approximately 600m from the shoreline and covered all of the seagrass growing within this area. The complex patterns in CDOM and chlorophyll *a* demonstrate the need to adequately characterize the variability in shallow seagrass areas. There is a danger in relying too heavily on discrete water samples to infer conditions. The nearest long-term water quality monitoring station is well outside the Kitchen yet data from this station are routinely used to evaluate the light environment over the seagrass. Without the use of a flow-through system, is evident management decisions designed to protect and restore seagrass could be based on erroneous conclusions.

3.2. Introduction

The need for more and better optical data is a constant challenge, especially for resource management agencies in Florida who are being tasked to develop transparency standards for protecting seagrass communities. Over the past two decades, there has been an impressive amount of research investigating the properties of the underwater light field and its effects on seagrass survival (Abal et al. 1994; Biber et al. 2008; Cummings and Zimmerman 2003; Dennison 1987; Dixon 2000; Enriquez 2005; Enriquez et al. 1992; Greening 2004; Kenworthy and Fonseca 1996; Miller and Mcpherson 1995; Ralph et al. 2007; Zimmerman 2003). All of these studies underscore the need for more spatial and temporal data, a common problem among budget conscious government agencies as well. Fortunately, technological advancements in hardware and data processing software have made it possible to sample large areas repeatedly without being cost prohibitive. Until recently, the lack of rugged and portably field instruments, such as spectrophotometers necessary to accurately characterize optical measurements like CDOM absorption and fluorescence, played a large part in contributing to the paucity of optical information (Hoge et al. 1993).

The use of a deck-mounted flow-through system to monitor optical conditions while underway promises to greatly enhance the way transparency data are being collected and analyzed. Flow-through systems have been in use for some time (Madden and Day 1992) but to date, none have been used in very shallow seagrass beds like those found in Tampa Bay, where depths rarely exceed 4m and are often less than 0.25m. Traditional methods of measuring in-water optical properties in Tampa Bay require a minimum depth of a t least 1.5m (Dixon and Leverone 1995; E.P.C.H.C. 2007; TBNEP 1996) which can create data bias, potentially resulting in erroneous conclusions.

To assist environmental resource management agencies in developing better monitoring techniques, a method of using a deck-mounted flow-through system in shallow seagrass areas is presented.

3.2.1 The underway flow-through system approach

An underway flow-through system, originally designed to be operated at sea, was employed in very shallow waters to characterize the optical properties of selected Seagrass Management Areas in Tampa Bay, FL. The payload included three chlorophyll fluorometers, two colored dissolved organic matter (CDOM) fluorometers, two backscatter meters, two transmissometers, a conductivity-temperature (CT) probe, and an onboard GPS (Table 3-1). While there are newer instruments on the market today, the payload used aboard this system included all the necessary hardware to collect optical data commonly used in seagrass and water quality management.

Table 2-1. Payload description of the underway flow-through system used for this project. The system in its current configuration includes redundant instrumentation for data validation and to account for operational differences among units.

Parameter	Unit	Orientation
CDOM Fluorescence	Wet Labs WET Star Fluorometer	Inline
	Wet Labs ECO Fluorometer	In-tank
Chlorophyll Fluorescence	Wet Labs WET Star Fluorometer	Inline
	Sea Tech Fluorometer	In-tank
	Wet Labs BB2F	In-tank
Red & Blue Backscatter	Wet Labs BB2F	In-tank
	HOBI Labs HyroScat-2	In-tank
Red & Blue Transmittance	Wet Labs C-star Transmissometer	In-tank
Conductivity / Salinity	Falmouth Scientific CTD	In Tank
Temperature	Falmouth Scientific CTD	In Tank

The concept of underway monitoring has been in around for some time (Buzzelli et al. 2003; Ensign and Paerl 2006; Madden and Day 1992; Paerl et al. 2009). In this study the concept is applied to modeling the inherent optical properties (IOP) of shallow waters within discrete Seagrass Management Areas (SMA). Thirty SMAs have been designated by the Tampa Bay Estuary Program and its partners based on a priori information related to historical seagrass coverage, water quality, hydrodynamics, and shoreline morphology (E.P.C.H.C. 2007).

Of special interest in Tampa Bay is the dominance of CDOM as a major absorber of blue light. Results from Chapter 1 indicated that seagrass in much of Tampa Bay are

blue-light limited. In Chapter 2, CDOM absorption accounted for as much as 60% of the total absorption of blue light in the SMAs studied. In addition, phytoplankton absorption made up an additional 20% of the total absorption of blue light.

In terms of the magnitude of CDOM and phytoplankton absorption, the Kitchen, located in eastern Tampa Bay was the most CDOM-rich area with the highest CDOM absorption occurring during the rainy season when inputs from river discharge and runoff are more prevalent. Chlorophyll absorption was also greatest in the Kitchen. Likely CDOM sources include a well established mangrove shoreline and direct river inputs of CDOM-rich waters from nearby streams.

The flow-through system was used to survey CDOM absorption in the Kitchen and other SMAs every other month for one year. The CDOM absorption coefficient at 440nm ($a_g(440)$) was empirically derived using raw CDOM fluorescence and $a_g(440)$ mesured from discrete water samples collected during each survey. The phytoplankton absorption coefficient at 440nm ($a_\phi(440)$) and the chlorophyll *a* concentration were als0 determined using empirical regression techniques. Surveys were designed using a "connect-the-dots" approach in which survey tracks passed over each discrete sample station creating a seamless record of optical measurements. This "connect-the-dots-approach" can be incorporated into existing monitoring programs as a way to repeatedly quantify differences between routine monitoring stations.

3.2.2 Principles of in-water fluorescence

While phytoplankton cells absorb light in the photosynthetically useable blue and red regions of the visible spectrum, they can also emit light. About 1% of the ambient light absorbed by phytoplankton cells is re-emitted as fluorescence in the red region centered around 685nm (Kirk 1994). Fluorescence can be induced by exciting cells with a light source of known intensity at a wavelength centered at 460nm and measuring the intensity of the emitted light at a wavelength centered at 695nm. Most in-water fluorometers use an LED as the excitation source. Some fluorometers use a halogen light source as does the SeaTech unit aboard the flow-through system used in this study. All others aboard the flow-through used LED light sources. CDOM fluoresces in the blue wavelengths when excited by light in the ultraviolet wavelengths. Peak fluorescence is

commonly found at 250nm and 350nm depending on its source (Coble 2007). Highest fluorescence efficiencies are found in fresh, terrestrial and deep marine waters while lowest efficiencies are typically found in offshore surface waters due in large part to photodegradation. Depending on the excitation (Ex) and emission (Em) peak wavelengths, specific components can be identified. Eight general types of fluorescence peaks have been identified. For example, an Ex/Em pair of 260nm/400nm-460nm indicates the presence of humic-like material and an Ex/Em pair of 275nm/305nm indicates a protein (tyrosine)-like component suggesting an autochthonous carbon source (Coble 2007). The excitation/emission wavelengths for the fluorometers aboard the flow-through system varied somewhat.

3.3. Materials and Methods

3.3.1. Flow-through system design and specification

An underway flow-through system allows continuous recording of optical data and affords the ability to detect spatial patterns not observable through traditional methods. The flow-through system payload included a conductivity/temperature sensor, blue and red transmissometers, chlorophyll fluorometers, CDOM fluorometers, and blue and red backscatterometers (Table 3-1). All underway instruments were mounted on a black metal frame which placed inside a large tank whose walls were painted black (Figure 3-1). Water was pumped through the chamber using a small pump with an average discharge rate of 38 liters per minute and was powered by an external 12V marine battery. At this discharge rate, residence time in the tank for a given parcel of water was approximately 3 minutes.

The flow-through system was designed with built-in redundancy to provide a backup in case of system failure and to cross-check measurements from units with different design specifications and operational characteristics (Cannizzaro et al. 2009). Redundant "in-line" chlorophyll *a* and CDOM fluorescence sensors provided a measure of any high frequency changes that may not have been detected by sensors in the tank. The advantage to operating the instruments in a closed tank rather than under ambient light conditions is that it eliminates the potential for contamination by solar-stimulated

fluoresced photons (Stramski et al. 2008). In order to minimize the chance that light emitted by one sensor is detected by another sensor, sensors were oriented within the chamber so that light emitted from one instrument would not directly enter the field of view of another instrument (Cannizzaro et al. 2009). The scatterometers were arranged inside the tank to maximize the distance between the instruments and the chamber walls reducing the likelihood of interference from reflected light off the tank walls. This is mainly a concern when operating in very clear waters and was not a concern in this study.
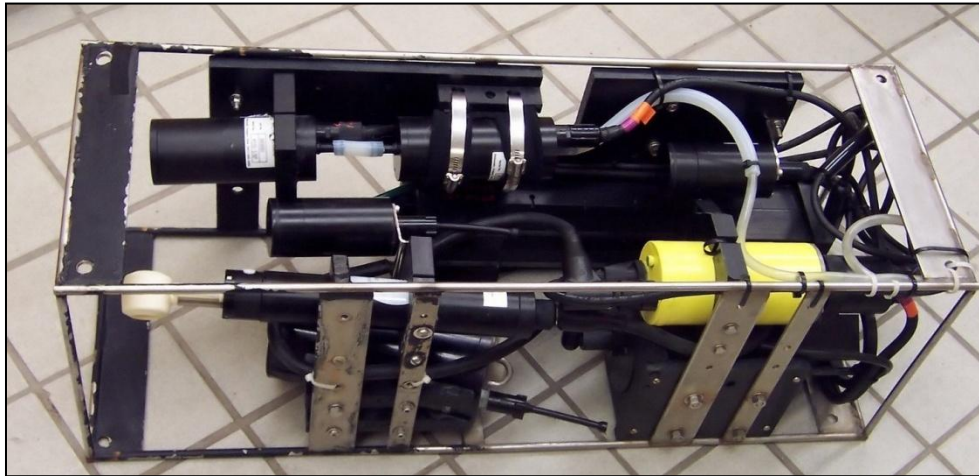
Figure 2-1. The deck mounted flow-through system used in this study.

3.3.2. Synoptic survey of Seagrass Management Areas

Synoptic surveys of the optical properties were conducted in selected Seagrass Management Areas in Tampa Bay, FL. Prior to leaving the laboratory on the morning of a survey, a full-systems test was conducted on all instruments. All cables and instruments were visually inspected and the system was connected to a ruggedized field laptop computer (Panasonic Toughbook CF-29). Except for the ECO fluorometer and the HydroScat 2 that were connected directly into the laptop via a serial-to-USB switch, all other instruments were routed through the CTD via an analog to digital converter to the laptop for logging. In addition to logging all flow-through data while underway, the laptop also provided positional information from a built-in GPS unit. All positional data were recorded in the WGS 1984 geographic coordinate system. The laptop also had navigational software (Fugawi ENC Ver4.5, Northport Systems, Inc., Ontario, Canada)

that allowed the overlay of the predetermined survey track onto a digital nautical chart. Optics were wiped clean of moisture and debris and then allowed to sit in air for approximately 10 minutes. Air measurements, in raw counts, were written down and compared to calibrated values to ensure they were within ±5%. Once the system passed its pre-cruise check, all cables were carefully disconnected and the system was prepared for transport to the field site.

Once onsite, the system was carefully loaded onto the boat and placed into the tank. Depending on the vessel used, the tank typically sat roughly between the center console and the bow. All cables were carefully reconnected and the system was turned on. A similar pre-cruise check was conducted in the boat while still onshore to make certain all systems were operating. This was a very important part of the pre-deployment process. Once the instruments passed their final pre-cruise check, they were set to begin logging. It was not necessary to stop logging data until the survey was complete unless there were problems with the system that necessitated immediate action.

A detailed field log was kept throughout the survey for mission reconstruction during the data evaluation phase of the project. Once the flow-through system was running and actively logging, the pump was connected to the tank and the pump intake affixed to the gunwale with the nose pointing in the direction of the flow path (ie. toward the bow) to minimize turbulence and air bubbles while underway. A small centrifugal wash-down pump (Water Puppy), with neoprene impellers to minimize damage to phytoplankton cells, was used, though ideally a diaphragm pump is preferred. This pump operated off of a standard 12V marine battery and had a discharge rate of 10gpm. At this flow rate, it took approximately three minutes to fill the tank. The hose leading from the pump to the tank was attached near the top of the tank. This was done primarily to allow sediments, or other large particles, to settle to the bottom of the tank instead of being repeatedly re-suspended by the incoming flow, as would happen if the hose were located near the bottom of the tank. Placing the inflow hose near the top also had the added advantage of allowing any air bubbles to escape out the top of the tank since the tank lid was not airtight. An inline y-valve was inserted just before the tank to divert some of the flow to the in-line CDOM and chlorophyll instruments. To minimize turbulence, flow

through the in-line fluorometers was adjusted to approximately 0.5gpm using the y-valve. Water leaving the tank drained out of a hole near the tank base opposite the inflow. A hose was connected to the drain and allowed to flow over the gunwale but away from the pump intake. The pump intake consisted of a ½" PVC intake pipe connected via a hose clamp to a flexible PVC hose attached to the pump. To keep the nose of the intake pointing at a downward angle of approximately 20° from the water surface, and to minimize yaw, the intake was weighted by two 10lb dive weights. The intake was attached to the gunwale such that the intake's pitch and height above the bottom could be adjusted on the fly. This was accomplished by attaching two lines from the intake to the boat. The forward or bow line was attached from the base of the intake pipe to a forward cleat. This line was used to adjust the pitch of the intake and was typically not adjusted once set. The aft or stern line was attached from the upper end of the intake and wrapped around an aft cleat. This line was used to adjust the depth of the intake and typically was handled by an operator for making quick depth adjustments.

Intake depth was usually between 0.25m and 0.50m and was located just below the boat hull. Minimum survey depth was 0.25m set by the boat's draft. At the intake nose, a mesh screen was attached to help exclude large floating particles from entering the tank. The screen was also designed to be a failsafe during those inevitable times when the intake dragged bottom in very shallow waters. When this occurred, the survey typically was stopped and the tank inspected for sedimentation. If it was determined that a large amount of sediment entered the tank, the flow-through system was lifted out of the tank, the tank was drained, and then rinsed with seawater. The entire process took several minutes and was documented in the underway log for data evaluation in the post-processing stage.

Survey areas in Tampa Bay varied from $3km^2$ - $12km^2$, and depending on the number of legs, survey times lasted between two and three hours. Maximum underway speed was approximately 5kts, above which excessive turbulence at the intake caused erratic backscatter measurements. Maximum speed was also constrained by depth along the shallow margins. While the Seagrass Management Areas were well delineated, the extent of the survey track was dependent on the desired spatial resolution. All survey

routes were delineated and plotted prior to starting the survey but occasionally needed to be edited in the field if depth conditions were too shallow or other circumstances made it impossible to follow the pre-plotted track. Track routes were based on a number of factors and in no small part to trial and error. A minimum of ten water sample locations per survey were selected for IOP determinations to allow for conversion of raw fluorescence data into absorption coefficients and chlorophyll concentrations. While these locations were initially chosen at random, some were adjusted to ensure that a wide cross section of optical conditions were captured (Figure 3-2). Occasionally it was necessary to move a sample location due to shallow water conditions preventing boat access.
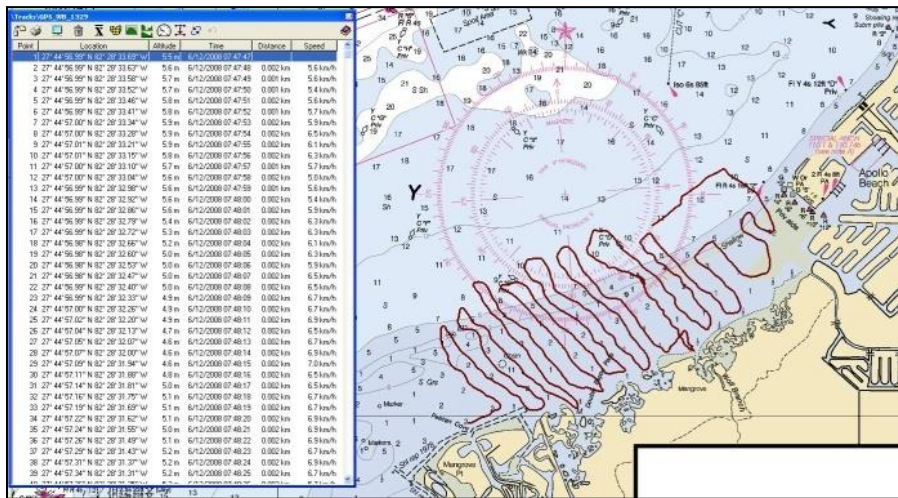
Figure 2-2. Example survey track from June 2008 for the Wolf Branch Seagrass Management Area.

This set the initial survey framework by which a connect-the-dots approach was applied (Figure 3-2). A secondary constraint was the addition of additional field measurements collected on the same cruise by other researchers, making it necessary to tailor track routes to accommodate these other sampling schemes. A third important constraint was depth. Early track routes were mostly based on depth data from nautical charts and limited local knowledge of the area, but as the project progressed, survey tracks were based more on actual depths, sometimes determined the hard way by running aground

and being forced to walk the boat off the bar. Over the course of a three hour survey, conditions did not remain static and by the time the boat reached the far end of the survey track the optical properties may have changed. This was an inherent bias when surveying large areas and must be kept in mind when analyzing spatial patterns over relatively large areas. Tidal stage, wind conditions, and currents were documented during each survey and were useful during post-mission reconstruction. Survey tracks were typically set up in a serpentine pattern (Figure 3-2) essentially creating a series of transects perpendicular to the shoreline that could be parsed out of the dataset to be analyzed as a standalone product. Each transect took approximately 30 minutes to complete.

Sea state was also a major concern and potential source of error. Because the flow-through system was originally designed to be on a large research vessel with plenty of cabin space, some design modifications were made to ruggedize the system for use on a small, open deck, boat. A secondary wiring box was added to the system housing any excess cable, the serial-to-USB converter box, and the instrument batteries. While this box was not completely waterproof it kept the electronics relatively dry. Another modification was to the tank locking mechanism which would no longer secure the tank's lid. This generally is a major problem when the seas are flat. However, during pre-deployment trials, whenever the sea state was greater than one foot, the tank lid would not stay closed and the flow-through system would experience excessive sloshing. The addition of adjustable straps eliminated this problem by securing the lid while still allowing some water to overflow the tank thus acting like a large de-bubbler.

3.3.3. Data management and analysis

All raw data were logged onto a hard drive mounted onboard the field laptop. Most of the instruments, with the exception of the ECO fluorometer, logged internally acting as a backup. The CTD acted as the main backup data logger for the in-line fluorometers, the transmissometers, and the CTD itself. At a data logging rate of half second intervals, a typical survey resulted in about 30,000 rows of data with as many as 30 parameters per row. This large quantity of data required a sophisticated data management strategy. The foundation of this strategy was based on four basic data levels. Each increasing level represents a more refined data product. Depending on the analysis

need, data from multiple levels may be used but generally analyses took place on Level 3 data.

Level 0 is the most basic level and represents raw data taken directly from the instruments. All data were logged by default at 0.5sec intervals unless otherwise specified. All raw data from the CTD and associated instruments were in units of digital counts from 0 to 4095. Geographical position data from the onboard laptop GPS was stored in a separate data file by the navigational software (Fugawi ENC).

All data stored as Level 1 data were binned to the nearest minute using a simple binning routine. CTD, GPS position, and backscatter data were stored in separate data files. All Level 1 CTD data remained in digital counts while BB2F and HS2 data were reported as the various scatter coefficients. Conversion of scatter data from raw counts occurred onboard the instruments using calibration files resident on the instruments. Data files containing raw signal counts were also saved and afforded the opportunity to apply locally derived constants to the scatter conversions.

At Level 2, optical fluorescence and transmittance data were converted into voltages and prepared for post mission reconstruction in which data were reviewed against the field logs. All instruments had an effective output range of $0 - 5$ VDC. Counts were converted into voltages using the simple equation:

$$VDC = \left(COUNTS/4095\right) \times 5 \qquad \text{Eq. 2.1}$$

Detailed notes entered into the field log were an invaluable tool when post processing because, as stated earlier, once the instruments were set to log prior to starting the actual survey, they did not stop logging until the survey was complete. On a typical mission, breaks in the survey track occurred at least half a dozen times for various reasons such as if the boat stopped at a fixed location to collect other data or when the boat ran aground in very shallow water and had to be pushed back into deeper waters. Data not part of the survey were simply parsed from the Level 2 dataset. Once all erroneous data were removed, GPS position data were merged with the CTD and backscatter datasets.

Data at Level 3 represented the final data products used for analysis. At this level, data were converted from voltages to relevant units. For the transmissometers, the conversion from voltage to beam attenuation was a two-step process. The first was to convert voltage into transmittance and then transmittance into beam attenuation as described in Chapter 2. Conversion of fluorescence voltage to absorption coefficients was done empirically using absorption coefficient data from selected grab samples (N≈200). Each survey mission included at least ten water samples taken back to the laboratory and analyzed for absorption by CDOM, phytoplankton, detritus as well as for chlorophyll concentration. The resultant regression equations were used to convert the rest of the survey data into relevant units.

3.4. Results and Discussion

Determinations of $a_g(440)$, $a_\phi(440)$, and chlorophyll *a* concentration, for the SMAs sampled in this study, were made from raw CDOM and chlorophyll a fluorescence using a combination of linear, non-linear, and multiple regression methods. The spatial variability in CDOM and chlorophyll *a* was mapped for the Kitchen SMA as a case study.

3.4.1. Inherent optical properties and fluorescence

Chlorophyll *a* fluorescence (FL_{Chl}) and $a_\phi(440)$ generally followed a linear fit across all SMAs. For IOP and chlorophyll *a* determinations, data from all stations were analyzed together to maximize the effective fluorescence ranges. All chlorophyll fluorescence data were compared for each instrument and while the response curves were very similar, there were some differences in the slopes, r^2, and y-intercepts (Table 3-2).

Table 2-2. Regression equations, with r^2, for each instrument aboard the flow-through system, used to convert raw fluorescence voltage (V) to corresponding absorption coefficients (m^{-1}) for chlorophyll $(a_\phi(440))$ and CDOM $(a_g(440))$, and chlorophyll concentration $(\mu g\ L^{-1})$.

$a_\phi(440) = 0.2392(FL_{chl}) - 0.0353$	$r^2 = 0.84$	WetStar Chl
$a_\phi(440) = 0.1306(FL_{chl}) + 0.0384$	$r^2 = 0.80$	SeaTech Chl
$a_g(440) = 0.1921(FL_{CDOM})^2 + 0.1952(FL_{CDOM}) + 0.1077$	$r^2 = 0.92$	WetStar
$a_g(440) = 0.8389(FL_{CDOM})^2 + 0.4278(FL_{CDOM}) + 0.0241$	$r^2 = 0.88$	ECO
$chl\ a = 11.423(FL_{chl}) - 4.4332$	$r^2 = 0.88$	WetStar Chl
$chl\ a = 6.2856(FL_{chl}) - 1.0473$	$r^2 = 0.88$	SeaTech Chl

The regression model between (FL_{Chl}) and $a_\phi(440)$, for the WetStar fluorometer, resulted in a good fit with $r^2 = 0.84$ and a y-intercept of -0.0353 (Figure 3-3). For the SeaTech fluorometer, the resultant best-fit line produced an $r^2 = 0.80$, and a y-intercept of 0.0384 (Figure 3.4).
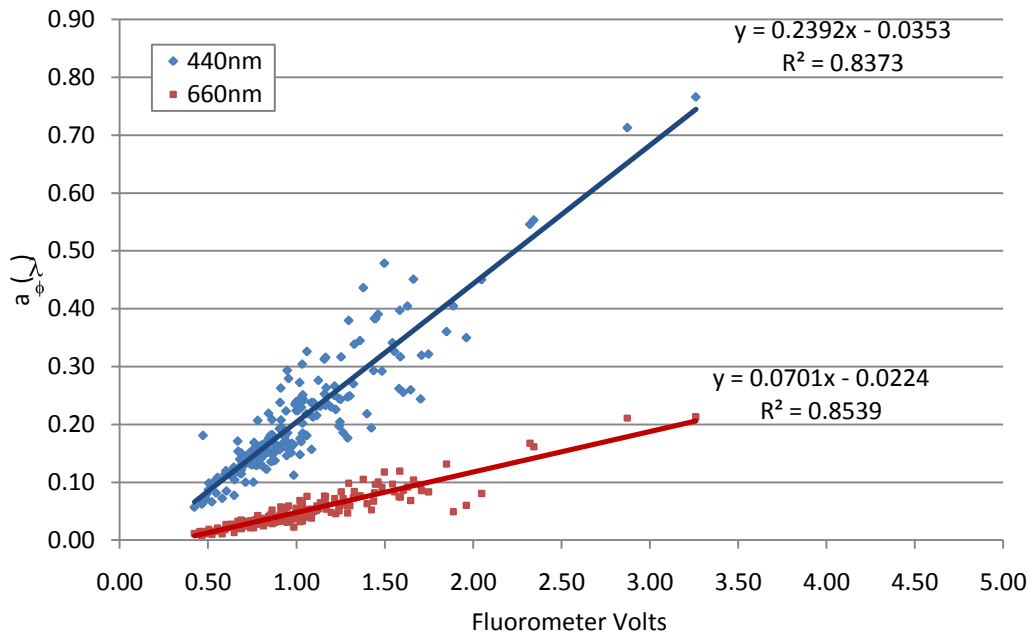

Figure 2-3. Relationship between WetStar chlorophyll fluorescence and the phytoplankton absorption coefficients $(a_\phi(\lambda))$ at 440nm and at 660nm.
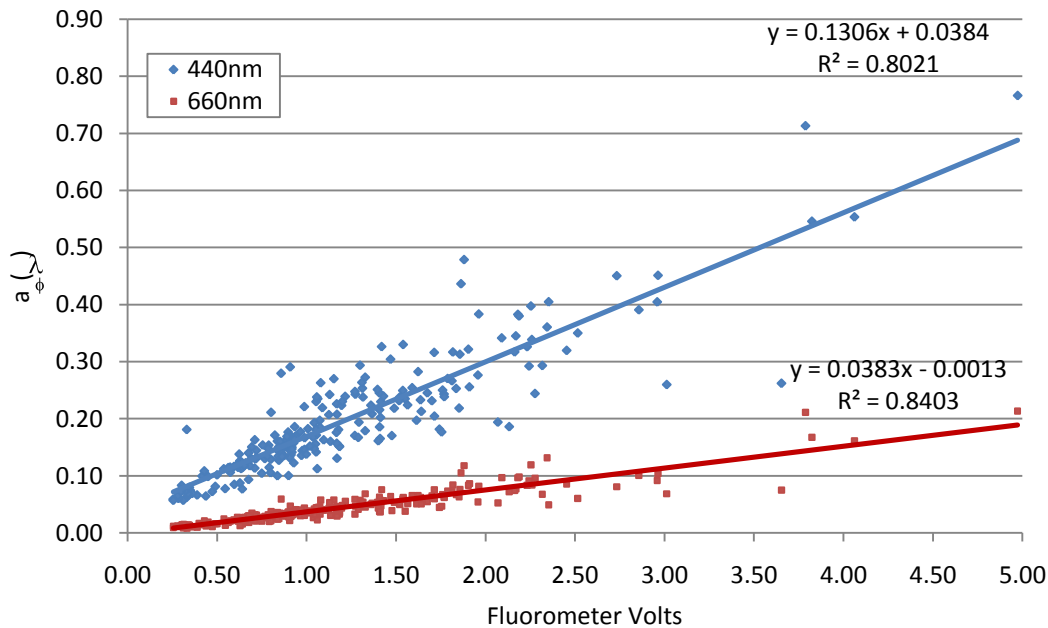
Figure 2-4. Relationship between SeaTech chlorophyll fluorescence and the phytoplankton absorption coefficients $(a_\phi(\lambda))$ at 440nm and at 660nm.

Using the absorption coefficient at 660nm yielded similar results for both WetStar $(r^2 = 0.88; \text{y-int} = -0.0229)$ and SeaTech fluorometers $(r^2 = 0.84; \text{y-int} = -0.0013)$ (Figure 3-4). Residuals increased as fluorescence increased and interference factors became more prevalent. Measuring *in-situ* fluorescence can sometimes be more art than science, and several confounding factors have to be considered when utilizing these types of relationships. For example, in waters with high phytoplankton biomass, pigment packaging effects can cause chlorophyll fluorescence variability (Bissett 1997). Another factor to consider is potential error due to CDOM and detritus. In this study, both CDOM and detritus absorption co-varied with chlorophyll fluorescence (ANOVA, p<0.01). This significance does not of course imply a cause and effect relationship but the slightly better fit between chlorophyll fluorescence and phytoplankton absorption at 660nm $(a_\phi(660))$ for both WetStar (Figure 3-3) and SeaTech (Figure 3-4) instruments suggests that there is a causal relationship. For both instruments the residuals increased with increasing absorption. This is to be expected as increases in fluorescence may be caused

104

by interference from CDOM and detrital absorption as well as scatter from both organic and inorganic particles at high concentrations.

Chlorophyll fluorescence plotted against chlorophyll concentration yielded a good fit though some non-linearity was visually evident in the Wet Star fluorometer when fluorescence was less than 1.0V (Figure 3-5).
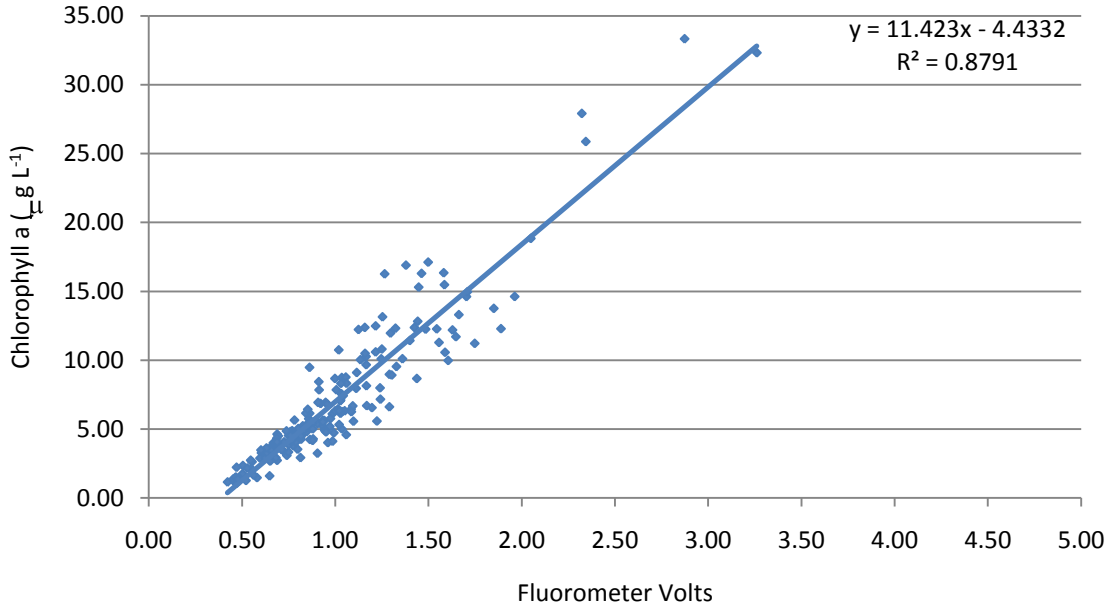
Figure 2-5. Relationship between WetStar chlorophyll fluorescence and chlorophyll concentration (μg L^{-1}).

For the SeaTech fluorometer the relationship between fluorescence and chlorophyll concentration was more linear, although, like the WetStar fluorometer, scatter about the best fit line increased with increasing chlorophyll concentration (Figure 3-6).
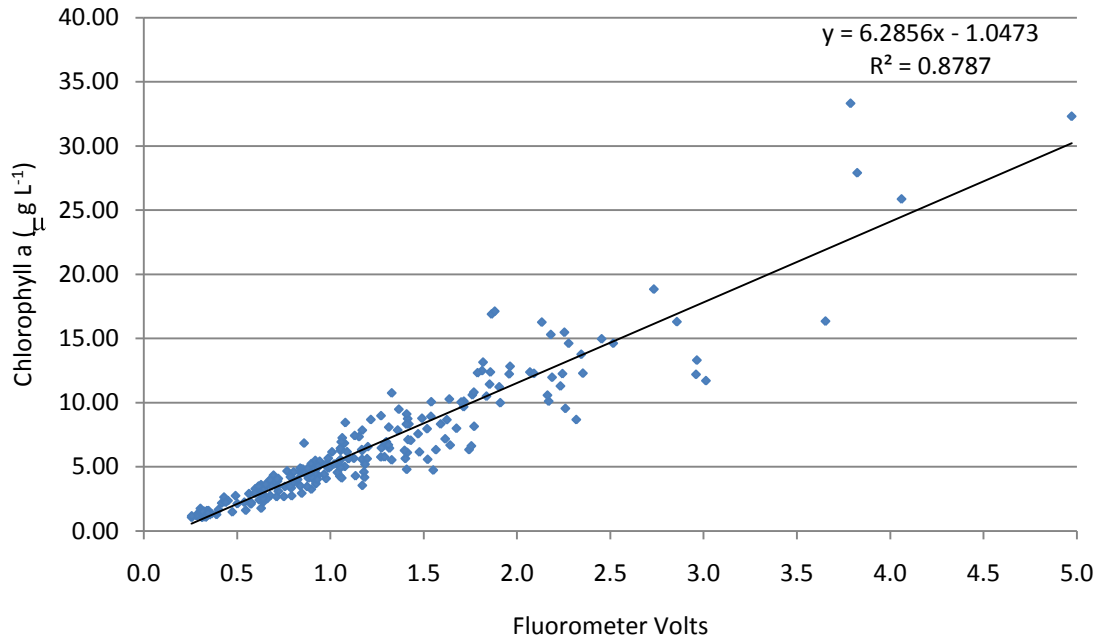
Figure 2-6. Relationship between SeaTech chlorophyll fluorescence and chlorophyll concentration (μg L^{-1}).

Also, the y-intercept for the resultant linear regression line was closer to the origin for the SeaTech fluorometer relative to the WetStar unit (Table 3-2).

Total scatter can also affect fluorescence by increasing the effective pathlength of the light source. However, when scatter was included in the multiple regression model, it was not significant (ANOVA, $p > 0.05$).

Measured FL_{CDOM} from both the ECO and WetStar fluorometers were plotted against $a_g(440)$ and resulted in very similar yet non-linear response curves (Figure 3-7).
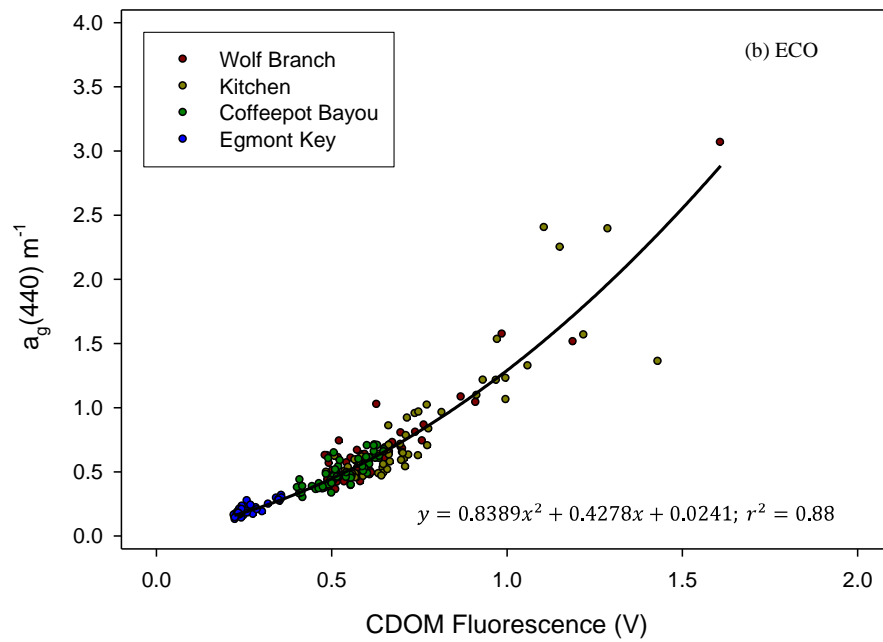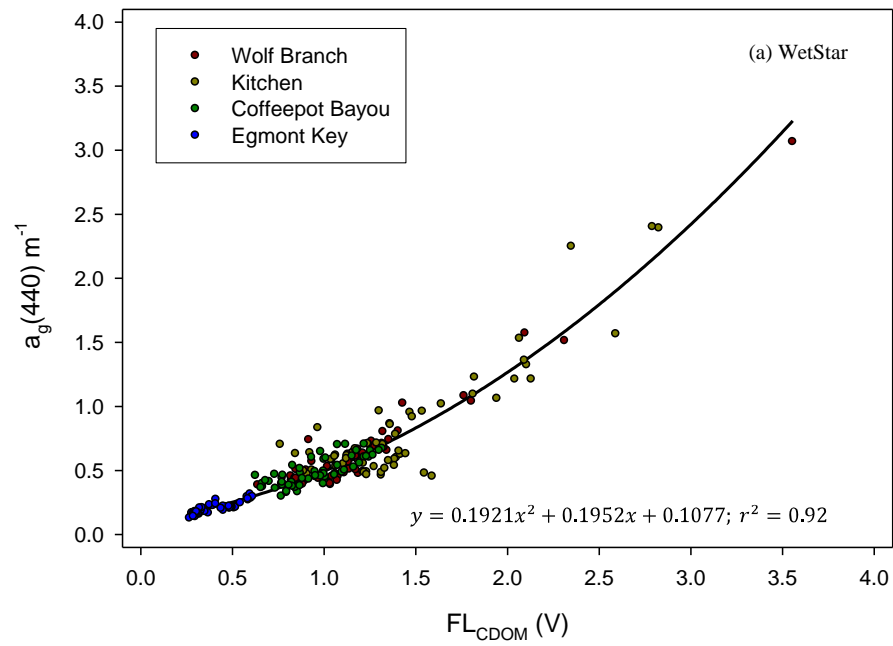
Figure 2-7. Relationship between CDOM fluorescence and the CDOM absorption coefficient $a_g(440)$ for the WetStar and ECO fluorometers. A second order polynomial is fitted to each of the curves.

Predictor equations for both WetStar and ECO fluorometers that best explained the variability in the data were second order polynomials of the form $y = ax^2 + bx + c$, with correlation coefficients of 0.88 and 0.92, respectively (Figure 3-7). The observed non-linearity between $a_g(440)$ and FL_{CDOM} was dependent on the wavelength of the CDOM absorption coefficient. The degree of non-linearity between $a_g(\lambda)$ and FL_{CDOM} decreased with decreasing wavelength, approaching a straight line at $a_g(312)$ (Figure 3-8) The differences between $a_g(312)$ and $a_g(440)$ can be seen in Figure 3-9.
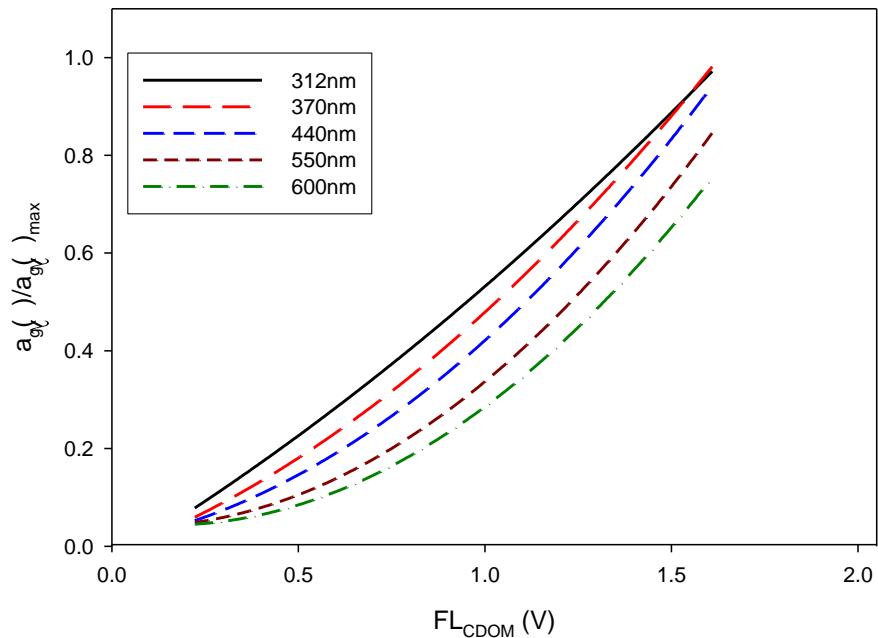
Figure 2-8. Wavelength dependence of the absorption coefficient on the relationship between FL_{CDOM} and $a_g(\lambda)$ for various wavelengths. For comparison purposes, $a_g(\lambda)$ was scaled to the maximum absorption coefficient for a given wavelength by dividing $a_g(\lambda)$ by $a_g(\lambda)_{max}$.
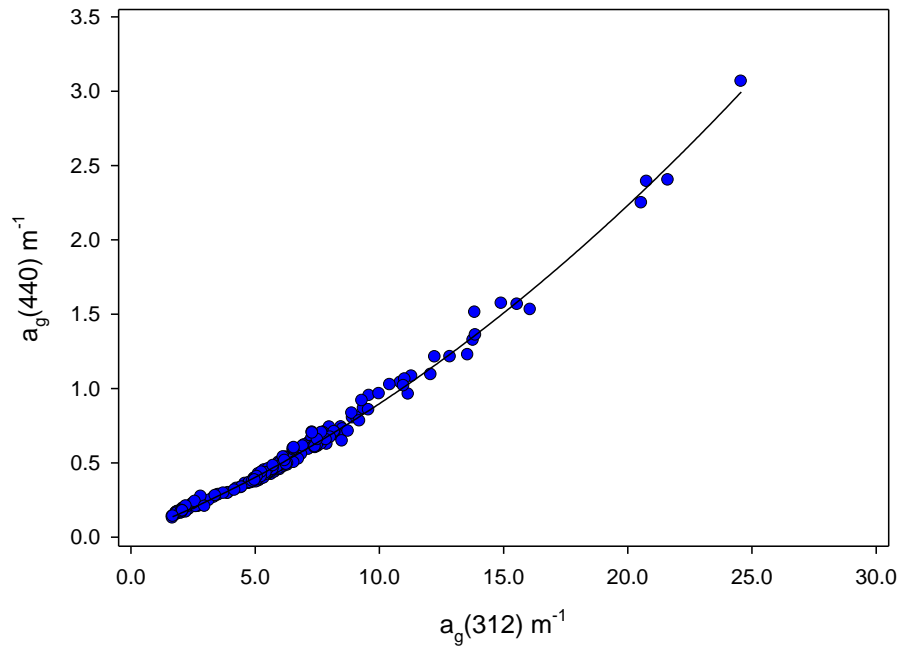
Figure 2-9. Plot of $a_g(312)$ and $a_g(440)$ for all sample data used in this study.

For $a_g(312)$, the relationship between the CDOM absorption coefficient and fluorescence intensity approximated a straight line for both the WetStar (Figure 3-10a) and ECO (Figure 3-10b) fluorometers, with correlation coefficients of 0.91 and 0.89, respectively.
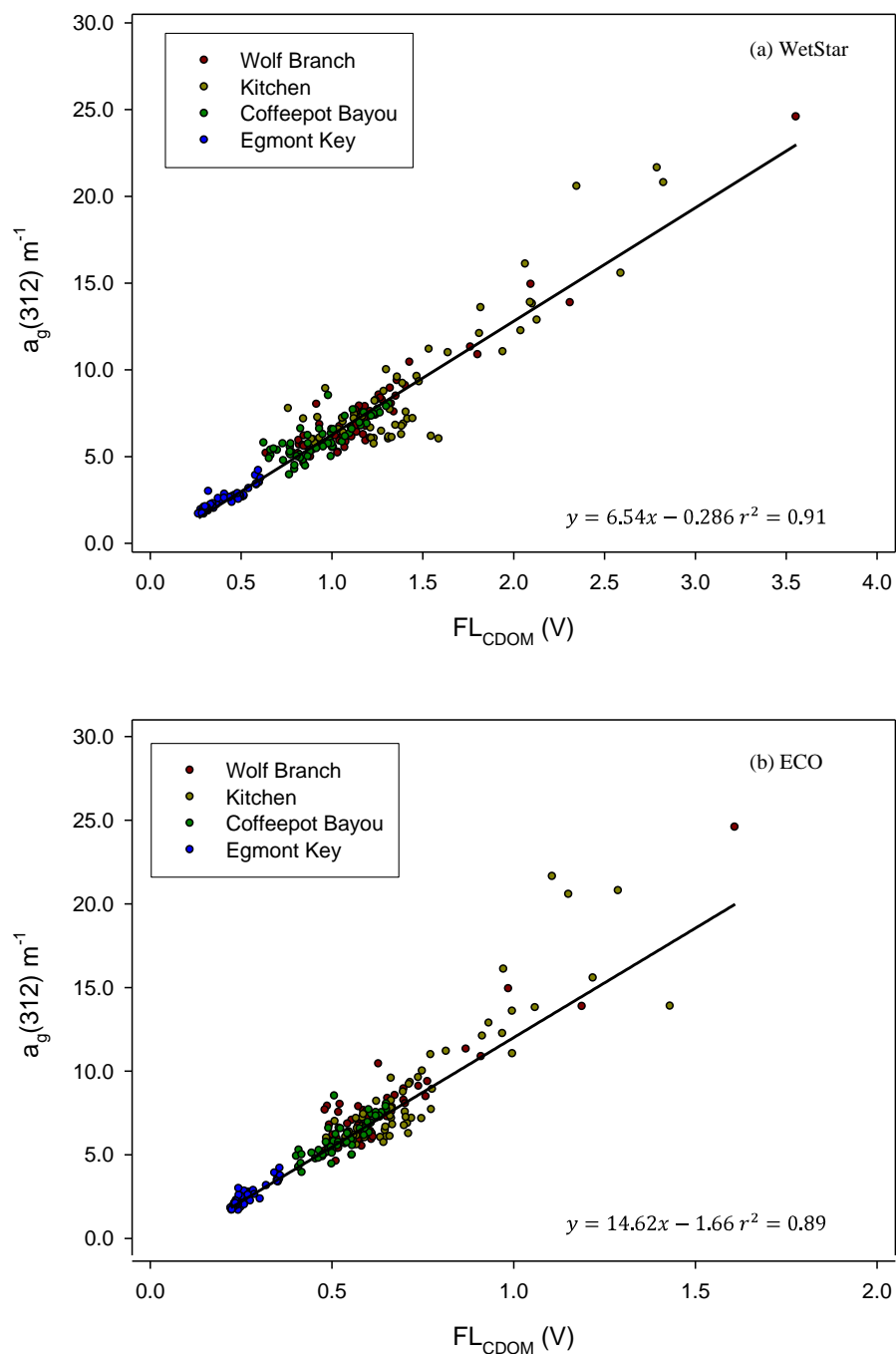
Figure 2-10. Relationship betweeen CDOM fluorescence and CDOM absorption at 312nm for the (a) WetStar and (b) ECO fluorometers.

The possibility of interference with the CDOM fluorescence signal by water column constituents other than CDOM, such as phytoplankton and detritus, was explored

using multiple regression techniques. In this study, $a_\phi(440)$, $a_d(440)$, and $a_p(440)$ all covaried with $a_g(440)$ (Figure 3-11).
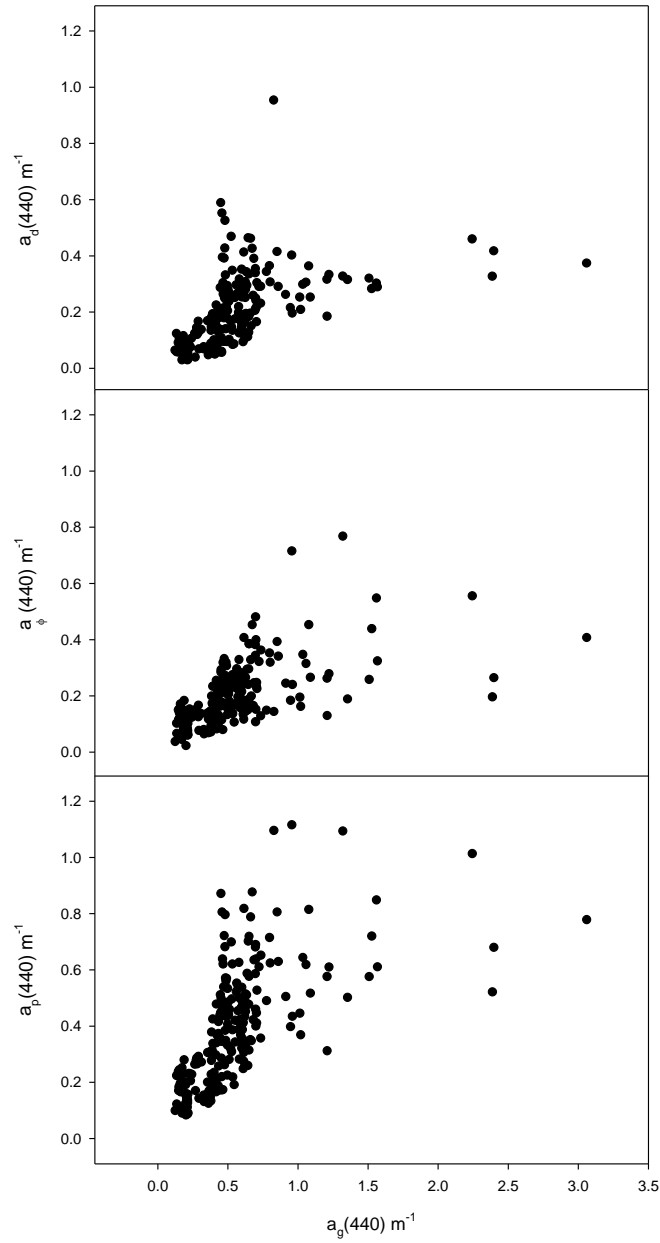
Figure 2-11. Comparison at 440nm of the CDOM absorption coefficient $(a_g(440))$ with the (a) detritus $(a_d(440))$, (b) phytoplankton $(a_\phi(440))$, and (c) particulate absorption $(a_p(440))$ coefficients. $(a_p(440) = a_d(440) + a_\phi(440))$.

While phytoplankton can contribute to the total CDOM pool, CDOM from terrestrial sources far exceeded any contribution from phytoplankton. The correlation between $a_g(440)$ and $a_\phi(440)$ was coincident on the fact that during wet periods, both CDOM concentration and phytoplankton productivity were elevated. The same conclusion can be inferred about detrital absorption and CDOM absorption.

A multiple regression model using FL_{CDOM}, measured with the ECO fluorometer, as the dependent variable, and $a_g(440)$, $a_\phi(440)$, and $a_d(440)$ as independent variables, resulted in strongly significant correlations at the 95% probability level for $a_g(440)$ and FL_{CDOM} (p<0.01), and $a_d(440)$ and FL_{CDOM} (p<0.01), but resulted in only a weakly significant correlation between $a_\phi(440)$ and FL_{CDOM} (p<0.05) (Table 3-3). Similar results were found using the WetStar fluorometer, except $a_\phi(440)$ and FL_{CDOM} were more strongly correlated (p<0.01) (Table 3-3). Multiple regression analyses were performed to investigate the dependence of FL_{CDOM} on $a_g(440)$. Chlorophyll fluorescence measured with the SeaTech fluorometer was not significantly correlated with $a_g(440)$ (ANOVA; p>0.10) (Table 3-3).

Because detritus absorption was significantly correlated with CDOM fluorescence, a multiple regression model was constructed using only $a_g(440)$ and $a_d(440)$ as independent variables. For the ECO and WetStar fluorometers, model results yielded correlation coefficients of 0.87 and 0.88, respectively (Table 3-3).

Table 2-3. Results of multiple regression analyses for establishing the relationship between CDOM fluorescence and the IOPs for shallow seagrass areas in Tampa Bay.

$FL_{CDOM} = 0.208 + 0.451a_g(440) + 0.137a_\phi(440) + 0.334a_d(440)$	ECO	$r^2 = 0.87$
$FL_{CDOM} = 0.252 + 1.03a_g(440) + 0.392a_\phi(440) + 0.604a_d(440)$	WetStar	$r^2 = 0.88$
$FL_{CDOM} = 0.213 + 0.467a_g(440) + 0.393a_d(440)$	ECO	$r^2 = 0.87$
$FL_{CDOM} = 0.264 + 1.08a_g(440) + 0.783a_d(440)$	WetStar	$r^2 = 0.88$
$a_g(440) = -0.295 + 1.50FL_{CDOM} + 0.022FL_{chl}$	ECO	$r^2 = 0.83$
$a_g(440) = -0.188 + 0.715FL_{CDOM} + 0.017FL_{chl}$	WetStar	$r^2 = 0.88$

3.4.2. CDOM and chlorophyll spatial variability

Survey data for CDOM fluorescence and chlorophyll concentration were converted into contour plots for the Kitchen SMA using a Kriging method in SURFER 8.0 (Golden Software) to examine the spatial patterns of CDOM and chlorophyll fluorescence. Survey results showed an increase in FL_{CDOM} along the immediate shoreline for August and, to a lesser extent, for April (Figure 3-12). While area-wide average $a_g(440)$ doubled from April to August (Table 3-4) and this increase was concentrated close to the shoreline.

Table 2-4. Annual summary of CDOM fluorescence voltage and corresponding CDOM absorption ($a_g(440)$) for the Kitchen Seagrass Management Area.

Month	Volts	$a_g(440)m^{-1}$			
	Mean ± stdev	Mean ± stdev	Median	Maximum	Minimum
April	1.32 ± 0.240	0.713 ± 0.185	0.656	1.40	0.530
June	1.15 ± 0.206	0.600 ± 0.139	0.578	1.17	0.406
August	2.14 ± 0.534	1.46 ± 0.630	1.28	4.21	0.650
October	1.36 ± 0.114	0.515 ± 0.083	0.504	0.772	0.387
December	1.13 ± 0.245	0.586 ± 0.161	0.539	1.03	0.359

Figure 2-12. Survey results of FL_{CDOM} (V) across the Kitchen Seagrass Management Area for (a) April and (b) August 2008.

In Chapter 2, it was shown that $a_g(440)$ was positively correlated with rainfall. The well established mangrove shoreline appears to be the major CDOM source in this case. Under very wet conditions, Bullfrog Creek and the Alafia River can contribute large high concentrations of CDOM to the Kitchen SMA. However, major incursions of high

CDOM water into the Kitchen were not observed from flow-through data collected during this study. A slight CDOM plume was detected at the mouth of Bullfrog Creek during the August survey (Figure 3-12a). Presumably, rainfall totals were not great enough to cause significant amounts of CDOM-rich river water to enter the Kitchen. Total rainfall, 30-days prior to sampling, was 29.6cm in August compared to only 6.63cm in April. This difference was expressed as lower CDOM in April, though FL_{CDOM} still increased shoreward (Figure 3-12b).

The CDOM-rich water mass concentrated over the existing seagrass beds. High CDOM concentrations may be beneficial to seagrass growing in average depths of less than 0.5m, where UV exposure could be lethal without this protective CDOM layer. While CDOM decreases with increasing distance away from the shoreline, any increase in light penetration is offset by increases in average depth.

Chlorophyll concentrations displayed a typical seasonal pattern with peak concentrations in August and minimum concentrations during the dry season (Table 3-5).

Table 2-5. Annual summary of chlorophyll concentrations (μg L^{-1}) calculated using chlorophyll fluorescence for the Kitchen Seagrass Management Area.

Month	Mean ± stdev	Median	Maximum	Minimum
April	5.93 ± 1.81	5.69	10.1	2.84
June	11.8 ± 5.08	10.1	30.6	5.04
August	16.3 ± 9.74	11.8	52.1	6.29
October	6.54 ± 1.78	6.09	11.0	4.14
December	6.95 ± 1.72	7.20	10.4	3.69

Unlike CDOM, no obvious spatial patterns for April, August, or any other month sampled, were readily evident. Phytoplankton dynamics are quite complex and involve a number of factors such as hydrodynamics, tide, season, and nutrient availability and therefore it is not surprising that a spatial pattern was not observed. There was however, a more subtle pattern that can be observed for the August survey, and to a lesser extent for the April survey as well, and that is the presence of small pockets of relatively high chlorophyll concentration located throughout the area (Figure 3-13). This was visually confirmed by sampling personnel during the actual surveys and therefore likely not an artifact of the contouring technique.
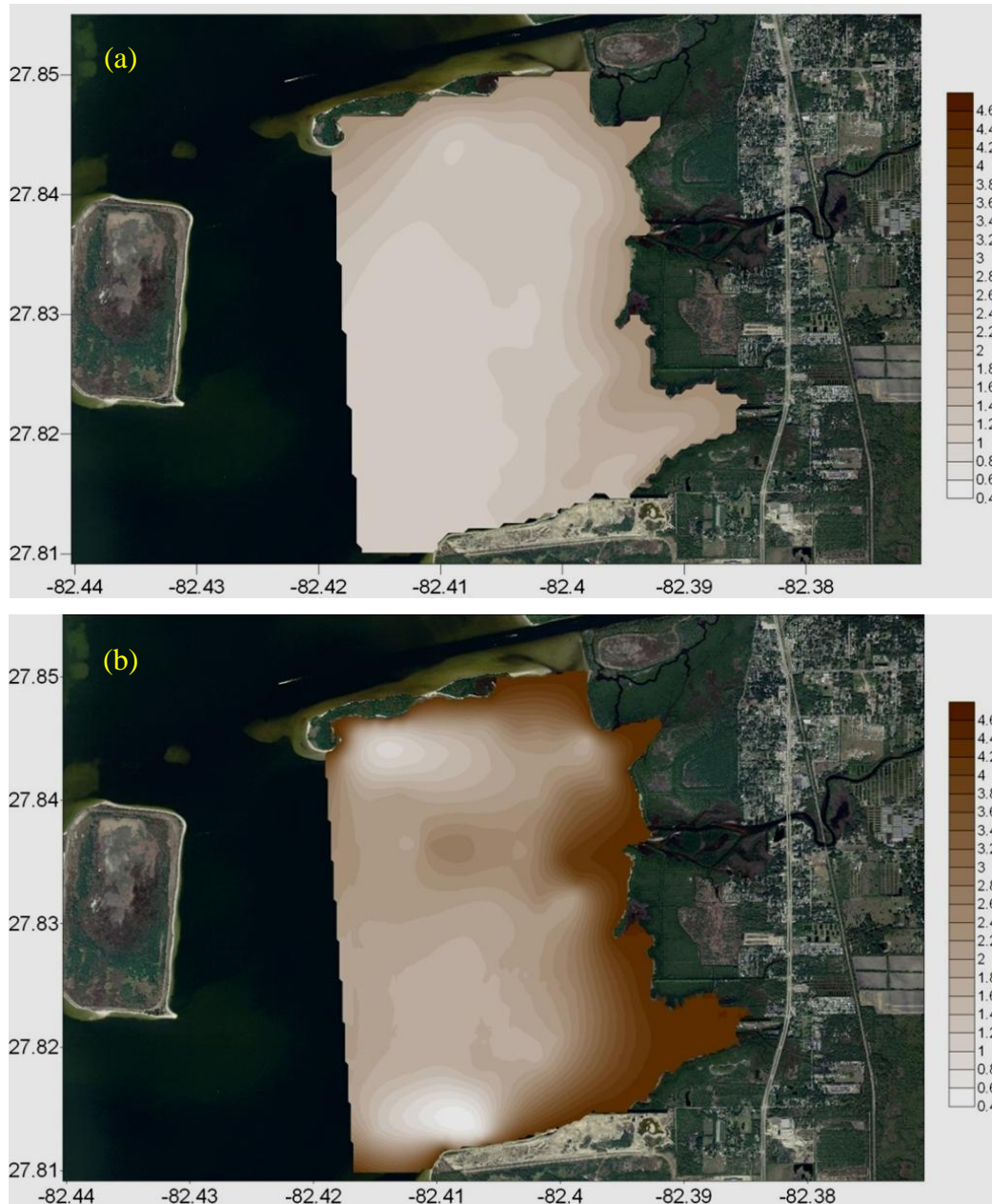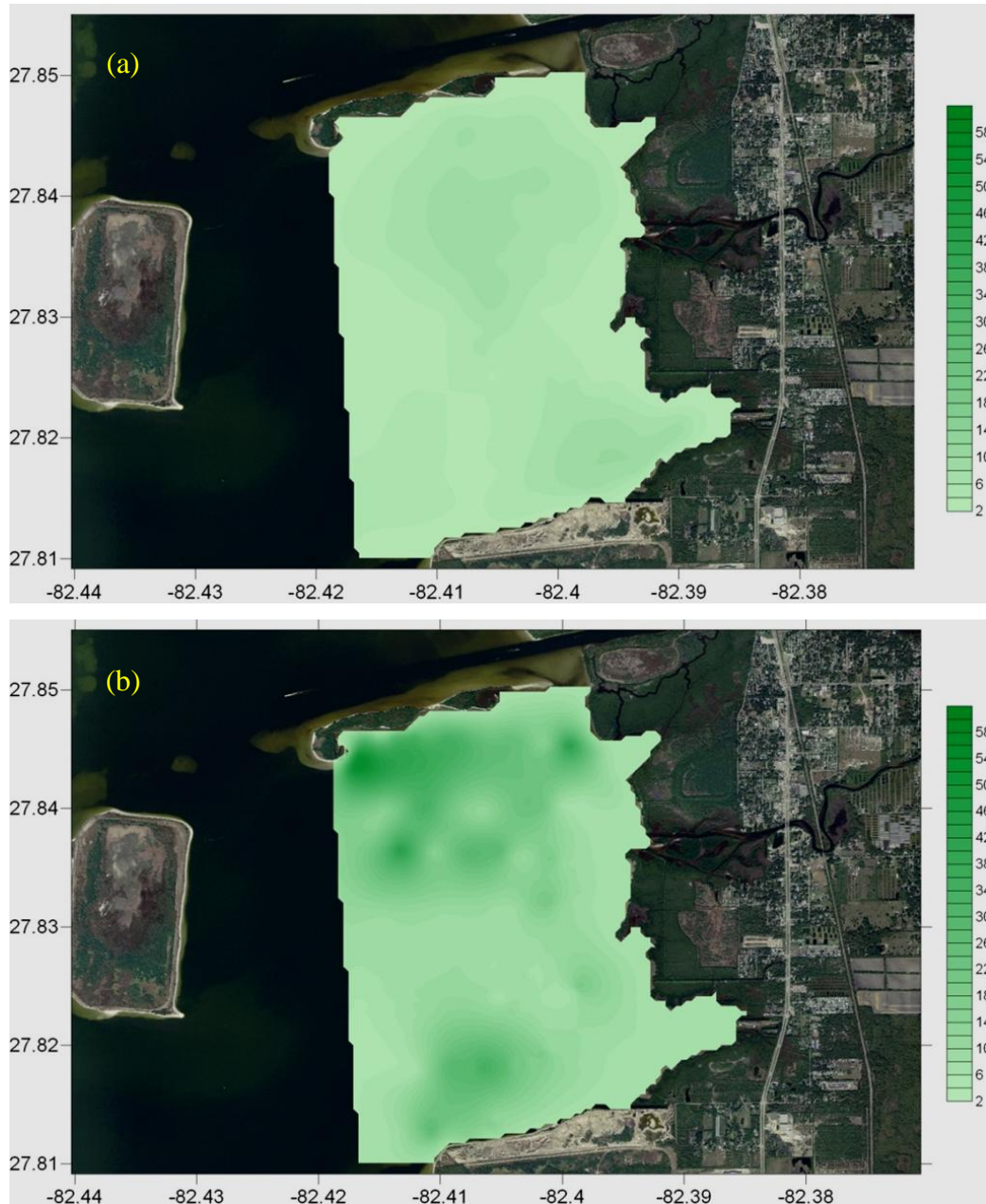
Figure 2-13. Survey results of FL_{Chl} across the Kitchen Seagrass Management Area for (a) April and (b) August 2008 expressed in concentration ($\mu g\ L^{-1}$).

3.5. Conclusions

      Using a deck-mounted flow-through system in shallow seagrass beds like the ones found in Tampa Bay is a novel approach. In this chapter the utility of using such a system

for monitoring the spatial variability of the optical environment within a Seagrass Management Area was clearly demonstrated for the Kitchen.

Raw flow-through data were collected in four SMAs under different conditions and times of the year. Despite these differences, the correlations between the IOPs and raw fluorescence produced good results. Overall, correlations using all available data were stronger than for individual surveys. This suggests that the underlying optical properties of these SMAs were similar. For example, CDOM slopes were similar across all SMAs indicating that CDOM may be originating from similar sources. That is not to say that this will always be the case across all SMAs or over all time periods, but it does suggest that at least in the SMAs studied here, predictor equations for calculating $a_\phi(440)$ and $a_g(440)$ are applicable across the SMAs. This work took place in 2008 which was a normal year for rainfall. It is possible that these equations would have to be re-calibrated during periods of strong El Niño or La Niña events or in the after the passage of a tropical storm. Further survey work should be conducted in other SMAs and under varying rainfall conditions to better refine the equations presented here.

The patterns in CDOM and chlorophyll demonstrate the inherent need to adequately characterize the variability in a complex area like the Kitchen. There is a danger in relying too heavily on discrete water samples to infer conditions in areas where conditions are markedly different. For example, the nearest long-term water quality monitoring station is will outside of the Kitchen SMA yet data from this station are routinely used to evaluate light availability over the seagrass.

Routine surveillance of SMAs should be part of a regional monitoring program in order to establish a base-line understanding of CDOM and phytoplankton dynamics. Incorporating this method to an existing program like the Hillsborough County EPC monthly monitoring of fixed stations throughout the bay, a "connect-the-dots" approach can be applied to establish optical characteristics between stations. The flow-through system used in this study was designed primarily for oceanographic research. Given the latest advancements in sensors and data processing, a flow-through system specifically designed for shallow water environments could easily be constructed and would provide

an operational and cost-effective tool for developing transparency criteria, as well as for other applications.

Conclusions

Seagrass are important indicators of estuarine health and, as such, their recovery and sustainability are of major importance to resource managers and regulatory interests. The work presented here demonstrated the importance of not only knowing the quantity of light reaching the bottom but also the quality of light. Light quality was defined in terms of its "end-user", in this case seagrass, by estimating the photosynthetically useable radiation at the seagrass deep edge. Using this method revealed that seagrass along the deep edge in Tampa Bay are blue-light limited and that most of the light being utilized for photosynthesis is coming from the red and even the green wavelengths. Using a GIS-based technique of calculating the percent subsurface light at the bottom relative to the surface revealed that on average seagrass are receiving $13.6\% - 18.1\%$ of the blue light at just below the water surface. By comparison, 32% - 39% of PAR originating at the surface reaches the bottom. This suggests that the current minimum light target for PAR of 20.5% is too low.

The attenuation of blue light in the Seagrass Management Areas studied here is primarily caused by CDOM absorption accounting for 60% of the total absorption. Detritus absorption accounted for an additional 20% of the total, leaving only 20% of the total absorption attributable to phytoplankton. This challenges the current seagrass management paradigm that chlorophyll a is the dominant absorber of light and that nitrogen limitation will have a direct effect on transparency. While it is important to consider CDOM and detritus when setting seagrass restoration and management goals, there may be little that can be done to manage CDOM or detritus.

Providing a linkage between the IOPs and parameters more typical of routine monitoring programs is important and adds value to existing datasets. In this study, Seagrass Management Area-specific correlations were derived for the various absorption and scatter coefficients. Given the resource management and regulatory importance of the light attenuation coefficient to establishing transparency criteria for Florida estuaries, an empirically-derived model originally developed using Monte Carlo simulation was used to calculate $K_d(480)$ from the total absorption and scatter coefficients.

A major challenge in modeling the underwater light field is capturing the spatial and temporal variability in the optical properties. In this study a deck-mounted flow-through system was used to survey the optical properties of shallow seagrass areas in Tampa Bay. Empirical relationships were derived between raw fluorescence and the IOPs. This system was very effective at providing a synoptic view of a given area using the Kitchen as a case study.

References

Abal, E. G., N. Loneragan, P. Brown, C. J. Perry, J. W. Udy, and W. C. Dennison. 1994. Physiological and morphological responses of the seagrass *Zostera capricorni* Ashers. to light intensity. Journal of Experimental Marine Biology and Ecology **178:** 113-129.

Arar, E. J., and G. B. Collins. 1997. *In vitro* determination of chlorophyll *a* and pheophytin *a* in marine and freshwater algae by fluorescence, p. 22. *In* N. E. R. Laboratory [ed.]. U.S. Environmental Protection Agency.

Belzile, C., C. S. Roesler, J. P. Christensen, N. Shakhova, and I. Semiletov. 2006. Fluorescence measured using the WETStar DOM fluorometer as a proxy for dissolved absorption. Estuarine, Coastal & Shelf Science **67:** 441-449.

Berwald, J., D. Stramski, C. D. Mobley, and D. A. Kiefer. 1995. Influences of absorption and scattering on vertical changes in the average cosine of the underwater light field. Limnology and Oceanography **40:** 11.

---. 1998. Effect of Raman scattering on the average cosine and diffuse attenuation coefficient of irradiance in the ocean. Limnology and Oceanography **43:** 13.

Biber, P., C. Gallegos, and W. Kenworthy. 2008. Calibration of a Bio-optical Model in the North River, North Carolina (Albemarle-Pamlico Sound): A Tool to Evaluate Water Quality Impacts on Seagrasses. Estuaries and Coasts **31:** 177-191.

Bissett, W. P., J. S. Patch, K. L. Carder, and Z. P. Lee. 1997. Pigment packaging and chl a-specific absorption in high-light oceanic waters. Limnology and Oceanography **42:** 961-968.

Blough, N. V., and R. D. Vecchio. 2002. Chromophoric DOM in the Coastal Environment. *In* D. A. Hansell and C. A. Carlson [eds.], Biogeochemistry of Marine Dissolved Organic Matter. Academic Press.

Bortone, S. A. 2000. Seagrasses : monitoring, ecology, physiology, and management. CRC Press.

Branco, A. B. A. J. N. K. 2005. The relative importance of chlorophyll and colored dissolved organic matter (CDOM) to the prediction of the difuse attenuation coefficient in shallow estuaries. Estuaries **28:** 643-652.

Bricaud, A., M. Babin, A. Morel, and H. Claustre. 1995. Variability in the chlorophyll-specific absorption coefficients of natural phytoplankton: Analysis and parameterization. Journal of Geophysical Research **100:** 13,321.

Bricaud, A., and D. Stramski. 1990. Spectral absorption coefficients of living phytoplankton and nonalgal biogenous matter: a comparison between the Peru upwelling area and the Sargasso Sea. Limnology and Oceanography **35:** 562-582.

Brock, J. C., C. W. Wright, A. H. Sallenger, W. B. Krabill, and R. N. Swift. 2002. Basis and methods of NASA airborne topographic mapper LIDAR surveys for coastal studies. Journal of coastal research : JCR **18:** 1-13.

Butler, W. L. 1962. Absorption of light by turbid materials. Journal of the Optical Society of America **52:** 292-299.

Buzzelli, C. P., J. Ramus, and H. W. Paerl. 2003. Ferry-based monitoring of surface water quality in North Carolina estuaries. Estuaries **26:** 975-984.

Cannizzaro, J. P. 2004. Detection and quantification of *Karenia brevis* blooms on the West Florida shelf from remotely sensed ocean color imagery. University of South Florida.

Cannizzaro, J. P., K. L. Carder, F. R. Chen, C. A. Heil, and G. A. Vargo. 2008. A novel technique for detection of the toxic dinoflagellate, *Karenia brevis*, in the Gulf of Mexico from remotely sensed ocean color data. Continental Shelf Research **28:** 137-158.

Cannizzaro, J. P., K. L. Carder, F. R. Chen, J. J. Walsh, Z. P. Lee, and C. Heil. 2004. A novel optical classification technique for detection of red tides in the Gulf of Mexico: Application to the 2001-2002 bloom event, p. 137-158. *In* F. F. a. W. C. C. a. I. O. C. o. UNESCO [ed.], Harmful Algae 2002.

Cannizzaro, J. P., C. Hu, D. C. English, K. L. Carder, C. A. Heil, and F. E. Muller-Karger. 2009. Detection of *Karenia brevis* blooms on the west Florida shelf using in situ backscattering and fluorescence data. Harmful Algae **8:** 898-909.

Carder, K. L., R. G. Steward, G. R. Harvey, and P. B. Ortner. 1989. Marine humic and fulvic acids: Their effects on remote sensing of ocean chlorophyll. Limnology and Oceanography **34:** 68-81.

Carder, K. L., Z. P. Lee, J. Marra, R. G. Steward, and M. J. Perry. 1995. Calculated quantum yield of photosynthesis of phytoplankton in the Marine Light - Mixed Layers (59°N, 21°W). Journal of Geophysical Research **100:** 6655-6663.

Chen, Z., C. Hu, R. N. Conmy, F. Muller-Karger, and P. Swarzenski. 2007. Colored dissolve organic matter in Tampa Bay, Florida. Marine Chemistry **104:** 98-109.

Cloern, J. E. 2001. Our evolving conceptual model of the coastal eutrophication problem. Marine ecology progress series **210:** 223-253.

Coble, P. G. 2007. Marine Optical Biogeochemistry: The Chemistry of Ocean Color. Chemical reviews **107:** 17.

Conmy, R. N. 2008. Temporal and Spatial Patterns in Optical Properties of Colored Dissolved Organic Matter on Florida's Gulf Coast: Shelf to Stream to Aquifer. Dissertation. University of South Florida.

Conmy, R. N., P. G. Coble, R. F. Chen, and G. B. Gardner. 2004. Optical properties of colored dissolved organic matter in the Northern Gulf of Mexico. Marine Chemistry **89:** 127-144.

Cummings, M. E., and R. C. Zimmerman. 2003. Light harvesting and the package effect in the seagrasses Thalassia testudinum Banks ex Konig and Zostera marina L : optical constraints on photoacclimation. Aquatic botany **75:** 261.

Dennison, W., C. and others 1993. Assessing water quality with submersed aquatic vegetation. BioScience **43:** 86-94.

Dennison, W. C. 1987. Effects of light on seagrass photosynthesis, growth, and depth distribution. Aquatic Botany **27:** 15-26.

Dennison, W. C., and R. S. Alberte. 1982. Photosynthetic response of *Zostera marina* L. (eelgrass) to in situ manipulations of light intensity. Oecologia **55:** 137-144.

Dixon, K. L., and J. R. Leverone. 1995. Light Requirements of *Thalassia testudinum* in Tampa Bay, Florida, p. 77. Mote Marine Laboratory.

Dixon, L. K. 2000. Establishing Light Requirements for the Seagrass *Thalassia testudinum*: An example from Tampa Bay, Florida. *In* S. A. Bortone [ed.], Seagrasses: Monitoring, Ecology, Phsiology, and Management. Marine science series. CRC Press.

Duarte, C. M. 1991. Seagrass depth limits. Aquatic Botany **40:** 363-377.

---. 2002. The future of seagrass meadows. Environmental Conservation **29:** 15.

Duarte, C. M., N. Marba, D. Krause-Jensen, and M. Sanchez-Camacho. 2007. Testing the Predictive Power of Seagrass Depth Limit Models. Estuaries and coasts : journal of the Estuarine Research Federation **30:** 5.

Durako, M. J. 2007. Leaf optical properties and photosynthetic leaf absorptances in several Australian seagrasses. Aquatic Botany **87:** 7.

EPCHC 2007. Tampa Bay Seagrass Management Area Determination, Status and Trends, and Water Quality Target Attainment, Technical Memorandum, p. 84. *In* E. R. M. Division [ed.].

Eaton, A. D., L. S. Clescerl, E. W. Rice, A. E. Greenberg, and M. A. H. Franson [eds.]. 2005. Standard Methods for Examination of Water & Wastewater: 21st Edition. American Public Health Association.

Enriquez, S. 2005. Light absorption efficiency and the package effect in the leaves of the seagrass Thalassia testudinum. Marine ecology progress series **289:** 10.

Enriquez, S., S. Agusti, and C. M. Duarte. 1992. Light absorption by seagrass Posidonia oceanica leaves. Marine ecology progress series **86:** 201-204.

Ensign, S. H., and H. W. Paerl. 2006. Development of an unattended estuarine nutrient monitoring program using ferries as data-collection platforms. Limnology and Oceanography: Methods **4:** 399-405.

Ferrari, G. M., and M. D. Dowell. 1998. CDOM absorption characteristics with relation to fluorescence and salinity in coastal areas of the southern Baltic Sea. Estuarine, Coastal & Shelf Science **47:** 91-105.

Ferrari, G. M., N. Hoepffner, and M. Mingazzini. 1996. Optical properties of the water in a deltaic environment: Prospective tool to analyze stellite data in turbid waters. Remote Sensing of Environment **58:** 69-80.

FDEP. 2009. Standard Operating Procedure for: Spectrophotometric Determination of Corrected and Uncorrected Chlorophyll a and Pheophytin, p. 14. *In* B. S. Bureau of Laboratories [ed.].

Fourqurean, J. W., N. Marba, and C. M. Duarte. 2003. Comment - Elucidating seagrass population dynamics: Theory, constraints, and practice. Limnology and oceanography **48:** 4.

Gallegos, and Kenworthy. 1996. Seagrass Depth Limits in the Indian River Lagoon (Florida, U S A): Application of an Optical Water Quality Model. Estuarine, Coastal & Shelf Science **42:** 22.

Gallegos, C. L. 1994. Refining habitat requirements of submersed aquatic vegetation: Role of optical models. Estuaries **17:** 187-199.

---. 2001. Calculating optical water quality targets to restore and protect submersed aquatic vegetation: Overcoming problems in partitioning the diffuse attenuation coeficient for photosynthetically active radiation. Estuaries **24:** 381-397.

---. 2005. Optical water quality of a blackwater river estuary: The Lower St. Johns River, Florida, USA. Estuarine, Coastal, and Shelf Science **63:** 57-72.

Gallegos, C. L., D. L. Correll, and J. W. Pierce. 1990. Modeling spectral diffuse attenuation, absorption, and scattering coefficients in a turbid estuary. Limnology and Oceanography **35:** 1486.

Gordon, H. R., D. K. Clark, J. W. Brown, O. B. Brown, R. H. Evans, and W. W. Broenkow. 1983. Phytoplankton pigment concentrations in the middle Atlantic Bight: Comparison of ship determinations and CSCZ estimates. Applied Optics **22:** 20-36.

Greening, H. 2004. Factors Influencing Seagrass Recovery in Feather Sound, Tampa Bay, Florida. Tampa Bay Estuary Program.

Griffen, L., and H. Greening. 2004. Factors influencing seagrass recovery in Feather Sound, Tampa Bay, Florida. *In* T. B. E. Program [ed.].

Guenther, G. C., A. G. Cunningham, P. E. Larocque, and D. J. Reid. 2000. Meeting the accuracy challenge in airborne LIDAR bathymetry, p. 28. European Assiciation of Remote Sensing Laboratories.

Hall, M. O., D. A. Tomasko, and F. X. Courtney. 1991. Responses of *Thalassia testudinum* to *in-situ* light reduction, p. 77-86. The Light Requirements of Seagrasses: Proceedings of a Workshop to Examine the Capability of Water Quality Criteria, Standards and Monitoring Programs to Protect Seagrasses.

Hansell, D. A., and C. A. Carlson [eds.]. 2002. Biogeochemistry of Marine Dissolved Organic Matter. Elsevier Science & Technology Books.

Hansen, M., M. Crane, C. Hearn, and K. Yates. 2005. Gulf of Mexico Integrated Science - Tampa Bay Study Watershed and Estuary Mapping. *In* U. S. G. Survey [ed.].

Hemminga, M. A., and C. M. Duarte. 2000. Seagrass Ecology. Cambridge University Press.

Herzka, S., and K. Dunton. 1997. Seasonal photosynthetic patterns in the seagrass *Thalassia testudinum* in the western Gulf of Mexico. Marine ecology progress series **152:** 103-117.

Hickman, G. D., and J. E. Hogg. 1969. Application of an airborne pulsed laser for near-shore bathymetric measurements. Remote Sensing of Environment **1:** 47-58.

Hill, K. 2002. Seagrass Habitats. Smithsonian Marine Station at Fort Pierce.

Hoge, F. E., A. Vodacek, and N. V. Blough. 1993. Inherent optical properties of the ocean: Retrieval of the absorption coefficient of chromophoric dissolved organic matter from fluorescence measurements. Limnology and Oceanography **38:** 1394-1402.

Holm-Hansen, O., and B. Rieman. 1978. Chlorophyll a determination: improvements in methodology. Oikos **30:** 438-447.

Janicki, A., R. Pribble, and K. Hackett. 2003. Nitrogen Loadings to Tampa Bay: Model Based Estimates of 1998 and 2010 Loads to Major Basins, and TN Load Reduction/Preclusion Apportionment. Tampa Bay Estuary Program.

Janicki, A., and D. Wade. 1996. Estimating critical external nitrogen loads for the Tampa Bay Estuary: An empirically based approach to setting management targets. Tampa Bay Estuary Program.

Janicki Environmental, I. 2001. Tampa Bay Estuary Program Model Evaluation and Update Model Evaluation and Update: Chlorophyll a - Light Attenuation Relationship, p. 35. Tampa Bay Estuary Program.

Kenworthy, W. J., M. J. Durako, S. M. R. Fatemy, H. Valavi, and G. W. Thayer. 1993. Ecology of Seagrasses in Northeastern Saudi Arabia One Year After the Gulf War Oil Spill. Marine pollution bulletin **27:** 213.

Kenworthy, W. J., and M. S. Fonseca. 1996. Light requirements of seagrasses *Halodule wrightii* and *Syringodium filiforme* derived from the relationship between diffuse light attenuation and maximum depth distribution. Estuaries **19:** 740-750.

Kiefer, D. A., and J. B. Soohoo. 1982. Spectral absorption by marine particles of coastal waters of Baja California. Limnology and Oceanography. Limnology and Oceanography **27:** 492-499.

Kirk, J. T. 1981. Estimation of the scattering coefficient of natrual waters using underwater irradiance measurements. Journal of Marine and Freshwater Research **32:** 533-539.

---. 1984. Dependence of relationship between inherent and apparent optical properties of water on solar altitude. Limnology and Oceanography **29:** 350-356.

---. 1994. Light and photosynthesis in aquatic ecosystems, Second Edition ed. Cambridge University Press.

Kirk, J. T. O. 1991. Volume scattering function, average cosines, and the underwater light field. Limnology and Oceanography **36:** 455-467.

---. 2003. The vertical attenuation of irradiance as a function of the optical properties of the water. Limnology and Oceanography **48:** 9.

Kishino, M., M. Takahashi, N. Okami, and S. Ichimura. 1985. Estimation of the spectral absorption coefficients of phytoplankton in the sea. Bulletin of Marine Science **37:** 634-642.

Kurz, R. 2002. Seagrass Mapping: Accuracy Issues, p. 246. *In* H. S. Greening [ed.], Seagrass Management: It's Not just Nutrients! Tampa Bay Estuary Program.

Lawson, S. E., P. L. Wiberg, K. J. Mcglathery, and D. C. Fugate. 2007. Wind-driven Sediment Suspension Controls Light Availability in a Shallow Coastal Lagoon. Estuaries and coasts : journal of the Estuarine Research Federation **30:** 11.

Lee, Z., K. L. Carder, C. D. Mobley, R. G. Steward, and J. S. Patch. 1998. Hyperspectral remote sensing for shallow waters: 1. A semianalytical model. Applied Optics **37:** 6329-6338.

Longstaff, B. J., and W. C. Dennison. 1999. Seagrass survival during pulsed turbidity events: The effects of light deprivation on the seagrasses *Halodule pinifolia* and *Halophila ovalis*. Aquatic Botany **65:** 105-121.

Madden, C. J., and J. W. Day. 1992. An instrument system for high-speed mapping of chlorophyll a and physico-chemical variables in surface waters. Estuaries **15:** 421-427.

Major, K. M., and K. H. Dunton. 2002. Variations in light-harvesting characteristics of the seagrass, Thalassia testudinum: evidence for photoacclimation. Journal of Experimental Marine Biology and Ecology **275:** 18.

Malick, L. A. 2004. Light quality and phytoplankton viability. University of South Florida.

Menon, H. B., A. Lotliker, and S. R. Nayak. 2006. Pre-monsoon bio-optical properties in estuarine, coastal and Lakshadweep waters. Estuaries and Coasts **63:** 211-223.

Miller, R. L., and B. F. Mcpherson. 1995. Modeling Light Available to Seagrasses in Tampa Bay, Florida. Florida scientist **58:** 116.

Miller, R. L. A. B. F. M. 1995. Modeling photosynthetically active radiation in water of Tampa Bay, Florida, with emphasis on the geometry of incident irradiance. Estuarine, Coastal, and Shelf Science **40:** 359-377.

Minor, E. C., J. Pothen, B. J. Dalzell, H. Abdulla, and K. Mopper. 2006. Effects of salinity changes on the photodegredation and ultra-violet-visible absorbance of terrestrial dissolved organic matter. Limnology and Oceanography **51:** 2181-2186.

Mobley, C. D. 1994. Light and Water: Radiative Transfer in Natural Waters. Academic Press.

128

Morel, A. 1978. Available, usable, and stored radient energy in relation to marine photosynthesis. Deep-sea Research **25:** 673-688.

---. 1991. Light and marine photosynthesis: a spectral model with geochemical and climatological implications. Progress in Oceanography **26:** 263-306.

Morel, A., and L. Prieur. 1977. Analysis of variations in ocean color. Limnology and Oceanography **22:** 709-722.

Nelson, N. B., and C. Y. Robertson. 1993. Detrital spectral absorption: laboratory studies of visible light effects on phytodetritus absorption, bacterial spectral signal, and comparison to field measurements. Journal of Marine Research **51:** 181-207.

Nielsen, S. L., K. Sand-Jensen, J. Borum, and O. Geertz-Hansen. 2002. Depth Colonization of Eelgrass (Zostera marina) and Macroalgae as Determined by Water Transparency in Danish Coastal Waters. Estuaries **25:** 8.

Paerl, H. W., K. L. Rossignol, R. Guajardo, N. S. Hall, A. R. Joyner, and B. L. Peierls. 2009. FerryMon: Ferry-based monitoring and assessment of human and climatically driven environmental change in the Albemarle-Pamlico Sound system. Environmental science & technology **43:** 7609-7613.

Pope, R. M., and E. S. Fry. 1997. Absorption spectrum (380nm-700nm) of pure water. II. Integrating cavity measurements. Applied Optics **36:** 8710-8723.

Preisendorfer, R. W. 1961. Application of radiative transfer theory to light measurements in the sea. IUGG Monographs **10:** 11-29.

Pribble, R., A. Janicki, H. Zarbock, S. Janicki, and M. Winowitch. 2001. Estimates of Total Nitrogen, Total Phosphorus, Total Suspended Solids, and Biochemical Oxygen Demand Loadings to Tampa Bay. Tampa Bay Estuary Program.

Prieur, L., and S. Sathyendranath. 1981. An optical classification of coastal and oceanic waters based on the specific spectral absorption curves of phytoplankton pigments, dissolved organic matter, and other particulate materials. Limnology and Oceanography **26:** 671-689.

Ralph, P. J., M. J. Durako, S. Enriquez, C. J. Collier, and M. A. Doblin. 2007. Impact of light limitation of seagrass. Journal of Experimental Marine Biology and Ecology **350:** 176-193.

Roesler, C. S., M. J. Perry, and K. L. Carder. 1989. Modeling in situ phytoplankton absorption from total absorption spectra in productive inland marine waters. Limnology and Oceanography **34:** 1510-1523.

Rowan, K. S. 1989. Photosynthetic Pigments of Algae. Cambridge University Press.

Siegel, D. A., and A. F. Michaels. 1996a. Quantification of non-algal light attenuation in the Sargasso Sea: Implications for biogeochemistry and remote sensing. Deep-sea research. Part II, Topical studies in oceanography **43:** 26.

---. 1996b. Quantification of non-algal light attenuation in the Sargasso Sea: Implications for biogeochemistry and remote sensing. Deep-Sea Research **43:** 321-345.

Smith, R. C., and K. S. Baker. 1978. The bio-optical state of ocean waters and remote sensing. Limnology and Oceanography **23:** 247-259.

Smith, R. C. A. K. S. B. 1981. Optical properties of the clearest natural waters (200-800 nm). Applied Optics **20:** 177-184.

Stedmon, C. A., S. Markager, and H. Kaas. 2000. Optical Properties and Signatures of Chromophoric Dissolved Organic Matter (CDOM) in Danish Coastal Waters. Estuarine, Coastal & Shelf Science **51:** 267-278.

Stedmon, C. A., Stiig Markager, Rasmus Bro. 2003. Tracing dissolved organic matter in aquatic environments using a new approach to fluorescence spectroscopy. Marine Chemistry **82:** 239-254.

Steinberg, D. K., N. B. Nelson, C. A. Carlson, and A. C. Prusak. 2004. RESEARCH ARTICLES - Production of chromophoric dissolved organic matter (CDOM) in the open ocean by zooplankton and the colonial cyanobacterium Trichodesmium spp. Marine ecology progress series **267:** 12.

Steward, J. S., and W. C. Green. 2007. Setting Load Limits for Nutrients and Suspended Solids Based upon Seagrass Depth-limit Targets. Estuaries and Coasts **30:** 657-670.

Steward, J. S., R. W. Virnstein, L. J. Morris, and E. F. Lowe. 2005. Setting seagrass depth, coverage, and light targets for the Indian River Lagoon. Estuaries and Coasts**:** 923-935.

Stramski, D. and others 2008. Relationships between the surface concentration of particulate organic carbon and optical properties in the eastern South Pacific and eastern Atlantic Oceans. Biogeosciences **5:** 171-201.

TBNEP. 1996. Charting the Course: The Comprehensive Conservation and Management Plan for Tampa Bay, p. 274. Tampa Bay National Estuary Program.

Thayer, G. W., K. A. Bjorndal, J. C. Ogden, S. L. Williams, and J. C. Zieman. 1984. Role of Larger Herbivores in Seagrass Communities. Estuaries **7:** 351-376.

Tomasko, D. A., C. J. Dawes, and M. O. Hall. 1996. The effects of anthropogenic nutrient enrichment on Turtle Grass (*Thalassia testudinum*) in Sarasota Bay, Florida. Estuaries **19:** 448-456.

Tomasko, D. A., and B. E. Lapointe. 1991. Productivity and biomass of *Thalassia testudinum* as related to water column nutrient availability and epiphytic levels: field observations and experimental studies. Marine ecology progress series **75:** 9-16.

Tomasko, D. A. B., D. L. , and J. A. Ott. 2001. Assessment of present and future nitrogen loads, water quality, and seagrass (*Thalassia testudinum*) depth distribution in Lemon Bay, Florida. Estuaries **24:** 926-938.

Twardowski, M. S., E. Boss, J. M. Sullivan, and P. L. Donaghay. 2004. Modeling the spectral shape of absorption by chromophoric dissolve organic matter. Marine Chemistry **89:** 69-88.

Twardowski, M. S., M. R. Lewis, A. H. Barnard, and J. R. Zaneveld. 2005. In-water instrumentation and platforms for ocean color remote sensing applications, p. 345. *In* R. Miller, C. E. D. Castillo and B. A. McKee [eds.], Remote Sensing of Coastal Aquatic Environments. Springer.

Tyler, D. and others 2007. Topobathymetric data for Tampa Bay, Florida: U.S. Geological Survey Open-File Report 2007-1051 (revised)

USEPA. 1999. Guidance Manual for Compliance with the Interim Enhanced Surface Water Treatment Rule: Turbidity Provisions. Office of Water.

Vanderbloemen, L. A. 2006. Satellite analysis of temporal and spatial chlorophyll patterns on the West Florida shelf (1997-2003). University of South Florida.

Warrior, H., and K. L. Carder. 2005. Production of hypersaline pools in shallow basins by evaporation. Geophysical Research Letters **32:** 5.

Weidemann, A. D., and T. T. Bannister. 1986. Absorption and scattering coefficients in Irondequoit Bay. Limnology and Oceanography **31:** 567-583.

Weiner, R. F., D. M. Osborn, D. Hinojosa, T. J. Heames, J. Penisten, and D. Orcutt. 2008. RADCAT 2.3 Users Guide. *In* S. N. Laboratories [ed.]. Sandia National Laboratories.

Yentsch, C. S. 1962. Measurement of visible light absorption by particulate matter in the ocean. Limnology and Oceanography **7:** 207-217.

Zieman, R. C., and R. T. Zieman. 1989. The ecology of the seagrass meadows of the west coast of Florida: A community profile. *In* U. S. F. a. W. Service. [ed.].

Zimmerman, R. C. 2003. A biooptical model of irradiance distribution and photosynthesis in seagrass canopies. Limnology and Oceanography **48:** 568-585.

About the Author

Chris Anastasiou started his PhD at the University of South Florida (USF) College of Marine Science (CMS) in 2004 while working full-time with the Southwest Florida Water Management District as an environmental scientist. In 2005, Chris began working for the Florida Department of Environmental Protection where he developed new techniques and technologies for coastal zone and estuarine resource management.

Before starting his PhD, Chris received his Bachelor's degree in Geography in 1994 at USF in Tampa and went on to receive his Master's degree in Biology in 2001 also at USF in Tampa.

In 2004 Chris also received his commission as a Navy Reserve Officer within the Naval Meteorology and Oceanography Command. He is currently a Lieutenant and the Executive Officer of the Naval Meteorology and Oceanography Reserve Activity aboard Naval Station Mayport, FL.